

**Implementation of synthetic cytokine biology aimed
at understanding immunological mechanisms in
pathological disorders**

Inaugural dissertation

for the attainment of the title of doctor
in the Faculty of Mathematics and Natural Sciences
at the Heinrich Heine University Düsseldorf

Presented by

Anna Rita Minafra

from Molfetta, Italy

Düsseldorf, July 2023

**Implementation of synthetic cytokine biology aimed
at understanding immunological mechanisms in
pathological disorders**

Inaugural-Dissertation

zur Erlangung des Doktorgrades
der Mathematisch-Naturwissenschaftlichen Fakultät
der Heinrich-Heine-Universität Düsseldorf

vorgelegt von

Anna Rita Minafra

aus Molfetta, Italy

Düsseldorf, Juli 2023

From the Institute of Biochemistry and Molecular Biology II
At the Heinrich Heine University Düsseldorf

Published by permission of the
Faculty of Mathematics and Natural Sciences
At Heinrich Heine University Düsseldorf

Supervisor: Prof. Dr. Jürgen Scheller
Co-supervisor: Prof. Dr. Hadi Al-Hasani

Date of the oral examination: 27.10.2023

Table of Contents

SUMMARY	6
LIST OF ABBREVIATIONS	7
AMINO ACIDS ABBREVIATION	10
1. INTRODUCTION	11
1.1 Cytokines.....	11
1.2 Synthetic cytokine biology	11
1.3 Interleukin (IL-)6-type cytokines	12
1.4 Interleukin (IL-)6	12
1.5 IL-6 signal transduction activated by different complexes of IL-6 and IL-6R	12
1.5.1 Classic IL-6 signaling	13
1.5.2 IL-6 trans-signaling	13
1.5.3 Cluster IL-6 signaling	14
1.6 IL-6 trans-signaling blockade as a potential therapeutic target	16
1.7 Obesity as metabolic disease associated with meta-inflammation	17
1.7.1 Role of IL-6 signaling in meta-inflammation in obesity.....	19
1.8 Beneficial effects of physical exercise	20
1.8.1 Skeletal muscle as “signaling organ” during exercise	20
1.8.2 Role of exercise-mediated IL-6 signaling	21
1.9 Generation of IL-6 trans-signaling mice	24
1.10 Immunoregulatory cytokines: TNF superfamily	26
1.11 Fas/CD95 as death receptor	27
1.12 Fas-mediated apoptosis signaling pathways	27
1.13 Synthetic cytokine receptors.....	30
1.14 Non-synonymous single nucleotide polymorphisms (SNPs) in Fas	30
1.15 Cytokimeras	31
2. Interleukin 6 receptor is not directly involved in regulation of body weight in diet-induced obesity with and without physical exercise.	33
3. Synthetic receptor platform to identify loss-of-function single nucleotide variants and designed mutants in the death receptor Fas/CD95.	46
4. Cytokimera GIL-11 rescued IL-6R deficient mice from partial hepatectomy-induced death by signaling via non-natural gp130:LIFR:IL-11R complexes.....	63
5. DISCUSSION	78

5.1 Revealing the role of IL-6 classic and trans-signaling in diet-induced obesity and physical exercise.	78
5.2 Implementation of a synthetic receptor platform underlines loss-of-function single nucleotide variants and novel functionally diverse mutants in the death receptor Fas/CD95 .	82
5.2.1 Application of Synthetic Fas receptor to complement CAR-T cell therapy	84
REFERENCES	86
ACKNOWLEDGEMENTS	93
EIDESSTATTLICHE ERKLÄRUNG	94

SUMMARY

Synthetic cytokine biology includes the study of engineered cytokines and their interacting receptors, in order to shed light on the related signaling pathways and biological response and individualize new therapeutic targets. During my doctoral studies, I have been focused on the roles of two key cytokine receptors from the Interleukin (IL)-6 and tumor necrosis factor (TNF) superfamilies: interleukin 6 receptor (IL-6R) and the synthetic Fas receptor.

IL-6 exerts its function through two main signaling pathways: IL-6 classic signaling and IL-6 trans-signaling, where IL-6 binds respectively a membrane-bound and a soluble form of IL-6R. In the past, IL-6 has been associated with body weight increase and, in obesity, with chronic low-grade inflammation, impaired glucose and insulin tolerance, leading to type 2 diabetes. On the other side, IL-6, increasing up to 100-fold after physical exercise, results to decrease inflammation, and generally induces anti-diabetogenic effects. Aiming at revealing the role of IL-6 trans-signaling in meta-inflammation, I metabolically characterized a novel mouse model that allows the specific activation of trans-signaling, while the classic signaling is abrogated, together with IL-6R globally deficient mice, and littermates wild-type control. Comprehensively, I monitored body weight and body composition, measured blood glucose and insulin level under fasting conditions, as well as determined metabolic substrate preference, following standard and high-fat diet, with and without physical exercise. Our data showed that neither classic signaling nor trans-signaling are involved in the described metabolic processes.

Synthetic receptors have been previously defined to fully phenocopy trimeric death receptors, in particular Fas, characterized by nanobodies as extracellular portion and natural transmembrane and intracellular domain. In the SNP database (dbSNP) for Fas, there are 17,889 single nucleotide variations (SNVs), of which 337 are missense mutations with mostly uncharacterized functional effects. Here, synthetic Fas has been used to experimentally screen a total of 35 single nucleotide polymorphisms (SNPs) associated with auto-immune diseases and cancer, and candidate loss-of-function (LOF) SNPs and structure-based mutations, testing for cellular proliferation, apoptosis, caspases 3 and 7, and dominant-negative effect. Furthermore, a few mutations were combined to obtain a stronger and milder gain-of-function (GOF) or LOF, as a potential clinical application to boost chimeric antigen receptor (CAR) T-cell therapy. Our findings revealed that 30 variations caused a partial or total LOF, whereas five variants caused a GOF, and the dominant-negative effect was confirmed for two LOF SNPs related to ALPS. In conclusion, we demonstrated that artificial cytokine receptors are a valid platform to experimentally validate LOF SNPs and novel functionally diverse mutants.

Taken together, the two central themes of the thesis rely on synthetic cytokine biology, specifically a novel synthetic sIL-6R mouse model and synthetic Fas, to shed light on the mechanisms underlying meta-inflammation and insulin resistance as well as to implement therapeutic approaches for screening and experimental characterizing immune diseases and cancer-associated mutations.

LIST OF ABBREVIATIONS

3' UTR 3' untranslated region

ALL acute lymphoblastic leukemia

ADAM a disintegrin and metalloproteinase

ALPS autoimmune lymphoproliferative syndrome

APAF-1 apoptotic protease-activating factor 1

APO-1 apoptosis antigen 1

BAIBA β -aminoisobutyric acid

BH3 Bcl-2 homology domain 3

BID BH3 interacting domain death agonist

BSF-2 human B cell stimulatory factor 2

C cytochrome c

CAR chimeric antigen receptor

CBD cytokine-binding domain

cDNA complementary DNA

CD40 cluster differentiation 40

CD40L cluster differentiation 40 ligand

CD95 cluster differentiation 95

CHO carbohydrate

CLC cardiotrophin-like-cytokine

CLF-1 cytokine-like factor 1 cm centimetre

ClinVar clinical variants

CNTF ciliary neurotrophic factor α -receptor

COVID-19 coronavirus disease 2019

CT-1 cardiotrophin-1

D domain

dbSNP SNP databes

DD death domain

DED death effector domain
DISC death-inducing signaling complex
DNA deoxyribonucleic acid
DR death receptor
E exon
FADD fas-associated death domain
Fas FS-7-associated surface antigen
FasL fas ligand
Fc fragment crystallisable
GFP green fluorescent protein
GOF gain-of-function
GLUT glucose transporter
gp130 glycoprotein 130
HA human influenza hemagglutinin
HFD high-fat diet
HIL-6 hyper IL-6
IBD inflammatory bowel disease
Ig immunoglobulin
IL interleukin
IL-6 interleukin 6
IL-6R interleukin 6 receptor
IL-11 interleukin 11
IL-11R interleukin 11 receptor
KO knock out
LIF leukaemia inhibitory factor
LOF loss-of-function
LT- α lymphotoxin-alpha
LT β R lymphotoxin beta receptor

M1 classically activated macrophages
M2 alternatively activated macrophages
mAb monoclonal antibody
MAPK mitogen-activated protein kinase
mRNA messenger RNA
MOMP mitochondrial outer membrane permeabilization
NK natural killer
OSM oncostatin M
SPARC secreted protein acidic and rich in cysteine
PI3K phosphoinositide 3-kinase
RA rheumatoid arthritis
Ras rat sarcoma virus
sgp130 soluble gp130
sIL-6R soluble IL-6 receptor
SNPs single nucleotide polymorphisms
SQ squamous cell carcinoma
STAT signal transducer and activator of transcription
SyCyR synthetic cytokine receptor
THD TNF homology domain
TNF tumor necrosis factor
TNFR tumor necrosis factor receptor
TNFSF TNF superfamily
TNFRSF TNFR superfamily
TRAF tumor necrosis factor receptor-associated factor
TRAIL TNF-related apoptosis-inducing ligand
VHH nanobody
JAK janus kinase
WT wild type

AMINO ACIDS ABBREVIATION

Amino Acid	Three letter code	Letter code
Alanine	Ala	A
Arginine	Arg	R
Asparagine	Asn	N
Aspartic acid	Asp	D
Cysteine	Cys	C
Glutamine	Gln	Q
Glutamic acid	Glu	E
Glycine	Gly	G
Histidine	His	H
Isoleucine	Ile	I
Leucine	Leu	L
Lysine	Lys	K
Methionine	Met	M
Phenylalanine	Phe	F
Proline	Pro	P
Serine	Ser	S
Threonine	Thr	T
Tryptophan	Trp	W
Tyrosine	Tyr	Y
Valine	Val	V

1. INTRODUCTION

1.1 Cytokines

Cytokines are defined as small proteins or peptides that are essential for cell signaling and communication. Released by different immune system cells as well as other cell types, such as fibroblasts and endothelial cells, they can control several cellular responses, such as proliferation, differentiation, and apoptosis, in an autocrine, paracrine, and endocrine manner (Dendorfer 1996).

Initially described as soluble factors released from one cell able to influence the behavior of other cells, cytokines today are also defined as integral membrane proteins never being released from a cell (Dinarello 2007).

Over the past 25 years, they have emerged as a crucial diagnostic, prognostic, and therapeutic tool in the treatment of human disease (Dinarello 2007).

1.2 Synthetic cytokine biology

Synthetic biology has emerged as a valuable tool and approach to studying signaling pathways to uncover fundamental mechanisms and to develop new personalized therapeutic strategies, for example, engineered adoptive T cells for cell-based cancer immunotherapy (Chakravarti and Wong 2015).

A new area of study is the interplay of synthetic biology and immunology, known as synthetic cytokines and synthetic cytokine receptor biology. In this field, scientists work to create new cytokines and/or cytokine receptors or alter those already existing in order to increase their therapeutic potential or better understand their mechanisms. This area has a great potential for creating novel treatments for a variety of diseases, especially those involving the immune system and inflammatory disorders (Zheng, Wu et al. 2022).

Here, I have used different paths of synthetic cytokine biology using engineered receptors of interleukin (IL)-6 and tumor necrosis factor (TNF) superfamilies. In particular, engineered soluble IL-6 receptor (sIL-6R) and IL-6 receptor (IL-6R) knock-out mice have been in vivo metabolically characterized in the context of obesity and insulin resistance, while synthetic cytokine receptors for Fas have been used in vitro to biochemically characterize non-synonymous SNPs, and cytokimera GIL-11 to rescue IL-6R deficient mice from partial hepatectomy.

1.3 Interleukin (IL)-6-type cytokines

The interleukin (IL)-6 cytokine family is composed of IL-6, interleukin (IL)-11, interleukin (IL)-30, interleukin (IL)-31, leukemia inhibitory factor (LIF), oncostatin M (OSM), ciliary neurotrophic factor (CNTF,) cardiotrophin-1 (CT-1), cardiotrophin-like cytokine (CLC) and neuropoeitin (Garbers, Hermanns et al. 2012, Garbers and Scheller 2013).

IL-6-type cytokines share conformational similarities with a conserved four-helical bundle structure, with marginal sequence homology (Bazan 1990). All those cytokines, except IL-31, signal through the common β -receptor glycoprotein 130 (gp130) (Grötzinger, Kernebeck et al. 1999), which functions as homodimer for IL-6 and IL-11, or heterodimer for the others, and activate the signal cascade through JAK/STAT, RAS/MAP kinase and phosphatidylinositol 3-kinase pathways (Taga 1997, Heinrich 1998).

Additionally, in order to bind to β -receptors, the IL-6-type cytokines IL-6, IL-11, and CNTF must interact with specific α -receptors, namely IL-6R, IL-11R, and CNTFR, respectively (Boulanger and Chow, McDonald, Panayotatos et al. 1995, Saggio, Gloaguen et al. 1995, Wagener, Aurich et al. 2014, Metcalfe, Aizel et al. 2020).

1.4 Interleukin (IL)-6

The immune cytokine IL-6 was described for the first time in 1986 by Hirano et al. They identified BSF-2 as a novel interleukin with 184 amino acids, which was later defined as a cytokine and given the name IL-6 (Hirano, Yasukawa et al. 1986).

IL-6 is now recognized as one of the key immunomodulatory cytokines regulating both health and disease (Jones and Jenkins 2018) and inhibitors of IL-6 and IL-6R have been used successfully to contrast several chronic inflammatory diseases, cancer, COVID-19 and cytokine storm consequent to CAR-T cell therapy (Rose-John, Jenkins et al. 2023).

1.5 IL-6 signal transduction activated by different complexes of IL-6 and IL-6R

Mechanistically, IL-6 can activate three distinct signaling pathways: classic IL-6 signaling, IL-6 trans-signaling, and IL-6 cluster signaling, represented in Figure 1. Interestingly, the common factor of the three signaling pathways is the activation of the homodimer of gp130, after binding of IL-6 to IL-6R, which can exist in the form of membrane-bound (mIL-6R) or soluble (sIL-6R) (Murakami, Hibi et al. 1993). Interaction and dimerization of gp130, which is a type I transmembrane receptor, is essential

for activation of downstream signaling pathways: activation of Janus kinase/signal transducer and activator of transcription (JAK/STAT) pathway, mitogen-activated protein kinase (MAPK) pathway, and phosphoinositide 3-kinase (PI3K) pathway (Garbers, Hermanns et al. 2012).

1.5.1 Classic IL-6 signaling

In the classic signaling, IL-6 binds the membrane-bound receptor (mIL-6R). This binding leads to recruitment and homo-dimerization of gp130 and consequent activation of signal transduction.

IL-6R is a protein consisting of 468 amino acids. Structurally, it can be divided into three regions: an extracellular region, a transmembrane domain, and a short cytoplasmic domain (Yamasaki, Taga et al. 1988).

The extracellular region is fundamental for ligand recognition and signal initiation and it is structurally composed of an immunoglobulin (IgG)-like domain (D1) and two fibronectin type III domains (D2 and D3), which are homologous to cytokine-binding domains (CBD) (Leahy, Hendrickson et al. 1992).

Initially, IL-6 binds CBD IL-6R with low affinity. After this, the complex binds to the signaling molecule gp130 to form a high-affinity and stable complex (Ward, Howlett et al. 1994).

Of note, IL-6R is expressed only on specific and restricted cell types, such as immune cells (lymphocytes B and T, neutrophils, macrophages, and monocytes), fibroblasts, and hepatocytes. (Oberg, Wesch et al. 2006, Scheller and Rose-John 2006, Chalaris, Garbers et al. 2011)

Recently, new evidences have proposed the hypothesis that IL-6R might be expressed also in adipocytes and myocytes (Päth, Bornstein et al. 2001, Keller, Steensberg et al. 2005, Sindhu, Thomas et al. 2015, Kistner, Pedersen et al. 2022).

1.5.2 IL-6 trans-signaling

IL-6 trans-signaling involves IL-6 binding to a soluble form of IL-6R (sIL-6R) generated by proteolytic cleavage by a disintegrin and metalloproteases 17 (ADAM-17), and by a minor extent ADAM-10 (Rose-John, Jenkins et al. 2023).

A soluble form of the IL-6R can also be generated by IL-6R mRNA alternative splicing, and this accounts in humans but not in mice and only for about 15% of the circulating IL-6R (Lust, Donovan et al. 1992, Schumacher, Meyer et al. 2015).

The soluble form of IL-6R is structurally composed of two domains: the extracellular portion and the stalk portion (Garbers, Hermanns et al. 2012). The activation of the signaling pathway is therefore induced by IL-6 binding to sIL-6R and consequent dimerization of gp130.

The advantage of trans-signaling is that it can be activated in all cell types since it requires the presence of gp130, which is a widely expressed protein in all the cell types (Heinrich, Behrmann et al. 2003), with the exception of granulocytes, on which it has been shown that gp130 is absent, thus resulting in lack of IL-6 activation (Wilkinson, Gartlan et al. 2018).

1.5.3 Cluster IL-6 signaling

Recently, a third mode of IL-6-mediated signaling has been described: the cluster signaling.

In this case, IL-6 interacts with mIL-6R expressed in the so-defined transmitter cell, and subsequently, the complex IL-6-IL-6R interacts with gp130 situated on the surface of a neighbouring receiver cell. The signal cascade is therefore activated in the receiver cell.

One example is the mechanism through which dendritic cells prime pathogenic Th17 cells using IL-6 trans-presentation (Heink, Yogev et al. 2017).

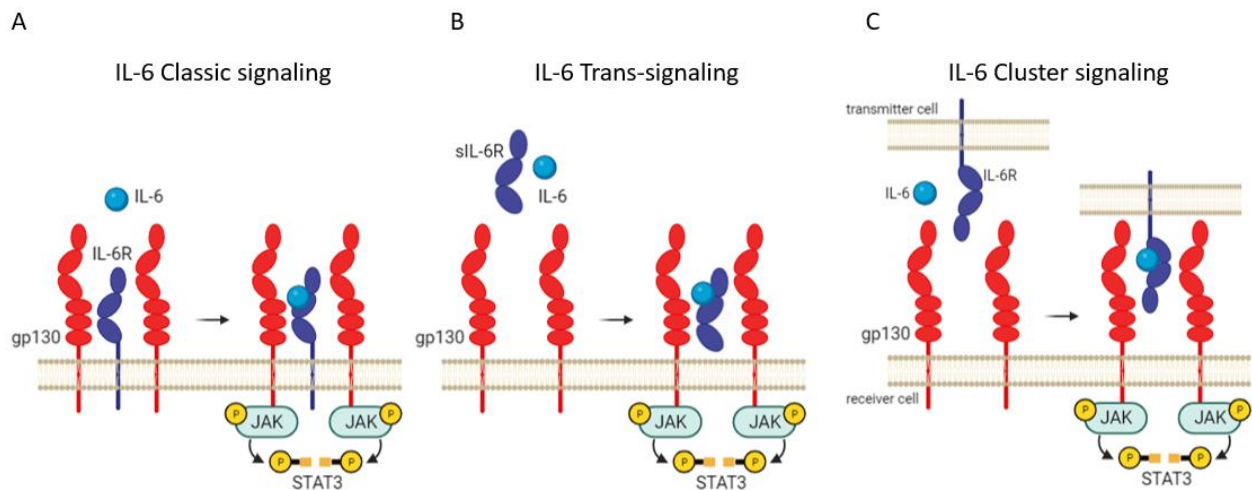


Figure 1: Schematic representation of IL-6 signaling modes.

- (A) Graphical representation of IL-6 classic signaling: IL-6 interacts with membrane-bound IL-6R leading to gp130 homodimerization and activation of intracellular pathway.
- (B) Graphical representation of IL-6 trans-signaling: IL-6 interacts with the soluble form of IL-6R followed by interaction and homodimerization of gp130 and activation of intracellular pathway.
- (C) Graphical representation of IL-6 cluster signaling: IL-6 interacts with the membrane-bound IL-6R expressed on the transmitter cell and the complex IL-6-IL-6R interact with homodimer gp130 expressed on the receiver cell, followed by activation of intracellular pathway in the receiver cell.

1.6 IL-6 trans-signaling blockade as a potential therapeutic target

While IL-6 classic signaling is primarily responsible for controlling homeostasis and acute pro-inflammatory processes, trans-signaling has been associated with chronic inflammation and pathological conditions.

Rapidly, inhibiting IL-6 signaling became a promising therapeutic strategy to treat several inflammatory diseases, such as viral and bacterial infections, plasma cell leukemia, Castleman disease, rheumatoid arthritis, and cytokine release syndrome. IL-6 signaling inhibitors were introduced and tested in the clinic, such as monoclonal antibodies that specifically bind to the IL-6R, e.g. tocilizumab and sarilumab, and monoclonal antibodies that directly target and neutralize IL-6, e.g. siltuximab (Rose-John, Jenkins et al. 2023).

However, none of these inhibitors of IL-6 signaling can distinguish between classic and trans-signaling. Globally inhibiting IL-6 might compromise its vital functions in maintaining organ homeostasis. In individuals with rheumatoid arthritis, for instance, inhibiting classic IL-6 signaling by antibodies may result in dysregulation of the immune response and subsequently raise the risk of infection (Navarro, Taroumian et al. 2014, Morel, Constantin et al. 2017).

In 2001, the research group of Stefan Rose-John generated a fusion protein composed of the extracellular region of gp130 and the Fc region of a human IgG1 antibody, called sgp130Fc, that interacted with IL-6-sIL-6R complexes and selectively blocked the IL-6 trans-signaling but did not affect classic signaling (Jostock, Müllberg et al. 2001).

The sgp130Fc variant, called olamkicept by the World Health Organization, has been initially tested in preclinical studies, demonstrating more favourable effects compared to global IL-6 blockage, for many inflammatory and neoplastic diseases, of note sepsis (Rakonczay, Hegyi et al. 2008), lung damage associated with pancreatitis (Zhang, Neuhöfer et al. 2013), bone healing (Kaiser, Prystaz et al. 2018), and recently myocardial infarction (George, Jasmin et al. 2021), as well as rheumatoid arthritis (Nowell, Williams et al. 2009), colon cancer (Becker, Fantini et al. 2004), atherosclerosis (Schuett, Oestreich et al. 2012).

Importantly, the application of olamkicept in several preclinical studies helped to shed light on the mechanisms behind several pathological condition and how specifically IL-6 trans-signaling plays a part in the progression of disease (Rose-John, Jenkins et al. 2023).

Olamkicept began clinical testing in phase I in 2012, and in phase IIa in 2021 with 16 patients who had inflammatory bowel disease (IBD), with a positive clinical response occurring in 44% and clinical

remission in 19% of cases (Schreiber, Aden et al. 2021). Furthermore, it recently demonstrated positive outcomes with clinical remission and mucosal repair in patients with moderate-to-severe ulcerative colitis in the phase IIb trial in 2021 (Chen, Zhang et al. 2021).

1.7 Obesity as metabolic disease associated with meta-inflammation

Over the past decades, especially in the Western countries, obesity has become a global health problem, reaching epidemic levels and affecting millions of people worldwide (Temple 2022).

Initially, obesity has been defined as excessive accumulation of body fat and adipocyte hypertrophy, often due to unhealthy dietary habits, lack of physical exercise, and, in some cases, genetic predisposition, hormonal imbalances, and specific medical conditions. Now, obesity is fully recognized as a metabolic disease, linked to chronic low-grade inflammation, known as meta-inflammation (Russo, Kwiatkowski et al. 2021).

Meta-inflammation is mainly characterized by the infiltration of immune cells, such as lymphocytes and neutrophils but in particular M1 pro-inflammatory macrophages, into adipose tissue, and consequently increased release of pro-inflammatory molecules, such as cytokine (e.g., IL-6 and tumor necrosis factor-alpha (TNF- α)), chemokines, and adipokines, that promote inflammation itself and disrupt metabolic processes in the adipose tissue and in the periphery, in particular in the skeletal muscles and liver (Esser, Legrand-Poels et al. 2014). A schematic overview of meta-inflammation linked to obesity is represented in Figure 2.

This phenomenon has drawn particular attention in recent years due to its potential role in the development and progression of various obesity-related complications, such as cardiovascular diseases, insulin resistance, impaired glucose homeostasis, and type 2 diabetes.

Multiple scientists have demonstrated that inhibiting inflammatory mediators and the signaling pathways they activate improve insulin sensitivity. In 1993, Hotamisligil and Shargill showed TNF- α production in adipose tissue in obese and diabetic rats and its blocking determined improved response to insulin and increased glucose uptake (Hotamisligil, Shargill et al. 1993). Furthermore, a key regulator of acute inflammation is the nuclear factor κ B (NF- κ B) and its activator IKK- β , and many evidences suggest their link with insulin resistance and type 2 diabetes. It has been shown how anti-inflammatory molecules, such as salicylates, increase insulin sensitivity in rodents, probably through IKK- β inhibition, while specific deletion of IKK- β in liver and myeloid cells causes respectively improved glucose uptake in the liver and systemic improved insulin sensitivity in high-

fat diet fed mice. (Hotamisligil, Shargill et al. 1993, Yuan, Konstantopoulos et al. 2001, Arkan, Hevener et al. 2005).

Hence, it is essential to comprehend the intricate mechanisms behind the interconnection between obesity and meta-inflammation in order to individualize efficient preventive and therapeutic strategies.

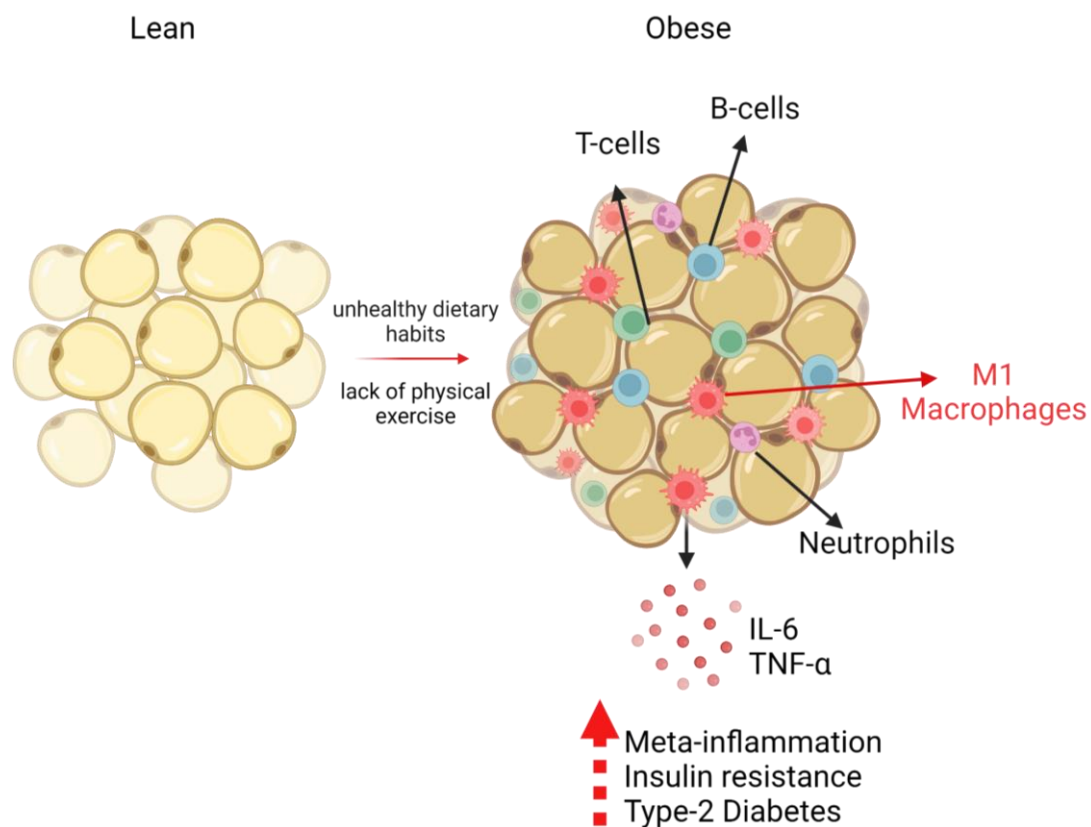


Figure 2: Obesity leads to meta-inflammation in adipose tissue

A transition from lean adipose tissue to obesity can occur as a result of an unhealthy diet and/or lack of exercise. This state is characterized by chronic low-grade immune cells infiltration, such as lymphocytes (T-cell in green and B-cells in blue), neutrophils (in pink), and pro-inflammatory macrophages (in red). These cells release an extensive amount of cytokines, such as IL-6 and TNF- α , which increase the inflammatory response and insulin resistance.

1.7.1 Role of IL-6 signaling in meta-inflammation in obesity

IL-6 has been identified as a key player in the regulation of meta-inflammation in obesity, released mainly by the pro-inflammatory M1 subtype macrophages that infiltrate the adipose tissue (Pal, Febbraio et al. 2014).

For the first time, Wallenius et al. in 2002 explored the role of IL-6 in the development of obesity and its impact on carbohydrate and lipid metabolism, using global IL-6-deficient mice. Their data suggested that IL-6 plays a fundamental role in regulating body weight and adiposity, as well as in causing imbalanced carbohydrates, in particular impaired glucose tolerance, and disturbances in lipid metabolism, such as increased levels of circulating triglycerides in females and increased leptin levels in both sexes (Wallenius, Wallenius et al. 2002, Pal, Febbraio et al. 2014).

A few years later, Matthews et al. confirmed the pivotal role of IL-6 in the regulation of body weight and glucose metabolism. In detail, CHO-fed mice lacking IL-6 developed obesity, systemic insulin resistance, reduced glucose tolerance, hepatic inflammation, and disrupted insulin signaling pathways in the liver, crucial for regulation of glucose metabolism (Matthews, Allen et al. 2010).

In contrast, unlike results were observed considering hepatocyte-specific IL-6 receptor deficiency mice. Indeed, in this regard, no differences were observed regarding body weight and body composition, leptin levels, daily food intake, activity, and respiratory exchange ratio, despite reduced glucose tolerance and insulin sensitivity (Wunderlich, Ströhle et al. 2010).

Interestingly, considering specific-astrocyte deficient IL-6 mice compared to specific-astrocyte deficient IL-6R mice, some differences were underlined. Firstly, increased body weight was observed only in male astrocytes IL-6 KO mice but not in females and remarkably also not in astrocyte-specific IL-6R KO mice (Quintana, Erta et al. 2013).

Furthermore, to evaluate the hypothesis that, in the context of obesity, IL-6 produced from adipocytes is linked to increased body weight and insulin resistance, recently, Whitham et al. confuted this suggestion proving that IL-6 in adipocytes is not directly influencing increase body weight, as well as glucose and insulin tolerance after high-fat diet (Whitham, Pal et al. 2019).

Likewise, Han et al. did not observe any changes in body weight, body composition, and insulin tolerance, following specific IL-6 depletion in adipocytes, but a minor improvement in glucose tolerance. Interestingly, they found that adipocyte IL-6 endorses adipose tissue inflammation and directly promotes the infiltration of pro-inflammatory M1 macrophages (Han, White et al. 2020).

In conclusion, it is yet unknown if IL-6 and/or IL-6R is the main factor that leads to the development of insulin resistance and obesity or if it is essentially needed to counteract the heightened inflammation occurring in the adipose tissue.

1.8 Beneficial effects of physical exercise

In the far 460 BC, the ancient Greek physician Hippocrates, known to be the founder of Western medicine, was the first person to formally acknowledge the health benefits of an active lifestyle, declaring that “Walking is man's best medicine.”

Today, it is well affirmed that physical exercise is essential for promoting general health and well-being, having a variety of beneficial effects on the body, and mind, as well as a strong potential for disease prevention.

Regular exercise can greatly improve flexibility, musculoskeletal strength, weight control, and cardiovascular health (Booth, Roberts et al. 2012).

Additionally, it correlates to better mood, less stress, increased cognitive function and memory, and higher-quality of sleep (Sharma, Madaan et al. 2006).

Contrary, lack of physical exercise has been associated with increased risk for several metabolic diseases, such as obesity, insulin resistance, and type 2 diabetes, colon, endometrial and breast cancers, in addition to cardiovascular problems and cognitive complications (Murphy, Watt et al. 2020).

1.8.1 Skeletal muscle as “signaling organ” during exercise

Beginning this century, it is now well accepted in the scientific community that skeletal muscle, besides their important role in movements and posture maintenance, is an important “signaling organ”. Especially during contraction, indeed, it actively secretes cytokines, peptides, and/or metabolites, defined as myokines, that execute their functions in an autocrine, paracrine, and/or endocrine manner, to communicate with the muscle itself and other organs such adipose tissue, liver, pancreas, bones, and brain (Pedersen and Febbraio 2012).

Examples include lactate, meteorin-like protein, glial cell differentiation (Metrnl), cathepsin B, and irisin, which increase during physical exercise and interact with the brain to enhance cognition and memory, IL-6 and BAIBA (β -aminoisobutyric acid), which engage with the liver, enhancing β -oxidation and energy disposal, and with the adipose tissue, inducing the browning, and finally

secreted protein acidic and rich in cysteine (SPARC), a myokine that rise during exercise in both mice and humans and guards against colon carcinogenesis (Murphy, Watt et al. 2020).

1.8.2 Role of exercise-mediated IL-6 signaling

Among the myokines, IL-6 holds a special place as the first myokine to be identified (Sprenger, Jacobs et al. 1992, Drenth, Van Uum et al. 1995, Nehlsen-Cannarella, Fagoaga et al. 1997, Pedersen and Hoffman-Goetz 2000).

In 1998, the research group of Professor Bente Klarlund Pedersen revealed that some cytokines (especially IL-6) levels in athletes' plasma are elevated during strenuous, prolonged exercise and it is also correlated to the intensity, duration, and engaged muscle mass during the exercise (Ostrowski, Hermann et al. 1998, Febbraio and Pedersen 2002)

The scientific community gradually began to consider that skeletal muscles must be the principal source of IL-6 production during contraction as more and more data came to support this theory. To begin with, rat muscle that had undergone concentric or eccentric electrically induced contractions had higher levels of IL-6 mRNA (Jonsdottir, Schjerling et al. 2000), while Ostrowski et al. and later Febbraio's research group observed both IL-6 mRNA and protein levels increase in skeletal muscle during physical exercise, and plasma IL-6 rises up to 100-fold (Ostrowski, Rohde et al. 1998, Steensberg, van Hall et al. 2000, Chan, Carey et al. 2004).

Only in 2001, this hypothesis was systematically confirmed by the group of Pedersen, who directly measured the net IL-6 released from legs during prolonged knee-extensor exercise. They successfully demonstrated that IL-6 production and subsequent release from skeletal muscle are not caused by an inflammatory response but rather are a result of muscle contractions following physical exercise activity. Furthermore, IL-6 release is directly influenced by pre-exercise glycogen availability (Steensberg, Febbraio et al. 2001).

Nowadays, there is evidence that myokine IL-6 has regenerative properties, temporarily suppresses immunological response, and possibly guards against obesity and insulin resistance, after physical exercise (Kistner, Pedersen et al. 2022).

Indeed, it has been demonstrated that IL-6 contributes to muscular recovery and hypertrophy and helps tissues heal after damage or injury (Serrano, Baeza-Raja et al. 2008).

Furthermore, although IL-6 is typically thought of as a cytokine that promotes inflammation, it also has immunomodulatory effects. Importantly, IL-6 can transiently reduce the immune functions: it

has been shown it is linked to increasing circulating levels of anti-inflammatory molecules, e.g. IL-10 and IL-1 receptor antagonist (IL-1ra), a cytokine that counteracts the effects of pro-inflammatory cytokine IL-1, as well as decreasing levels of pro-inflammatory cytokines, e.g. TNF- α (Schindler, Mancilla et al. 1990, Starkie, Ostrowski et al. 2003, Steensberg, Fischer et al. 2003, Petersen and Pedersen 2005).

Interestingly, it has been shown that IL-6 can reduce inflammation also via promoting M2 macrophage phenotype (Deng, Wehling-Henricks et al. 2012, Fernando, Reyes et al. 2014) .

Finally, IL-6 secreted by contracting muscles is involved in the regulation of energy homeostasis and metabolic processes, being defined as “energy sensor”. As demonstrated, during physical activity, IL-6 stimulates cell surface glucose transporter 4 (GLUT4) translocation in muscle cells, promoting blood glucose elimination and blood glucose uptake in skeletal muscles, and can improve insulin sensitivity (Pal, Febbraio et al. 2014). Consuming glucose while exercising reduces circulating IL-6 levels induced by exercise and stops humans' skeletal muscles from releasing IL-6 (Pedersen and Febbraio 2012).

Additionally, important is the cross-talk between skeletal muscle and adipose tissue after physical exercise. IL-6 might boost fatty acid uptake, lipolysis, and free fatty acids oxidation from skeletal muscles and adipocytes as well, thus defining IL-6 as a lipolytic factor (Petersen, Carey et al. 2005).

In a study conducted by Wan et al. in 2012, the data revealed that IL-6 activates signal transducer STAT3 in the adipose tissue during exercise, indirectly associated with activation of glyceroneogenic enzymes, which are involved in the lipid metabolism, thereby contributing to general energy disposal (Wan, Perry et al. 2012). Furthermore, other studies reported a direct correlation between IL-6 and intramuscular lipid and glycogen content (Lukaszuk, Bialuk et al. 2012, Wan, Perry et al. 2012, Chowdhury, Schulz et al. 2020).

In summary, the main functions of IL-6 as myokine, up to date reported in the literature, are represented in Figure 3: released from skeletal muscle during contraction, IL-6 has been associated with enhanced fatty acid uptake and oxidation, lipolysis, and inhibition of inflammation in the adipose tissue, as well as increased glucose disposal and up-take and better insulin sensitivity in the skeletal muscles.

However, it should be considered that the roles of IL-6 influencing the immune responses, cell proliferation and differentiation, as well as metabolic regulations, result to be intricate and context-

dependent, and the precise mechanisms involved are still unknown, thus needing further investigations.

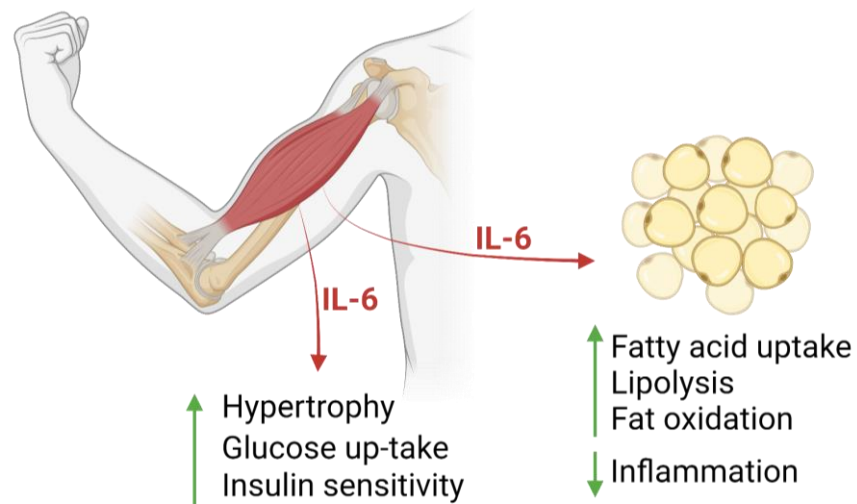


Figure 3: The main functions of IL-6 released from skeletal muscles during physical exercise

IL-6 has been associated to numerous beneficial effects when released from skeletal muscle during contraction. In particular, it has been linked to hypertrophy, increase of glucose disposal and glucose up-take, and improved insulin sensitivity in the skeletal muscles, but also increased fatty acid uptake and oxidation, lipolysis, and inhibition of inflammation in the adipose tissue.

1.9 Generation of IL-6 trans-signaling mice

As stated above, it is now well-established that IL-6, when acting as an adipokine, promotes meta-inflammation, and insulin resistance, and causes type 2 diabetes, whereas, when acting as a myokine, is primarily accountable for reducing inflammation, raising insulin sensitivity, enhancing glucose metabolism, and generally improving energy expenditure during physical activity. However, it is not yet known, whether the metabolic actions of IL-6 primarily depend on classic or trans-signaling.

Previously, soluble IL-6R (sIL-6R) mice were generated (Fazel Modares, Polz et al. 2019). These animals were the result of genetic engineering that resembles ADAM10/17 hyperactivation, which is produced by Cre-mediated deletion of the genetic material coding for the transmembrane and intracellular domain of the IL-6R. More in detail, the IL-6R gene (gene ID: 16194) is composed of ten exons: the transmembrane domain and the initial portion of the intracellular domain are encoded by exon 9 (E9), while the final portion and the 3' untranslated region (3' UTR) is encoded by exon 10 (E10). To mimic the natural proteolytic cleavage, those two exons were fused, via removal of intron 9, and a 2A-GFP-KDEL was inserted to substitute the endogenous codon stop, before the final 3'UTR.

A 2A peptide, commonly referred to as a "self-cleaving 2A peptide," is a short peptide sequence with the distinctive ability to self-process or self-cleave, since its ability to mediate a co-translational "ribosome skipping" event during protein translation. It is, thus, able to generate two distinct proteins, in this case, IL-6R and GFP, from a single mRNA transcript.

Furthermore, two LoxP sites were inserted at the beginning and end of the E9-E10-GFP cassette. Following Cre recombination, the described cassette was removed, leading to the production of an mRNA that exclusively encoded for the soluble IL-6R.

As a result, these mice selectively engage in trans-signaling, whereas classic signaling is abrogated. A schematic representation of sIL-6R mice, where only trans-signaling is active, compared to global IL-6R deficient mice (IL-6R KO), where both classic and trans-signaling are abolished, is in Figure 4.

Importantly, as previously tested in liver regeneration after partial hepatectomy (Fazel Modares, Polz et al. 2019), IL-6 trans-signaling can fully compensate the lack of classic signaling. Indeed, sIL-6R mice were able to survive following partial hepatectomy, compared to IL-6R global deficient mice, which resulted severely harmed.

In conclusion, selectively executing only trans-signaling and abrogating classic signaling, this mouse model represents an accurate methodologic strategy to reveal through which mechanisms IL-6 exerts its function in the context of diet-induced obesity and physical exercises.

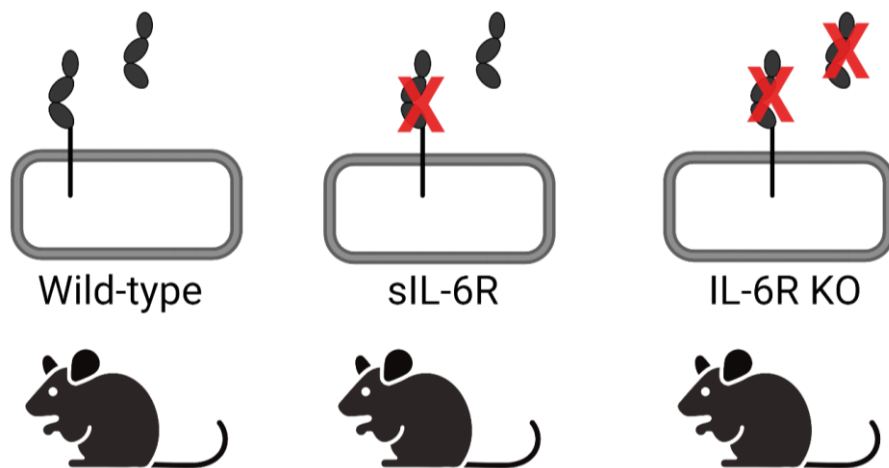


Figure 4: Graphical representation of sIL-6R mice versus IL-6R KO mice.

sIL-6R mice can execute only trans-signaling while classic signaling is abrogated due to a deletion of genetic portions codifying for the transmembrane and intracellular IL-6R domains, mimicking the endogenous proteolytic activity of ADAM 10/17. IL-6R KO mice are instead characterized by total ablation of IL-6R expression, thus not being able to execute classic or trans-signaling.

1.10 Immunoregulatory cytokines: TNF superfamily

The TNF (Tumor Necrosis Factor) superfamily is a group of cytokines and cell surface receptors that play critical roles in regulating immune responses and inflammation, cell survival, proliferation, and differentiation.

The superfamily is named after the first member, TNF- α , discovered in late 1975 by Carswell et al. for its capacity to cause tumor necrosis (Carswell, Old et al. 1975). Since then, numerous other members have been discovered, each with its own unique roles and mechanisms of action.

Based on their functional characteristics, the TNF superfamily can be classified into two primary groups: 19 ligands, which compose the cytokine-like molecules (TNFSF), and 29 associated receptors (TNFR), which compose the TNF receptor superfamily (TNFRSF).

Most of the TNF superfamily's ligands are homo- or heterotrimers and have structural traits in common. Typically, they are type II transmembrane proteins composed of extracellular domain (C-terminus), transmembrane, and intracellular domain (N-terminus). The extracellular domain is characterized by a conserved distinctive motif defined as TNF homology domain (THD), which contains a characteristic arrangement of beta strands and alpha helices, that allows trimeric structure formation, necessary for binding to trimeric TNFR (Bodmer, Schneider et al. 2002).

Several noteworthy ligands are tumor necrosis factor-alpha (TNF- α), a very effective pro-inflammatory molecule, lymphotoxin-alpha (LT- α) or TNF- β , engaged in immunological reactions and the development of lymphoid organs, CD40 Ligand (CD40L), expressed on activated lymphocytes to induce release of antibodies and immune cell activation, Fas Ligand (FasL), which causes apoptosis in target cells by interacting with the Fas receptor, and TRAIL (TNF-related apoptosis-inducing ligand), which promotes apoptosis in tumor cells and infected cells (Bodmer, Schneider et al. 2002).

The TNF superfamily's receptors, moreover, are mainly type I transmembrane proteins. They have an extracellular domain (N-terminus) that binds to ligands, a transmembrane domain, and an intracellular domain (C-terminus) that transmits signaling.

Of note, based on their structures, TNFRSF can be classified into two distinct groups: death receptors, characterized by the presence of a death domain (DD), and non-death receptors. The DD is a conserved 80-amino acid motif present in the intracellular portion. Lacking a DD, non-death

receptors usually enlist TRAFs to trigger signaling pathways that regulate cell survival, proliferation, and cytokine release.

Death receptors include TNFR1, TNFR2, Fas (CD95), death receptor 3 (DR3), TNF-related apoptosis-inducing ligand receptors 1 and 2 [TRAIL-R1 (DR4), TRAIL-R2 (DR5)], and death receptor 6 (DR6). Examples of non-death receptors are CD40 and lymphotoxin β receptor (LT β R) (Dostert, Grusdat et al. 2019).

1.11 Fas/CD95 as death receptor

Fas, also known as CD95 or APO-1, is one of the members of the TNF superfamily, and in particular, it belongs to the death receptor group. It exerts a pivotal role in triggering apoptotic cell death.

Fas protein is encoded by the Fas gene, or TNFRSF6, located on human chromosome 10, which is composed of nine exons and eight introns. While exon 6 encodes for the transmembrane domain, exon 9 encodes for the death domain (Price, Shaw et al. 2014).

Structurally, it is a type I transmembrane receptor, composed by an extracellular domain, containing cysteine-rich regions essential for binding to Fas ligand (FasL), a transmembrane domain, that anchors it to the cell membrane, and an intracellular domain, including the death domain, fundamental for initiating the signal transduction (Dostert, Grusdat et al. 2019).

Fas-mediated apoptosis is crucial for maintaining immune tolerance and preventing autoimmunity. For instance, activated T cells or autoreactive T cells undergo apoptosis following the interaction of Fas with FasL, expressed on the cell surface of cytotoxic T cells or NK cells, in order to suppress overactive immune responses (Stranges, Watson et al. 2007).

1.12 Fas-mediated apoptosis signaling pathways

Upon Fas-FasL binding, conformational changes in the Fas structure occur: a reversible transition from a closed to an open structure of the intracellular domain allows recruitment and subsequent aggregation of additional Fas proteins, thus forming a trimeric structure, essential for signal transduction (Figure 4) (Scott, Stec et al. 2009).

Following Fas trimerization, the intracellular DD recruits the adaptor molecule Fas-associated death domain (FADD), which directly interacts with the DD. A death effector domain (DED), localized in FADD, is then responsible for recruiting and inducing the activation of pro-caspase 8, which shifts to its active form through autocatalytic cleavage.

Fas DD, FADD, and pro-caspases 8 form the so-called death-inducing-signaling complex (DISC).

Finally, caspase 8 activates the effector caspases-3 and -7 that trigger apoptosis. This is the so-defined extrinsic pathway.

Alternatively, in the intrinsic pathway, also referred to as the mitochondrial pathway, active caspase 8 can cleave BID (a mitochondrial BH3-only protein), which can translocate to the mitochondria and induce permeabilization of the mitochondrial outer membrane (MOMP), which leads to cytochrome c release. Once in the cytosol, the cytochrome c interacts with other proteins, such as apoptotic protease-activating factor 1 (APAF-1) and procaspase-9, to form the apoptosome. Active caspase-9 in turn activates downstream effector caspases-3 and -7 to induce apoptotic cell death.

While the extrinsic pathway is primarily involved in immune surveillance, eliminating infected or damaged cells, and maintaining tissue homeostasis, the intrinsic pathway is activated by intracellular signals arising from cellular stress or DNA damage caused by external factors, like chemicals, radiation, and growth factor withdrawal (Figure 5) (Dostert, Grusdat et al. 2019).

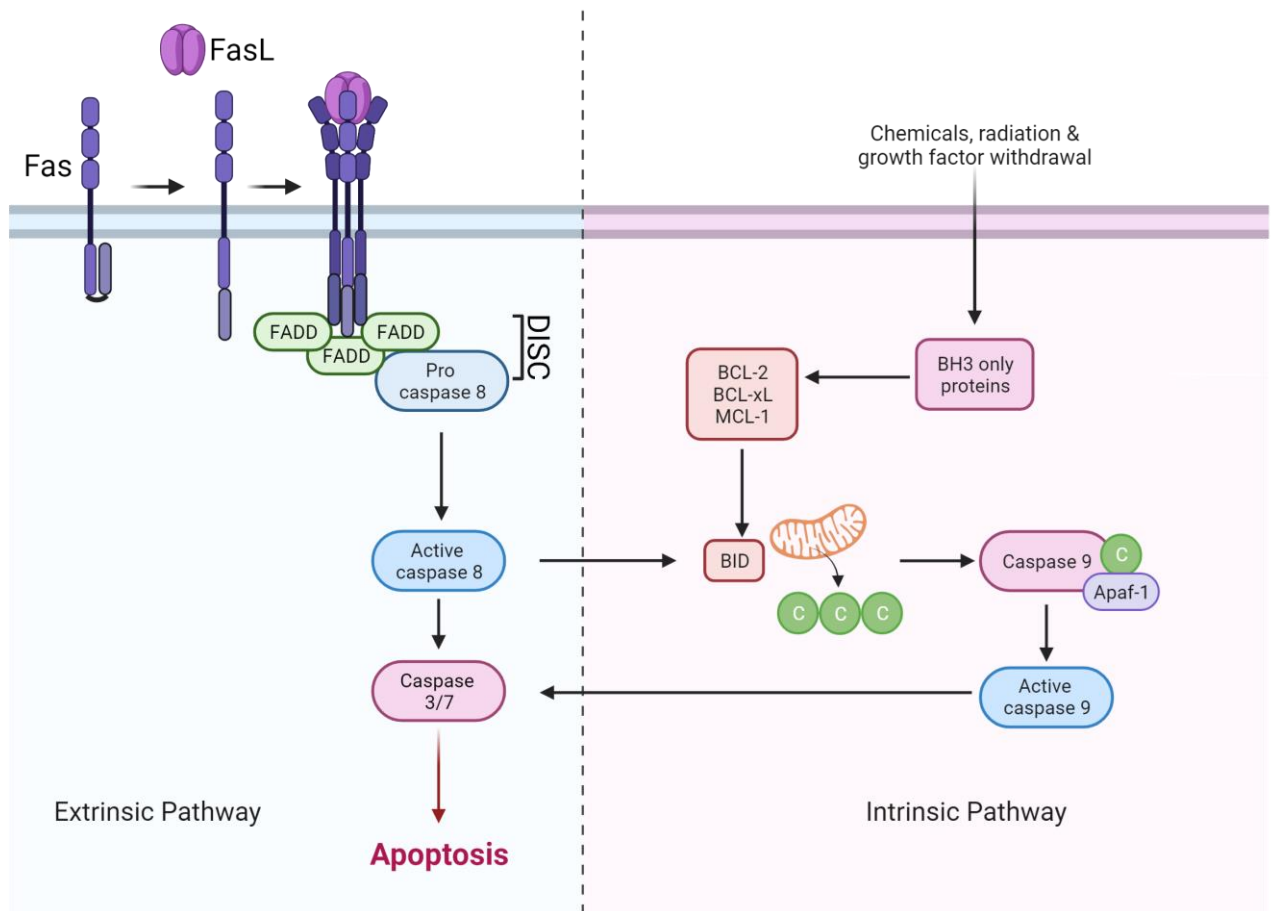


Figure 5: Schematic overview of Fas-induced apoptotic pathways.

Normally, Fas resides in a closed conformation. In the presence of FasL, the intracellular Fas domain shift from a closed to an open, transient conformation that allows interaction with additional Fas molecules, thus forming a trimeric structure, as well as interactions with FADD. Together with pro-caspase 8, Fas-FADD forms the DISC complex. In the extrinsic pathway, pro-caspase 8 undergoes auto-catalytic cleavage and activates effector caspases 3 and 7, inducing apoptosis. Vice versa, in the intrinsic pathway, active caspase 8 induces mitochondrial outer membrane permeabilization, through BID cleavage, which causes the release of cytochrome c (C), which interacts with Apaf-1 and caspase 9. This, in the active form, induces activation of caspases 3 and 7, inducing apoptosis

1.13 Synthetic cytokine receptors

Synthetic biology enables the design and construction of synthetic cytokine receptors (SyCyRs). This approach allows the systematic study of receptor-ligand interactions and their impact on downstream cellular responses in a controlled and customizable manner, providing opportunities for therapeutic applications and enhancing our understanding of cytokine-mediated processes in health and disease.

Of note, first approved gene therapy has been the chimeric antigen receptor (CAR) T cell immunotherapy for acute lymphoblastic leukemia (ALL) (June, O'Connor et al. 2018).

In the research group of Prof. Scheller, initially dimeric SyCyRs have been designed and engineered to phenocopy IL-6/IL-23 and IL-22 signaling (Engelowski, Schneider et al. 2018, Mossner, Kuchner et al. 2020).

Recently, also prototypical trimeric receptors for TNF and FasL have been created. The extracellular portion of the receptor has been substituted with nanobodies (VHH), which correspond to the variable region of a heavy chain of a Camelid antibody (Rothbauer, Zolghadr et al. 2008, Wesolowski, Alzogaray et al. 2009, Fridy, Li et al. 2014), fused to the transmembrane and intracellular domain of the specific receptors and function as bio-sensors for homo- or heteromeric ligands, such as fusion protein of green fluorescent protein (GFP) and mCherry (Mossner, Phan et al. 2020).

Following the binding of trimeric synthetic ligand to trimeric synthetic receptor, it has been previously demonstrated that endogenous receptor-specific activation of signaling pathway takes place, which is via NF- κ B signaling or Caspase-induced apoptosis, respectively for TNF and FasL (Engelowski, Schneider et al. 2018, Mossner, Kuchner et al. 2020).

1.14 Non-synonymous single nucleotide polymorphisms (SNPs) in Fas

Human DNA contains around 3 billion bases. Although on average 99.6% of the human genome sequence is identical, we are all genetically unique.

Single nucleotide polymorphisms (SNPs) are single nucleotide variation within human DNA sequence. They can occur anywhere in the genome, including within genes, and are the most prevalent sort of genetic variation across individuals, at least in 1% of the population.

Fas gene is associated with 17.889 SNPs reported in SNP database (dbSNP), of which 337 non-synonymous missense mutations, of which 39 listed in clinical variants (ClinVar) database.

SNPs within the FAS gene have been studied to understand their association with various diseases and phenotypes, such as autoimmune disorders, cancer susceptibility, and infectious diseases, particularly development of autoimmune lymphoproliferative syndrome (ALPS) and squamous cell carcinoma (de Carvalho-Neto, Santos et al. 2013, Rieux-Laucat 2017).

In general, mutations in the gene's sequence can cause variations in gene expression, protein folding, localization, stability, and/or function (Rauscher and Ignatova 2018, Robert and Pelletier 2018).

Discovering the genetic variations, including SNPs, within the FAS gene can provide insights into disease susceptibility, prognosis, and potential therapeutic targets. However, the majority of non-synonymous SNPs found in a random-like genome sequencing approaches, lack of functional analysis. It is crucial to understand the molecular mechanism behind each of those mutations, specially loss-of function mutations that interfere with apoptosis, to fully comprehend the complex relationships between FAS SNPs and disease phenotypes.

To handle the increasing SNP landscape, systematic bioinformatics and experimental methods must be combined. In-depth structure-guided analysis (Pettersen, Goddard et al. 2021) or simple online data processing methods like Provean (Kumar, Henikoff et al. 2009) can both predict functionally important SNPs. In addition, current advances in artificial intelligence allow for the in-silico prediction of protein and protein complex structures (Service 2021). The structural comprehension of amino acid exchanges can be aided by these deep learning algorithms, such as RoseTTAFold (Baek, DiMaio et al. 2021) and AlphaFold (Jumper, Evans et al. 2021), either in the examination phase to screen for functionally relevant SNPs or in the post-laboratory phase to understand the biochemically approved gain- or loss-of-function (GOF, LOF) SNPs.

However, at least for gain- and loss-of-function mutants, in-silico characterisation needs to be experimentally confirmed.

1.15 Cytokimeras

Chimeric cytokines, also known as cytokimeras, are characterized by the backbone of a natural cytokine which is modified with a minimum of one receptor binding site of another cytokine with structural similarity (Kallen, Grötzinger et al. 1999).

One exemplary cytokimera from the IL-6-type cytokines family is IC7, described in the literature for the first time in 1999. In this case, Kallen et al. transferred the LIFR binding site from CNTF to IL-6,

obtaining a chimeric cytokine able to bind to IL-6R and to signal via a heterodimer of gp130 and LIFR (Kallen, Grötzinger et al. 1999).

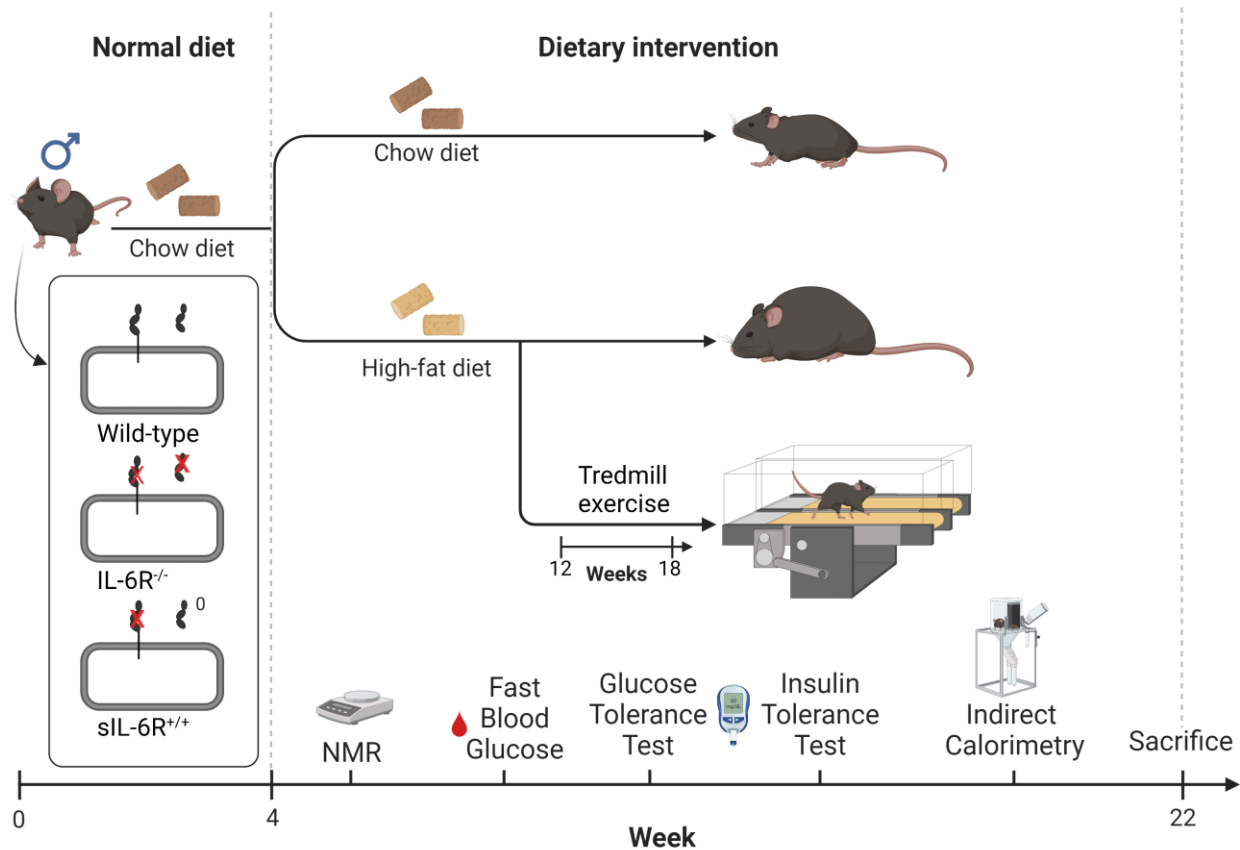
The biggest advantage of the cytokimera is essentially its specificity, since, in the case of IC7, it can exert its function only in cells expressing gp130, IL-6R, and LIFR, rather than being active after binding IL-6R and gp130, in the case of IL-6, or CNTFR, LIFR, and gp130, in the case of CNTF.

The aim is to overcome the central problem of pronounced pro-inflammatory response that follows IL-6 therapeutic administration and the production of neutralizing antibodies after CNTF usage in patients (Ettinger, Littlejohn et al. 2003).

Notably, the use of IC7 in preclinical research on mice has demonstrated anti-diabetogenic effects, enhanced glucose tolerance, and weight loss prevention (Findeisen, Allen et al. 2019).

Certainly, the cytokimeras set up a novel approach that encourages greater research for potential therapeutic applications.

2. Interleukin 6 receptor is not directly involved in regulation of body weight in diet-induced obesity with and without physical exercise.



Status: published, Front Endocrinol (Lausanne), 2022 Oct 27; 13:1028808.

doi: 10.3389/fendo.2022.1028808.

Impact factor: 6.055

Contribution: 80%

Designed and conducted all the experiments, entirely written and drafted the manuscript, as well as prepared and illustrated all the figures.



OPEN ACCESS

EDITED BY
Rosalia Rodriguez-Rodriguez,
International University of Catalonia,
Spain

REVIEWED BY
Karim Bouzakri,
Université de Strasbourg,
France
Ildiko Szanto,
Hôpitaux universitaires de Genève
(HUG), Switzerland

*CORRESPONDENCE
Jürgen Scheller
jscheller@uni-duesseldorf.de

SPECIALTY SECTION
This article was submitted to
Obesity,
a section of the journal
Frontiers in Endocrinology

RECEIVED 26 August 2022
ACCEPTED 04 October 2022
PUBLISHED 27 October 2022

CITATION
Minafra AR, Chadt A, Rafii P,
Al-Hasani H, Behnke K and Scheller J
(2022) Interleukin 6 receptor is not
directly involved in regulation of body
weight in diet-induced obesity with
and without physical exercise.
Front. Endocrinol. 13:1028808.
doi: 10.3389/fendo.2022.1028808

COPYRIGHT
© 2022 Minafra, Chadt, Rafii, Al-Hasani,
Behnke and Scheller. This is an open-
access article distributed under the
terms of the [Creative Commons
Attribution License \(CC BY\)](#). The use,
distribution or reproduction in other
forums is permitted, provided the
original author(s) and the copyright
owner(s) are credited and that the
original publication in this journal is
cited, in accordance with accepted
academic practice. No use,
distribution or reproduction is
permitted which does not comply with
these terms.

Interleukin 6 receptor is not directly involved in regulation of body weight in diet-induced obesity with and without physical exercise

Anna Rita Minafra¹, Alexandra Chadt^{2,3}, Puyan Rafii¹,
Hadi Al-Hasani^{2,3}, Kristina Behnke¹ and Jürgen Scheller^{1*}

¹Institute of Biochemistry and Molecular Biology II, Medical Faculty, Heinrich-Heine-University, Düsseldorf, Germany, ²Institute for Clinical Biochemistry and Pathobiochemistry, German Diabetes Center, Medical Faculty, Heinrich-Heine-University, Düsseldorf, Germany, ³German Center for Diabetes Research Deutsches Zentrum für Diabetesforschung e.V. (DZD), Partner Düsseldorf, München, Neuherberg, Germany

High level of interleukin 6 (IL-6), released by adipocytes in an obesity-induced, low grade inflammation state, is a regulator of insulin resistance and glucose tolerance. IL-6 has also regenerative, anti-inflammatory and anti-diabetogenic functions, when secreted as myokine by skeletal muscles during physical exercise. IL-6 mainly activates cells via two different receptor constellations: classic and trans-signalling, in which IL-6 initially binds to membrane-bound receptor (IL-6R) or soluble IL-6 receptor (sIL-6R) before activating signal transducing gp130 receptor. Previously, we generated transgenic soluble IL-6 receptor ^{+/+} (sIL-6R^{+/+}) mice with a strategy that mimics ADAM10/17 hyperactivation, reflecting a situation in which only IL-6 trans-signalling is active, whereas classic signalling is completely abrogated. In this study, we metabolically phenotyped IL-6R deficient mice (IL-6R-KO), sIL-6R^{+/+} mice and wild-type littermates fed either a standard chow (SD) or a high-fat diet (HFD) in combination with a 6-weeks treadmill exercise protocol. All mice were subjected to analyses of body weight and body composition, determination of blood glucose and insulin level under fasting conditions, as well as determination of substrate preference by indirect calorimetry. Neither classic IL-6 nor trans-signalling do influence the outcome of diet-induced obesity, insulin sensitivity and glycaemic control. Furthermore, IL-6R deficiency is not impairing the beneficial effect of physical exercise. We conclude that the IL-6R does not play a requisite role in regulation of body weight and glucose metabolism in diet-induced obese mice.

KEYWORDS

interleukin 6 (IL-6), obesity, exercise, diet, mouse model

Introduction

In the last two decades, obesity has been described not only as elevated amount of fat cells caused by excess of nutrients and a low degree of physical inactivity, but also associated with an inflammatory state. The transition from healthy lean to obese adipose tissue is accompanied by a chronic low-grade inflammation and immune dysregulation, as well as the enhanced release of pro-inflammatory cytokines, which can consequently interfere with peripheral insulin signalling and glucose metabolism. Among others, IL-6 has been frequently associated with the impaired immune control in obese adipose tissue (1).

Among several studies, Wallenius et al. showed that mice lacking IL-6 developed mature-onset obesity, associated with a disturbed carbohydrate and lipid metabolism (2). These data were subsequently supported by Matthews et al., who observed increased body weight, impaired glucose tolerance and exacerbated insulin resistance in IL-6 KO mice (3). Moreover, enhanced inflammation in liver and skeletal muscles and insulin resistance was observed in hepatocyte-specific IL-6R deficient animals (4), as well as increased insulin resistance in whole-body IL-6 KO mice (5) and increased body weight in astrocyte-specific IL-6 deficient mice (6). In contrast, adipocyte-specific deletion of IL-6 in the context of diet-induced and genetic obesity had no effect on body weight and fat content, glucose tolerance and insulin resistance (7) or, in another study, it determined slightly reduced high fat diet (HFD)-induced glucose intolerance (8).

Taken together, it is still unclear whether IL-6 is a primary trigger for the development of obesity and insulin resistance or whether it is actually required to counteract the increased inflammation associated with obesity. Additionally, this intricate scenario is complicated further by the observed beneficial effect of IL-6 produced by skeletal muscles following physical exercise.

Indeed, during intense exercise, both IL-6 mRNA and protein levels increase in skeletal muscles (9, 10) and plasma IL-6 rises up to 100-fold (11). In addition, there are many lines of evidence that IL-6 has also regenerative effects, transiently downregulates immune function and can actually protect from obesity and insulin resistance. Indeed, during physical exercise, IL-6 promotes blood glucose disposal and blood glucose uptake in skeletal muscles by stimulating cell surface glucose transporter 4 (GLUT4) translocation in muscle cells (1). In addition, it may increase fatty acid uptake, lipolysis and free fatty acids release from adipocytes and skeletal muscles, respectively (12, 13). Moreover, IL-6 has been shown to stimulate pancreatic insulin production and insulin sensitivity in peripheral tissues, including skeletal muscle and adipose tissue, together with enhancing skeletal muscle hypertrophy and bone remodelling (14).

Mechanistically, two main signalling pathways can be activated by IL-6. In the classic signalling pathway, IL-6 binds to its membrane-bound receptor (IL-6R), followed by

dimerization of glycoprotein 130 (gp130) and activation of JAK/STAT, MAPK, and PI3K/AKT (15). In the *trans*-signalling pathway, IL-6 can bind soluble IL-6 receptor (sIL-6R) molecules which are generated *via* ectodomain shedding by metalloproteases (ADAM-10 and ADAM-17) (16) or through alternative splicing of IL-6R mRNA (17).

Of note, activation of classic IL-6 signalling is limited to specific tissues, since IL-6R is only expressed in distinct cell types, such as immune cells and hepatocytes. Some studies suggest that IL-6R might be expressed also in adipocytes and myocytes (18–20). Thus, it is not yet clear whether metabolic functions of IL-6 mainly rely on classic or *trans*-signalling. Accordingly, here, we metabolically characterized the previously generated IL-6 *trans*-signalling mice, which were genetically engineered to execute IL-6 *trans*-signalling, with a strategy that mimics ADAM10/17 hyperactivation generated by Cre-mediated deletion of the genetic information coding for the transmembrane and intracellular domain of the IL-6R. Due to this lack, IL-6R is directly secreted as soluble IL-6R. Consequently, these mice selectively execute *trans*-signalling, whereas classic signalling is abrogated (21).

Here, we analyzed IL-6R deficient mice in diet-induced obesity and physical exercise. Albeit also IL-6 deficient mice have shown contradictory results, IL-6R deficient mice phenotypically strongly deviate from IL-6 deficient mice in wound healing (22) but not in liver regeneration (21). We were, therefore, interested if IL-6R deficient mice phenocopy IL-6 deficient mice in diet-induced obesity. Furthermore, we hypothesize that IL-6 *trans*-signalling is mainly involved in glucose metabolism regulation in diet-induced obesity and may be affected by physical activity, while classic signalling is linked to a homeostatic regulation.

Results

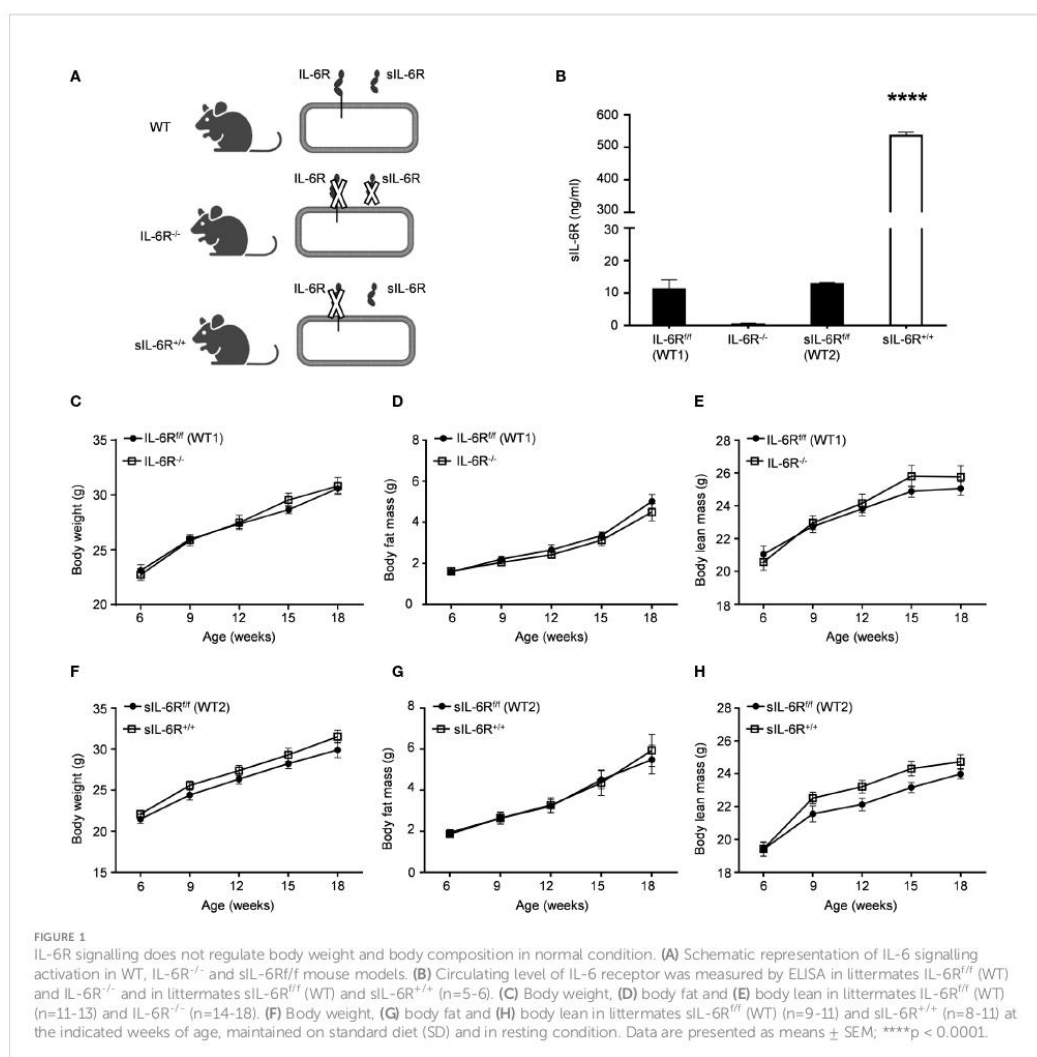
Specific activation of IL-6 *trans*-signalling and deficiency of classic and *trans*-signalling does not influence body composition of mice under standard diet

We first generated transgenic *soluble* IL-6R^{+/+} (sIL-6R^{+/+}) mice, as previously described (21). Shortly, in these mice, the endogenous hyper-activation of ADAM10/17 is mimicked by Cre-mediated deletion of the genetic information coding for the transmembrane and intracellular domain of the IL-6R, reflecting a situation in which only *trans*-signalling is active, whereas classic signalling is abrogated. According to this mouse model, membrane-bound IL-6R is entirely converted into soluble IL-6R (sIL-6R) allowing only endogenous IL-6 *trans*-signalling. To endorse our model, we initially tested the plasma level of sIL-6R, using wild-type (WT) littermate controls and a mouse model with complete deficiency of IL-6R (IL-6R-KO), where both IL-6

trans and classic signalling are abrogated (Figure 1A). As expected, the circulating level of sIL-6R was increased in sIL-6R^{+/+} mice (approximately 536 ng/ml) and completely absent in IL-6R deficient mice in comparison to the strain control mice with 12.8 ng/ml for sIL-6R^{+/+} (wild-type 1 for sIL-6R^{+/+}) and 11.2 ng/ml for IL-6R^{+/+} (wild-type 2 for IL-6R^{+/+}) (Figure 1B).

We monitored body composition in resting condition and under standard diet (SD) in IL-6 trans-signalling mice, IL-6R deficient mice and the appropriate wild-type littermates. After 18 weeks, we did not observe any differences in body weight, body fat and lean mass due to different genotypes but a similar progressive tendency throughout the 12 weeks (Figures 1C-H). Next, we

tested the effect of sIL-6R over-expression and IL-6R deficiency on glucose and insulin tolerance under standard diet by intraperitoneal glucose tolerance test after 16 h fasting at 12 weeks and at older age of 20 weeks. There was no detectable variation in glucose disposal related to different IL-6 signalling activation (Figures 2A-H). We also measured blood glucose levels following an insulin injection for 15, 30, and 60 minutes, with no differences observed for the different genotypes in insulin sensitivity (Figures 2I-L). In summary, we did not observe any influence of specific activation of IL-6 trans-signalling and deficiency of IL-6R classic and trans-signalling on body weight gain, glucose and insulin tolerance following standard diet.



IL-6R signalling does not regulate basal metabolism in resting conditions

In human and animal trials, indirect calorimetry is frequently used to assess the total energy expenditure together with the respiratory exchange ratio (RER), calculated as ratio between O_2 and CO_2 consumption, index of glucose, protein or fat oxidation as a fuel source (23). We therefore tested the basal metabolic capacity in sIL-6R^{+/+} and IL-6R deficient mice. As expected, we noticed a slight increase of RER during the dark phase, index of a metabolic shift towards glucose oxidation (Figures 3A–D). Despite a decreased respiratory quotient in sIL-6R^{+/+} in comparison to WT mice in both light and dark phases, no correlation with different genotypes was statistically significant. Whole carbohydrate oxidation rates were partially elevated while fatty acids oxidation rates were moderately reduced in appropriate WT controls compared to IL-6R deficient and sIL-6R^{+/+} mice, but the differences were not statistically significant (Figures 3B, C, E, F). Whole carbohydrates and fatty acids oxidation rate were calculated as previously described (24). From these data we conclude that nor IL-6 classic or trans-signalling is influencing the basal metabolism under resting conditions.

Diet-induced obesity and treadmill exercise does not induce changes in body composition in sIL-6R^{+/+} and IL-6R deficient mice

It has been shown that IL-6 has an important role in obesity and insulin resistance but also is cardinal in driving the beneficial effects of physical exercise in glucose and insulin sensitivity as well as body composition (1). Therefore, sIL-6R trans-signalling mice, IL-6R deficient mice and appropriate wild-type mice were fed with high fat diet (HFD) starting from week 4 until week 18 including a treadmill protocol after 9 weeks of high fat diet for the total duration of 6 weeks, 5 days per week. HFD feeding determined an increase in body weight and changes in body composition trajectory in comparison to SD. A similar trend was observed in body weight and body composition before starting the treadmill training. After 6 weeks of training, a significant increase of body weight was observed in appropriate WT mice compared to trained WT and IL-6R deficient mice, due to beneficial effect of exercise, but no differences were attributable to different genotype (Figure 4A). After training, we observed a reduction in body fat mass but not in lean mass (Figures 4B, C). We did not observe any significant change in body weight, body fat and lean mass in sIL-6R^{+/+} and control mice after training (Figures 4D–F). Taken together, no differences in energy metabolism due to IL-6R genotype were underlined following high-fat diet and physical exercise.

IL-6 signalling does not rescue HFD-induced hyperglycaemia before and after training

IL-6 signalling has been reported to be involved not only in regulation of weight loss but also in improved glucose and insulin sensitivity induced by physical activity (14). Considering that, fasting blood glucose was measured at the beginning of the HFD at 4 weeks and no variations between genotypes were observed (Figures 5A, B). We repeated the same experiments at the beginning of the training at 12 weeks and similarly glucose level was not impaired (Figures 5C, D). HFD led to an increased blood glucose level after intraperitoneal glucose tolerance test measured at 11-week-old before training compared to SD-fed mice but no significant differences were observed between the genotypes (Figures 5E–H).

To test whether exercise training has any impact, equally, glucose in addition to insulin tolerance was determined in high-fat diet-fed and trained sIL-6R^{+/+} and IL-6 deficient mice and littermate controls. Physical exercise significantly improved glucose tolerance in IL-6R littermate WT mice but only slightly in IL-6 deficient mice (Figures 5I, J), while no differences were observed between sIL-6R^{+/+} and littermate control mice (Figures 5K, L). Likewise, insulin tolerance after treadmill training in IL-6R deficient and sIL-6R^{+/+} mice was comparable to the sedentary group (Figures 5M–P).

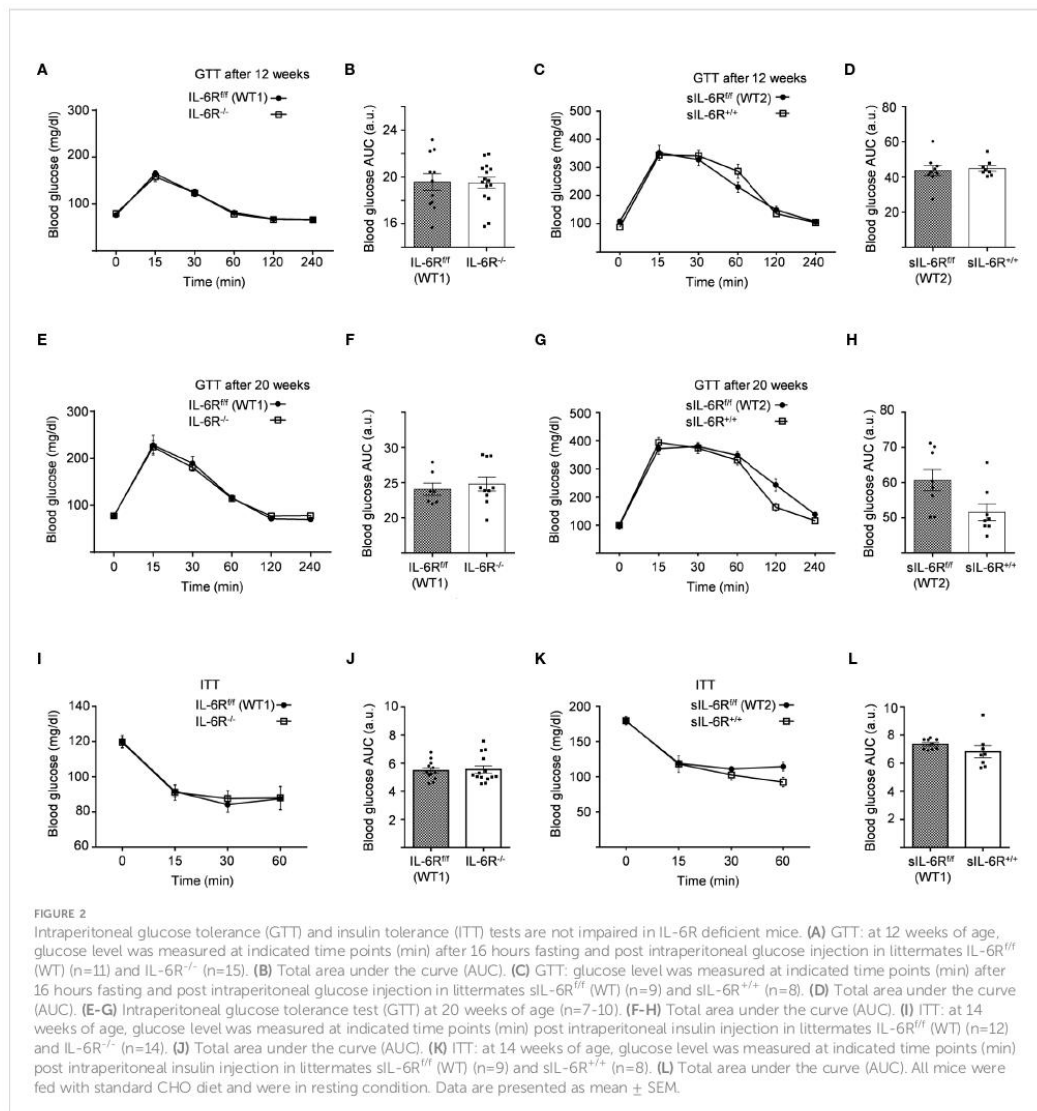
In brief, lack of membrane-bound and soluble IL-6R did not regulate fast blood glucose level following 8 weeks of high-fat diet and did not influence glucose and insulin tolerance tests during high-fat diet and after physical exercise.

IL-6 signalling does not influence basal metabolism in HFD-fed mice before and after training

To better understand the consequences of high-fat diet as well as the impact of physical exercise on the whole-body metabolism in sIL-6R^{+/+} and IL-6 deficient mice, we assessed substrate utilization and whole-body carbohydrate and fatty acid oxidation rate two weeks before the start of the treadmill training and after 4 weeks of exercise.

We found that substrate utilization was not influenced by physical exercise and was not different between sIL-6R^{+/+} and IL-6R deficient mice and respective WT mice (Figures 6A, D, G, H, K, L). Based on our results shown in Figures 6B, C, E, F, I, J, M, N, IL-6R signalling did not regulate the whole-body carbohydrate and fatty acid oxidation and they are not significantly influenced by exercise.

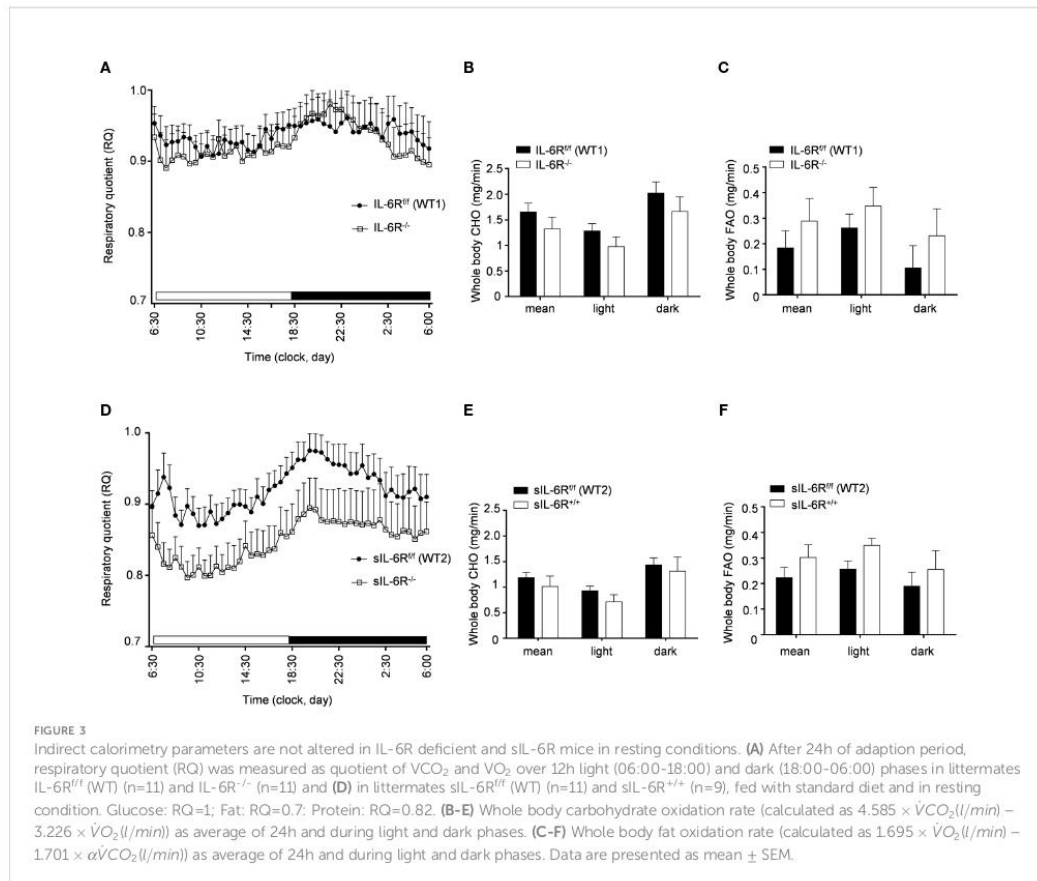
In conclusion, the respiratory quotient and the carbohydrate and fatty acid basal metabolism are not changed in high-fat diet fed IL-6R deficient mice and following treadmill training.



Discussion

Using IL-6R deficient and sIL-6R^{+/-} trans-signalling mice, we analysed the specific role of IL-6 classic and trans-signalling in diet-induced obesity and physical exercise. In contrast to previous studies, mainly centred around IL-6 KO mouse models, our data suggested that both classic and trans-signalling have no considerable impact on body weight increase and distorted glucose metabolism following standard CHO diet and/or high-fat diet. Interestingly, sIL-6R^{+/-} mice showed modest increase in

body weight in comparison to controls under CHO diet, majorly attributable to enhanced body lean mass; this phenomenon could be partially due to the observed gain of fatty acid utilization during light and dark periods that could explain the lack of increase in adipose tissue. Moreover, we did not observe any impaired blood glucose level after 9 weeks of HFD in IL-6R deficient mice and respective wild-type control. Lastly, deficiency of IL-6R did not critically regulate the beneficial effects of physical exercise on body weight, body composition, glucose and insulin tolerance, as well as basal metabolism.

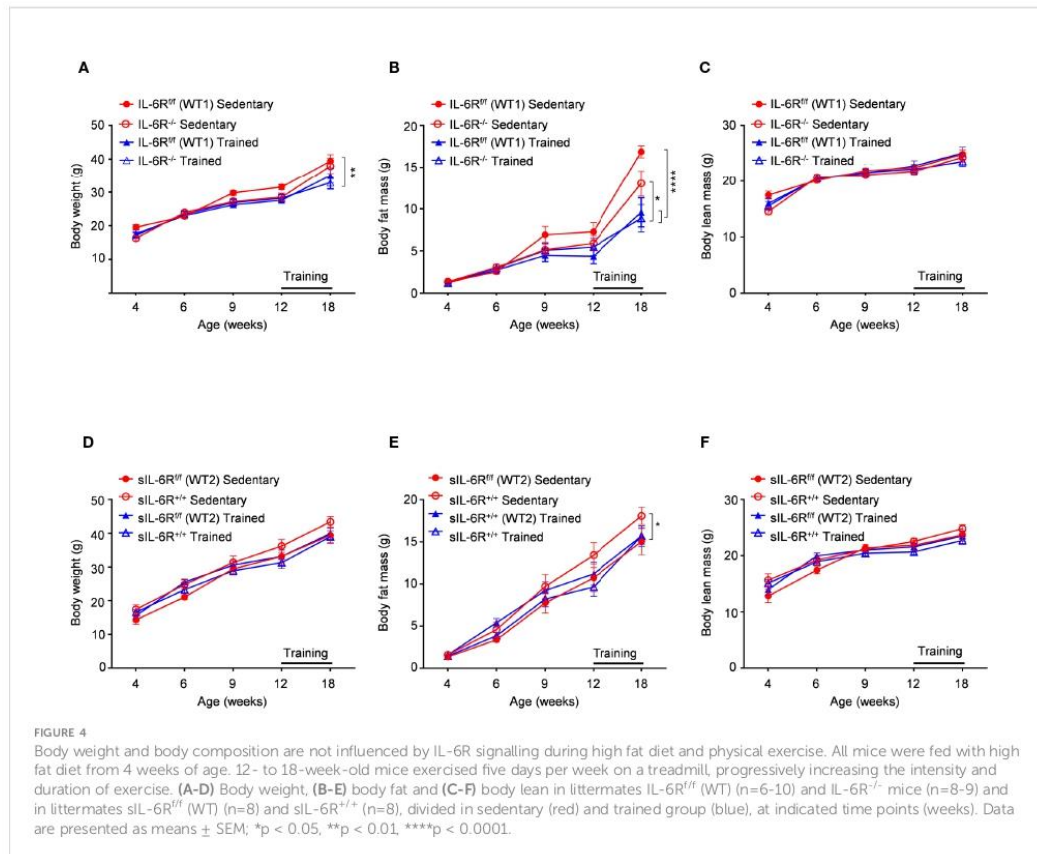


For the first time in the context of obesity, we characterized the sIL-6R^{+/+} mouse model (21), an approach to simulate ADAM10/17 hyperactivation for the specific target protein IL-6R by a Cre-mediated deletion of the genetic sequence coding for transmembrane and intracellular domains that consequently lead to specific trans-signalling execution. This is a unique system to study solely the IL-6 trans-signalling, without the classic signalling activation, during patho-physiological conditions, including, in our case, obesity associated with insulin signalling and glucose metabolism distortion, as well as physical exercise. Based on our data, following high-fat diet, circulating sIL-6R is increased up to 48-fold in sIL-6R^{+/+} mice compared to appropriate littermate controls, suggesting that our model specifically executes trans-signalling and abrogates classic signalling. To support our statement, we have shown that mRNA levels of IL-6R in sIL-6R^{fl/fl} and IL-6R^{fl/fl} were comparable to wild-type mice while a significant increase was detected in sIL-6R^{+/+}, and immunochemistry data additionally highlighted IL-6R being detectable in wild-type but not in IL-6R

deficient and sIL-6R^{+/+} mice, demonstrating how membrane-bound IL-6R is being converted to sIL-6R and rapidly secreted (21). Collectively, this explains the notable increase of sIL-6R levels in our mouse model.

The present study was designed to clarify whether IL-6R deficient mice phenocopy the IL-6 deficient mice in diet-induced obesity and physical exercise exposure. The majority of studies linked IL-6 deficiency to development of obesity, glucose intolerance and insulin resistance, such as Wallenius et al., who indicated IL-6 KO mice to developed mature-onset obesity and insulin resistance (2), although a few years later Di Gregorio et al. reported no differences in obesity in 8 months old mice and after 3 months of high-fat diet (25).

Remarkably, our data did not show a similar phenotype between IL-6 KO and IL-6 receptor KO mice, since we did not observe any increase in body weight, changes in body composition or alterations of glucose and insulin sensibility or variations in basal metabolism, e.g. indirect calorimetry measurements. A similar scenario has been observed by McFarland-Mancini et al., where



mice lacking IL-6R showed different phenotype compared to IL-6-deficient mice in delayed wound healing process, despite some similarities in inflammatory deficits (22). Of note, in this study, the combined deficiency of IL-6 and IL-6R had the similar phenotype than IL-6R. Although we did not provide comparative data for IL-6 KO, due to the high number of studies already reported in literature, we speculate that IL-6R KO plays a minor role in development of the phenotypes compared to IL-6 KO. On this basis, a plausible explanation of our adverse results could be a previously unidentified function of IL-6R that does not involve IL-6 but other cytokines or receptors. This would highlight the feasibility of the hypothesis previously formulated by McFarland-Mancini et al. that IL-6 might execute its function binding to a different receptor. Furthermore, one cannot exclude a compensatory mechanism that involves other cytokines, belonging to the IL-6 family. For instance, Schuster et al. revealed that human CNTF as well can bind and activate signalling via IL-6R, although with an affinity 50-fold inferior to IL-6 (26).

Another important factor to be considered is the genetic background differences that could affect the results. There are many examples of how genetic background could cause opposite

effects on metabolism, for instances different murine strains have opposing effects on muscle and liver insulin sensitivity (27). It cannot be excluded that there are additional genetic variations into the mouse lines, diverse breeding strategies, divergent use of control animals (littermates or general WT), different age, as well as different methodology, environmental or dietary factors that could play a key role in causing variances between the studies. Notably, we observed surprising differences between the two control strains IL-6R^{fl/fl} and sIL-6R^{fl/fl} with respect to body weight and body composition, as well as blood glucose levels and RQ, equally in standard condition and after high-fat diet and physical exercise, independent of IL-6R genotype, with the same C57/BL6 background and identical experimental techniques. This underlines the importance of comparing the results with littermate controls rather than universal WT mice.

Together with genotype and environmental factors, an additional variable that could influence the different pathophysiology of obesity in different mice lines is the gut microbiota. It has been shown that diet-induced obese mice have different amounts of the two dominant bacterial divisions, the Bacteroidetes and the Firmicutes, and this affects the metabolic

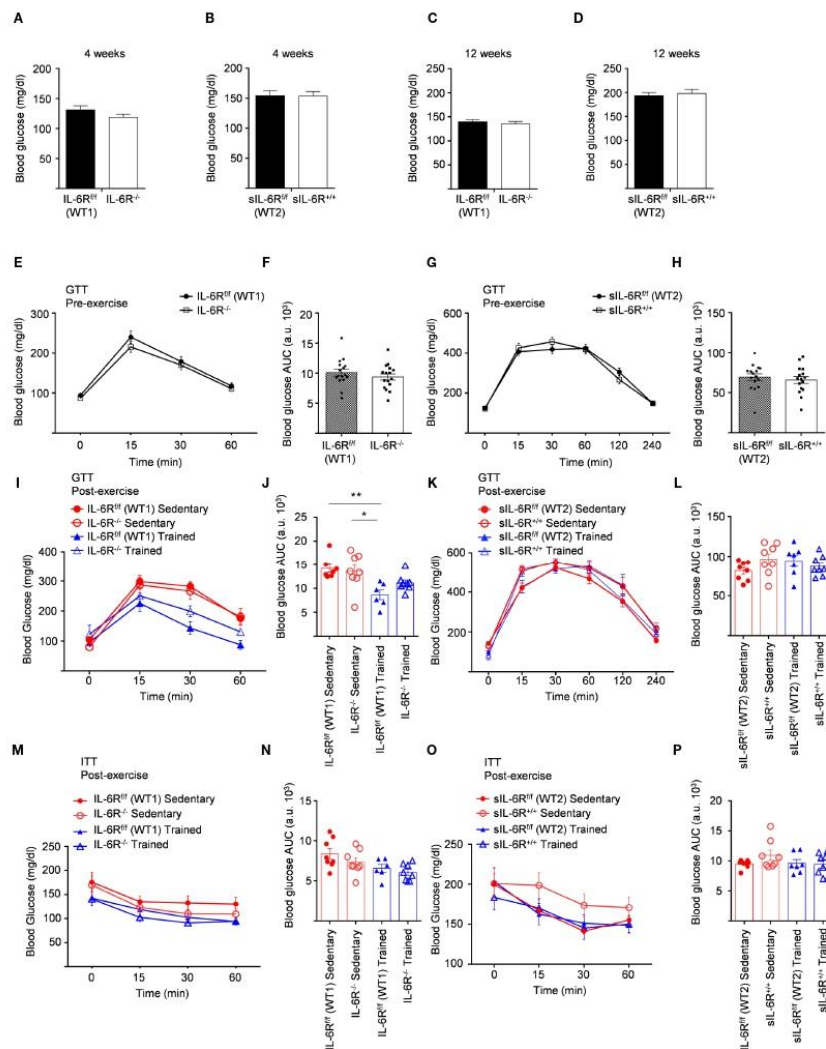
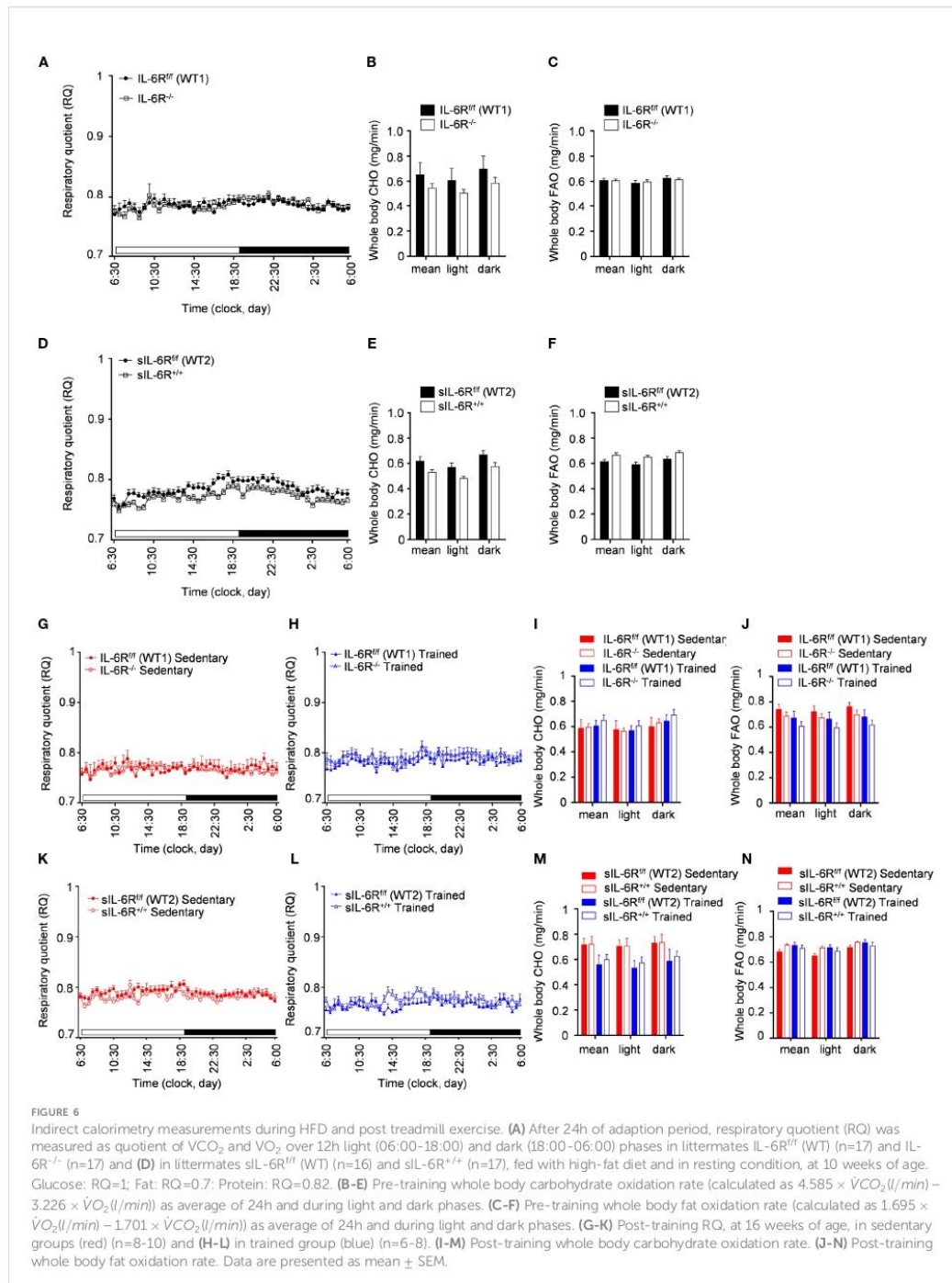


FIGURE 5

Unimpaired glucose and insulin tolerance in sIL-6R^{+/±} and IL-6R-KO mice following high fat diet and treadmill exercise. All mice were fed with high fat diet from 4 weeks of age. 12- to 18-week-old mice exercised five days per week on a treadmill, progressively increasing the intensity and duration of exercise. (A) FBG: fast blood glucose level was measured at 4 weeks of age in littermates IL-6R^{fl/fl} (WT) (n=11) and IL-6R^{-/-} (n=16) and (B) in littermates sIL-6R^{fl/fl} (WT) (n=16) and sIL-6R^{-/-} (n=16). (C, D) FBG at 12 weeks of age, after 8 weeks of high-fat diet (HFD) (n=15-16). (E-I) GTT: blood glucose level was measured pre and post training at indicated time points (min) after 16 hours fasting and post intraperitoneal glucose injection in littermates IL-6R^{fl/fl} (WT) and IL-6R^{-/-} (pre-training: n=16 WT and n=16 KO; post-training: n=7 WT and n=8 KO sedentary (red) and n=6 WT and n=8 KO trained (blue)). (F-L) Total area under the curve (AUC). (G-K) GTT in littermates sIL-6R^{fl/fl} (WT) and sIL-6R^{-/-} (pre-training: n=16 WT and n=16 sIL-6R^{+/±}; post-training: n=8 WT and n=8 sIL-6R^{+/±} sedentary (red) and n=8 WT and n=8 sIL-6R^{+/±} trained (blue)). (H-L) Total area under the curve (AUC). (M-O) ITT: at 15 weeks of age, blood glucose level was measured at indicated time points (min) post intraperitoneal insulin injection in littermates IL-6R^{fl/fl} (WT) and IL-6R^{-/-} (sedentary (red): n=8 WT and n=8 sIL-6R^{+/±}; trained (blue): n=6 WT and n=8 sIL-6R^{+/±}) and in littermates sIL-6R^{fl/fl} (WT) and sIL-6R^{-/-} (sedentary (red): n=8 WT and n=8 sIL-6R^{+/±}; trained (blue): n=7 WT and n=8 sIL-6R^{+/±}). (N-P) Total area under the curve (AUC). Data are presented as mean ± SEM. *p < 0.05, **p < 0.01.



profile, leading to increased capacity for dietary energy harvest and higher body fat contents (28).

In summary, nor membrane-bound IL-6R and/or sIL-6R seems to be involved in regulating glucose and insulin metabolism in diet-induced obesity, although previous reports defined IL-6 as the major trigger of inflammation in adipose tissue in obese conditions and consequent glucose and insulin intolerance in peripheral tissues. Our results add new crucial information to what is the already known as the complex scenario related to the role of IL-6 signalling in the above mentioned mechanisms. This paves the way to address new questions that need further investigations regarding a plausible novel mechanism of IL-6R in adipocytes and skeletal muscles.

Material and methods

Animals

All experiments were approved by the Ethics Committee of the State Office for Nature, Environment and Consumer Protection NRW (LANUV, North Rhine-Westphalia, Germany – 84-02.04.2020.A278) and conducted at the animal facility of the German Diabetes Center. Unless otherwise specified, three to six mice per cage were housed at 22°C with a 12-hour light–dark cycle and free access to food and water. Following weaning, male animals were fed a regular chow diet (Ssniff, Soest, Germany, 11% Fat) or fed with high fat diet (HFD, Research diet, rodent, 60 kcal% Fat) from the age of 4 weeks and used for experiments from the age of 4 to 21 weeks.

Floxed sIL-6R and global sIL-6R^{+/+} mice were generated as previously described (21). IL-6R^{-/-} mice (22) were obtained from the Heinrich-Heine University of Düsseldorf's animal facility ZETT – Zentrale Einrichtung für Tierforschung und wiss. Tierschutzaufgaben.

Analysis of body weight and body composition

Body weight was measured every 2–3 weeks with an electronic scale (Sartorius), and body composition (body fat and lean mass) was determined by a nuclear magnetic resonance spectrometer (Bruker-Minispac NMR-Analyzer mq10; Bruker Optics).

Fast blood glucose tolerance test

Mice fasted for 6 h before the experiments. Fast blood glucose level was measured from the tail tip. This experiment has been performed at the age of 4 weeks and 12 weeks.

Intraperitoneal glucose tolerance test

Mice were fasted for 16 h before the experiment and subsequently were injected intraperitoneally with sterile glucose (2 g/kg body weight, 20% solution, 10 µL/g). Basal blood glucose was determined at the tail tip at 0, 15, 30, 60, 120 and 240 minutes after injection. This experiment has been performed at the age of 12 and 20 weeks, under CHO-diet, and at the age of 11 weeks (pre-exercise) and 17 weeks (post-exercise), under high fat diet.

Intraperitoneal insulin tolerance test

Subsequently to blood glucose level measurement from the tail tip, mice were injected intraperitoneally with 10 µL/g insulin (Actrapid, Novo Nordisk, 100 U/ml). Basal blood glucose was determined from the tail tip at 0, 15, 30 and 60 min after injection.

Indirect calorimetry

After a 24-hour adaption period, the respiratory quotient (RQ) of the animals was assessed using indirect calorimetry (Hartmann & Braun). The flow rate was 0.5 L/min, and the rates of oxygen consumption (VO₂) and carbon dioxide production (VCO₂) were measured at 22°C for 23 h. Water and food were freely available to the animals. The RQ is the quotient of VCO₂/VO₂. The following formulae were used to compute whole-body carbohydrate and fat oxidation rates (g/min): *carbohydrate oxidation rate* = $4.585 \times \dot{V}CO_2(l/min) - 3.226 \times \dot{VO}_2(l/min)$; *fat oxidation rate* = $1.695 \times \dot{VO}_2(l/min) - 1.701 \times \dot{VCO}_2(l/min)$ (24).

ELISA quantification of sIL-6R in serum

To quantify mouse serum sIL-6R, the enzyme-linked immunosorbent assay (Mouse IL-6Ra DuoSet, cat. #DY1830, R&D Systems, Minneapolis, MN, USA) was used. Microtitre plates (Nunc maxi sorb, Sigma Aldrich, Munich, Germany) were incubated overnight with goat anti-mouse IL-6R capture antibody diluted in PBS (R&D Systems, 1.6 g/ml working concentration). After overnight incubation, the plates have been washed three times with 300 µL washing buffer (R&D Systems, cat. #WA12) prior blocking with 300 µL of PBS with 1% BSA for 1 h at RT. Subsequently, diluted serum samples from sIL-6R^{fl/fl}, sIL-6R^{+/+}, IL-6R^{-/-} mice and wt littermates were added (100 µL/well) and incubate for 2 h at RT. Plates were washed three times and biotinylated goat anti-mouse IL-6R mAbs (R&D Systems) were used to identify bound sIL-6R.

Exercise

Mice aged 12 to 18 weeks ran on a treadmill 5 days a week for 6 weeks. The treadmill program was designed to gradually increase the intensity and duration of exercise, beginning with a warm-up and 10 m/min for 20 minutes totally (0° inclination) and progressing to 15–22 m/min for a total of 60 min of training with a 10° inclination.

Statistics

Data are described as means \pm SEMs. Significant differences were determined using one-way ANOVA, as indicated in the figure legends. P value <0.05 were considered statistically significant.

Data availability statement

The raw data supporting the conclusions of this article will be made available by the authors, without undue reservation.

Ethics statement

All experiments were approved by the Ethics Committee of the State Office for Nature, Environment and Consumer Protection NRW (LANUV, North Rhine-Westphalia, Germany – 84-02.04.2020.A278) and conducted at the animal facility of the German Diabetes Center.

Author contributions

ARM. carried out the experiments and wrote the manuscript with support from JS. JS conceived the original idea and supervised the project. PR helped with mouse experiments and

contributed to the project discussion. AC and HA-H helped in supervising the project. KB contributed to preparation of animal documentation. All authors provided constructive criticism and contributed to the development of the study. All authors contributed to the article and approved the submitted version.

Funding

Funded by the Deutsche Forschungsgemeinschaft, Graduiertenkolleg VIVID.

Acknowledgments

The authors thank RTG 2576 “Vivid- *In vivo* investigations towards the early development of type 2 diabetes” for funding this project. We thank Lena Espelage, Anna Schedl, Carina Heitmann and Birgit Knobloch for technical assistance.

Conflict of interest

The authors declare that the research was conducted in the absence of any commercial or financial relationships that could be construed as a potential conflict of interest.

Publisher's note

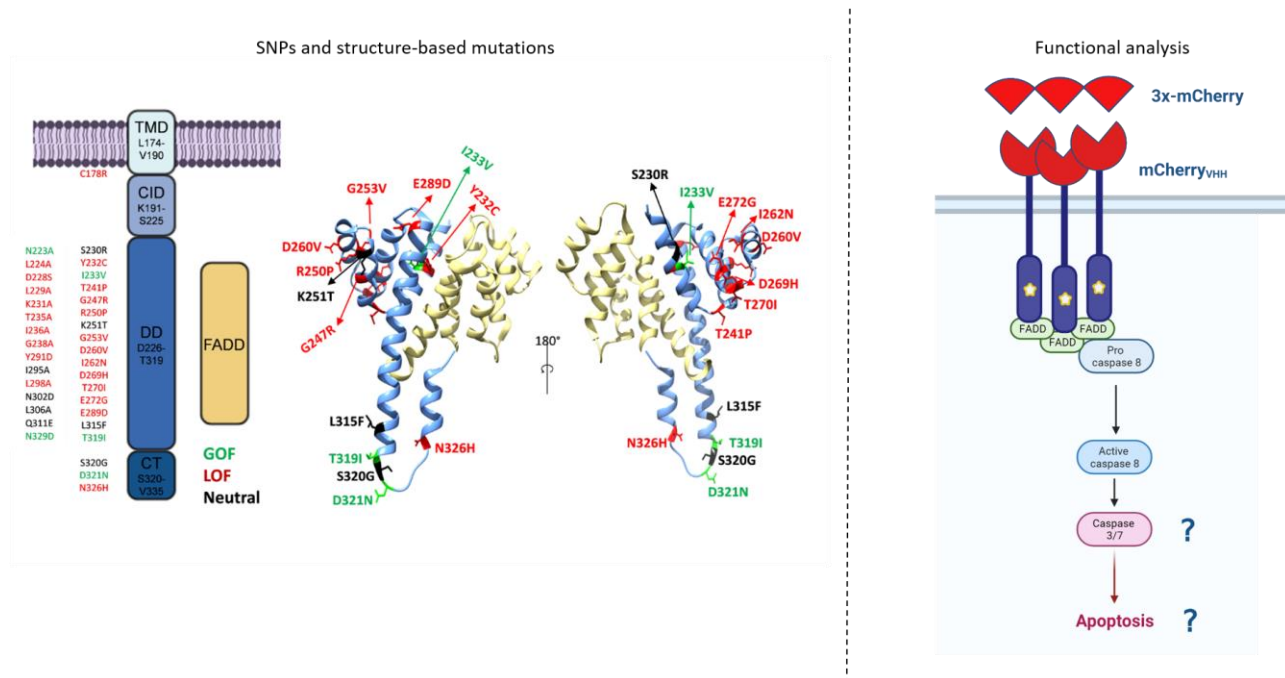
All claims expressed in this article are solely those of the authors and do not necessarily represent those of their affiliated organizations, or those of the publisher, the editors and the reviewers. Any product that may be evaluated in this article, or claim that may be made by its manufacturer, is not guaranteed or endorsed by the publisher.

References

1. Pal M, Febbraio MA, Whitham M. From cytokine to myokine: the emerging role of interleukin-6 in metabolic regulation. *Immunol Cell Biol* (2014) 92(4):331–9. doi: 10.1038/icb.2014.16
2. Wallenius V, Wallenius K, Ahrén B, Rudling M, Carlsten H, Dickson SL, et al. Interleukin-6-deficient mice develop mature-onset obesity. *Nat Med* (2002) 8(1):75–9. doi: 10.1038/nm0102-75
3. Matthews VB, Allen TL, Risis S, Chan MHS, Henstridge DC, Watson N, et al. Interleukin-6-deficient mice develop hepatic inflammation and systemic insulin resistance. *Diabetologia* (2010) 53(11):2431–41. doi: 10.1007/s00125-010-1865-y
4. Wunderlich FT, Ströhle P, Köner AC, Gruber S, Tovar S, Brönneke HS, et al. Interleukin-6 signaling in liver-parenchymal cells suppresses hepatic inflammation and improves systemic insulin action. *Cell Metab* (2010) 12(3):237–49. doi: 10.1016/j.cmet.2010.06.011
5. Wan Z, Ritchie I, Beaudoin MS, Castellani L, Chan CB, Wright DC, et al. IL-6 indirectly modulates the induction of glyceroneogenic enzymes in adipose tissue during exercise. *PLoS One* (2012) 7(7):e41719. doi: 10.1371/journal.pone.0041719
6. Quintana A, Erta M, Ferrer B, Comes G, Giral M, Hidalgo J, et al. Astrocyte-specific deficiency of interleukin-6 and its receptor reveal specific roles in survival, body weight and behavior. *Brain Behav Immun* (2013) 27:162–73. doi: 10.1016/j.bbi.2012.10.011
7. Whitham M, Pal M, Petzold T, Hjorth M, Egan CL, Brunner JS, et al. Adipocyte-specific deletion of IL-6 does not attenuate obesity-induced weight gain or glucose intolerance in mice. *Am J Physiol-Endocrinol Metab* (2019) 317(4):E597–604. doi: 10.1152/ajpendo.00206.2019
8. Han MS, White A, Perry RJ, Camporez JP, Hidalgo J, Shulman GI, et al. Regulation of adipose tissue inflammation by interleukin 6. *Proc Natl Acad Sci* (2020) 117(6):2751–60. doi: 10.1073/pnas.1920004117

9. Ostrowski K, Rohde T, Zacho M, Asp S, Pedersen BK. Evidence that interleukin-6 is produced in human skeletal muscle during prolonged running. *J Physiol* (1998) 508(3):949–53. doi: 10.1111/j.1469-7793.1998.949bp.x
10. Chan MH, Carey AL, Watt MJ, Febbraio MA. Cytokine gene expression in human skeletal muscle during concentric contraction: Evidence that IL-8, like IL-6, is influenced by glycogen availability. *Am J Physiology-Regul Integr Comp Physiol* (2004) 287(2):R322–7. doi: 10.1152/ajpregu.00030.2004
11. Steensberg A, Hall van G, Osada T, Sacchetti M, Saltin B, Pedersen BK, et al. Production of interleukin-6 in contracting human skeletal muscles can account for the exercise-induced increase in plasma interleukin-6. *J Physiol*. (2000).
12. Chowdhury S, Schulz L, Palmisano B, Singh P, Berger JM, Yadav VK, et al. Muscle-derived interleukin-6 increases exercise capacity by signaling in osteoblasts. *J Clin Invest* (2020) 130(6):2888–902. doi: 10.1172/JCI133572
13. Lukaszuk B, Bialuk I, Górski J, Zajackiewicz M, Winnicka MM, Chabowski A, et al. A single bout of exercise increases the expression of glucose but not fatty acid transporters in skeletal muscle of IL-6 KO mice. *Lipids* (2012) 47(8):763–72. doi: 10.1007/s11745-012-3678-x
14. Kistner TM, Pedersen BK, Lieberman DE. Interleukin 6 as an energy allocator in muscle tissue. *Nat Metab* (2022) 4(2):170–9. doi: 10.1038/s42255-022-00538-4
15. Garbers C, Hermanns HM, Schaper F, Müller-Newen G, Gröttinger J, Rose-John S, et al. Plasticity and cross-talk of interleukin 6-type cytokines. *Cytokine Growth Factor Rev* (2012) 23(3):85–97. doi: 10.1016/j.cytogfr.2012.04.001
16. Scheller J, Chalaris A, Schmidt-Arras D, Rose-John S. The pro- and anti-inflammatory properties of the cytokine interleukin-6. *Biochim Biophys Acta (BBA)-Mol Cell Res* (2011) 1813(5):878–88. doi: 10.1016/j.bbamcr.2011.01.034
17. Lust JA, Donovan KA, Kline MP, Greipp PR, Kyle RA, Maible NJ, et al. Isolation of an mRNA encoding a soluble form of the human interleukin-6 receptor. *Cytokine* (1992) 4(2):96–100. doi: 10.1016/1043-4666(92)90043-Q
18. Keller C, Steensberg A, Hansen AK, Fischer CP, Plomgaard P, Pedersen BK, et al. Effect of exercise, training, and glycogen availability on IL-6 receptor expression in human skeletal muscle. *J Appl Physiol* (2005) 99(6):2075–9. doi: 10.1152/japplphysiol.00590.2005
19. AlMuraikhi N, Alaskar H, Binhamdan S, Alotaibi A, Kassem M, Alfayez M. JAK2 inhibition by fedratinib reduces osteoblast differentiation and mineralisation of human mesenchymal stem cells. *Molecules* (2021) 26(3):606. doi: 10.3390/molecules26030606
20. Püth G, Bornstein SR, Gurniak M, Chrousos GP, Scherbaum WA, Hauner H, et al. Human breast adipocytes express interleukin-6 (IL-6) and its receptor system: Increased IL-6 production by β -adrenergic activation and effects of IL-6 on adipocyte function. *J Clin Endocrinol Metab* (2001) 86(5):2281–8. doi: 10.1210/jcem.86.5.7494
21. Fazel Modares N, Polz R, Haghighi F, Lamertz L, Behnke K, Zhuang Y, et al. IL-6 trans-signaling controls liver regeneration after partial hepatectomy. *Hepatology* (2019) 70(6):2075–91. doi: 10.1002/hep.30774
22. McFarland-Mancini MM, Funk HM, Paluch AM, Zhou M, Giridhar PV, Mercer CA, et al. Differences in wound healing in mice with deficiency of IL-6 versus IL-6 receptor. *J Immunol* (2010) 184(12):7219–28. doi: 10.4049/jimmunol.0901929
23. Arch J, Hislop D, Wang S, Speakman J. Some mathematical and technical issues in the measurement and interpretation of open-circuit indirect calorimetry in small animals. *Int J Obes* (2006) 30(9):1322–31. doi: 10.1038/sj.ijo.0803280
24. Chadt A, Immisch A, de Wendt C, Springer C, Zhou Z, Stermann T, et al. Deletion of both Rab-GTPase-activating proteins TBC1D1 and TBC1D4 in mice eliminates insulin- and AICAR-stimulated glucose transport. *Diabetes* (2015) 64(3):746–59. doi: 10.2337/db14-0368
25. Di Gregorio GB, Hensley L, Di Lu T, Ranganathan G, Kern PA. Lipid and carbohydrate metabolism in mice with a targeted mutation in the IL-6 gene: Absence of development of age-related obesity. *Am J Physiology-Endocrinol And Metab* (2004) 287(1):E182–7. doi: 10.1152/ajpendo.00189.2003
26. Schuster BR, Kovaleva M, Sun Y, Regenhart P, Matthews V, Gröttinger J, et al. Signaling of human ciliary neurotrophic factor (CNTF) revisited: The interleukin-6 receptor can serve as an α -receptor for CNTF. *J Biol Chem* (2003) 278(11):9528–35. doi: 10.1074/jbc.M210044200
27. Colombo C, Haluzik M, Cutson JJ, Dietz KR, Marcus-Samuels B, Vinson C, et al. Opposite effects of background genotype on muscle and liver insulin sensitivity of lipotrophic mice: Role of triglyceride clearance. *J Biol Chem* (2003) 278(6):3992–9. doi: 10.1074/jbc.M207665200
28. Turnbaugh PJ, Ley RE, Mahowald MA, Magrini V, Mardis ER, Gordon JJ, et al. An obesity-associated gut microbiome with increased capacity for energy harvest. *Nature* (2006) 444(7122):1027–31. doi: 10.1038/nature05414

3. Synthetic receptor platform to identify loss-of-function single nucleotide variants and designed mutants in the death receptor Fas/CD95.



Status: Published, Papers in Press, June 29, 2023; Journal of Biological Chemistry.

<https://doi.org/10.1016/j.jbc.2023.104989>

Impact factor: 5.48

Contribution: 80%

Designed and conducted all the experiments, entirely written and drafted the manuscript, as well as prepared and illustrated all the figures.



Synthetic receptor platform to identify loss-of-function single nucleotide variants and designed mutants in the death receptor Fas/CD95

Received for publication, December 21, 2022, and in revised form, May 17, 2023 Published, Papers in Press, June 29, 2023,

<https://doi.org/10.1016/j.jbc.2023.104989>

Anna Rita Minafra¹, Puyan Rafii¹, Sofie Mossner¹, Farhad Bazgir¹, Doreen M. Floss¹, Jens M. Moll^{1,2}, and Jürgen Scheller^{1,*}

From the ¹Institute of Biochemistry and Molecular Biology II, Medical Faculty, Heinrich-Heine-University, Düsseldorf, Germany;

²PROvendis GmbH, Muelheim an der Ruhr, Germany

Reviewed by members of the JBC Editorial Board. Edited by Peter Cresswell

Synthetic biology has emerged as a useful technology for studying cytokine signal transduction. Recently, we described fully synthetic cytokine receptors to phenocopy trimeric receptors such as the death receptor Fas/CD95. Using a nanobody as an extracellular-binding domain for mCherry fused to the natural receptor's transmembrane and intracellular domain, trimeric mCherry ligands were able to induce cell death. Among the 17,889 single nucleotide variants in the SNP database for Fas, 337 represent missense mutations that functionally remained largely uncharacterized. Here, we developed a workflow for the Fas synthetic cytokine receptor system to functionally characterize missense SNPs within the transmembrane and intracellular domain of Fas. To validate our system, we selected five functionally assigned loss-of-function (LOF) polymorphisms and included 15 additional unassigned SNPs. Moreover, based on structural data, 15 gain-of-function or LOF candidate mutations were additionally selected. All 35 nucleotide variants were functionally investigated through cellular proliferation, apoptosis and caspases 3 and 7 cleavage assays. Collectively, our results showed that 30 variants resulted in partial or complete LOF, while five lead to a gain-of-function. In conclusion, we demonstrated that synthetic cytokine receptors are a suitable tool for functional SNPs/mutations characterization in a structured workflow.

Immunoregulatory cytokines, including tumor necrosis factor (TNF) and FasL, control immune-related events and are critically involved in pathophysiological processes such as autoimmunity and cancer (1). Fas/CD95 is a death receptor belonging to the TNF superfamily, characterized by a conserved intracellular death domain (DD) (2). Upon trimerized FasL binding, conformational changes in the intracellular DD result in the binding of the adapter molecule fas-associated death domain (FADD) and activation of procaspase 8 via the death-inducing–signaling complex (3). Following autocatalytic cleavage, active caspase 8 promotes downstream signaling, including effector caspases 3 and 7 that lead to final apoptosis (4).

Synthetic biology has become an alternative option to analyze cytokine signal transduction as well as for the development of personalized therapies (5). Recently, we generated fully synthetic cytokine receptors to phenocopy prototypical trimeric receptors for TNF and FasL (6). In our synthetic cytokine receptors for Fas (Fas-SyCyR), we use nanobodies as extracellular ligand-binding domains (7, 8), fused to the transmembrane and intracellular domain of the receptor of interest. The nanobodies serve as biosensors for homomeric or heteromeric ligands, for example, fusion proteins of GFP and mCherry (9). Activation of the endogenous signaling pathway is followed by binding of the synthetic ligand to the synthetic receptor (10, 11).

Nonsynonymous SNPs in Fas eventually cause defects in lymphocyte apoptosis leading to autoimmune diseases and cancer, such as the development of autoimmune lymphoproliferative syndrome (ALPS) (12) and squamous cell carcinoma (SCC) (13). In general, SNPs might influence gene expression, protein folding, stability, localization, or function (14, 15). Apropos of Fas, functional analysis of most non-synonymous, coding SNPs to understand the molecular mechanism(s) that could cause defective apoptosis and/or a link to disease has not been investigated or found for the vast majority of nonsynonymous SNPs, most likely because they were found in more random-like genome sequencing approaches and not by an underlying disease-driven sequencing strategy. Therefore, combining systematic bioinformatics and experimental approaches is needed to manage the expanding SNP landscape. Functionally relevant SNPs can be predicted by in-depth structure-guided analysis (16) or by basic online data processing tools such as Proven (17). Moreover, recent developments in artificial intelligence enable the *in silico* prediction of structures of proteins and protein complexes (18). These deep learning algorithms including RoseTTAFold (19) and AlphaFold (20) will aid the structural understanding of amino acid exchanges either in the exploration phase to screen for functionally relevant SNPs or in the postlaboratory phase to understand the biochemically approved gain-of-function (GOF) or loss-of-function (LOF) SNPs. However, *in silico* characterization

* For correspondence: Jürgen Scheller, jscheller@uni-duesseldorf.de.



Synthetic Fas receptor platform

has to be experimentally validated, at least for GOF and LOF mutants.

Here, we developed an experimental workflow for the Fas-SyCyR system to functionally characterize SNPs and structure-predicted mutations within the transmembrane and intracellular (death) domain of Fas/CD95. We used the SNP database (dbSNP) and clinical variants (ClinVar) database, compilations of all known polymorphisms and polymorphisms with a clinical correlation. Provean and structure-guided analysis were used for the preselection of candidate GOF and LOF mutations. Mutations were introduced into Fas-SyCyR, followed by a functional quantitative characterization including cellular proliferation, apoptosis, and effector caspases 3 and 7 cleavage assays.

In summary, our results showed that among the 35 functionally characterized mutants, 22 were strong LOF, eight were mild LOF, and five led to a mild GOF. We comprehensively demonstrated that the Fas-SyCyR system is a valid tool to functionally and systematically characterize LOF and GOF variants.

Results

Selection of SNPs in the transmembrane and intracellular domain of Fas/CD95

Among the 17,889 SNPs found in the Fas gene, we surveyed the listed 337 nonsynonymous missense SNPs of the transmembrane and intracellular domain, of which 39 were listed in ClinVar. From the 337 missense SNPs, 23 were reported in peer-reviewed publications, 19 had a direct disease association but only 13 were experimentally validated (21, 22).

Nonsynonymous SNPs reported in ClinVar have a high probability of being LOF, whereas SNPs listed only in dbSNP might have no effect on protein function. To identify further nonsynonymous SNPs with potential LOF characteristics among the ones listed in dbSNP, we analyzed all nonsynonymous dbSNPs with Provean. We then selected ten previously uncharacterized nonsynonymous SNPs from

ClinVar and five Provean predicted SNPs from dbSNP (ClinVar: C178R, G253V, I262N, E272G, E289D, L315F, T319I, S320G, D321N, N326H; Provean: S230R, I233V, G247R, K251T, D269H). Moreover, we included the five previously characterized nonsynonymous LOF SNPs Y232C, T241P, R250P, D260V, and T270I located in the intracellular DD, which were reported to be associated with ALPS and SCC (23–30). Figure 1 shows the structural localization of the selected SNPs in the Fas/FADD complex structure.

LOF SNPs in Fas-SyCyR failed to inhibit the proliferation of Ba/F3-gp130 cells

The 20 selected nonsynonymous missense SNPs were introduced into the complementary DNA (cDNA) coding for the synthetic Fas-SyCyR (C_{VHH} Fas) receptor and introduced into Ba/F3-gp130 cells. Cell surface expression of mutant C_{VHH} Fas (with N-terminal human influenza hemagglutinin [HA]-tag) was verified by flow cytometry using HA antibodies (Fig. 2, A and B).

Apoptosis of Ba/F3-gp130- C_{VHH} Fas cells was induced upon addition of trimeric mCherry (3C) fused to an Fc part of an IgG1 antibody (6). The IC_{50} of the synthetic FasL ligand was determined to be in the range of 0.5 and 3.2 ng/ml, demonstrating that low quantitative doses were sufficient to efficiently prevent Hyper-IL-6 (HIL-6)-induced proliferation of Ba/F3-gp130 cells expressing synthetic Fas as control (Fig. 3, A and B). HIL-6 is a fusion protein of IL-6 and the soluble IL-6R, which specifically activates gp130 receptor signal transduction and proliferation of Ba/F3-gp130 cells (6).

As expected, the five previously characterized LOF SNPs (Y232C, T241P, R250P, D260V, T270I) failed to inhibit HIL-6-induced proliferation (Fig. 3A). Among the 15 additional candidates, eight variants were also unable to inhibit HIL-6-induced cellular proliferation, thereof were six SNPs from ClinVar (C178R, G253V, I262N, E272G, E289D, N326H) and two SNPs predicted by Provean (G247R and D269H) (Fig. 3B).

Contrary, the remaining four SNPs from ClinVar (L315F, T319I, S320G, D321N) and three mutants from the dbSNP/

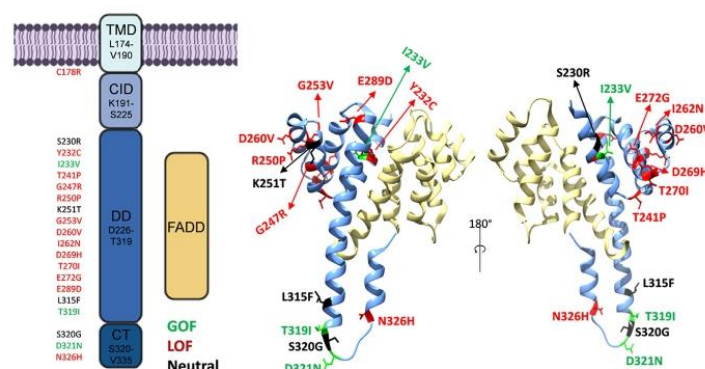


Figure 1. Schematic representation of Fas synthetic receptor and SNPs localization. Graphic representation of transmembrane domain (TMD) and intracellular domain (ICD) of Fas synthetic receptor, including calcium-inducing domain (CID), death domain (DD) interacting with FADD, and COOH-terminal region (CT) (3E2Q). All the selected SNPs' location is highlighted in the Fas TMD, DD, and CT. The final activity is indicated by the following color legend: red, LOF; green, GOF; and black, neutral. GOF, gain-of-function; LOF, loss-of-function.

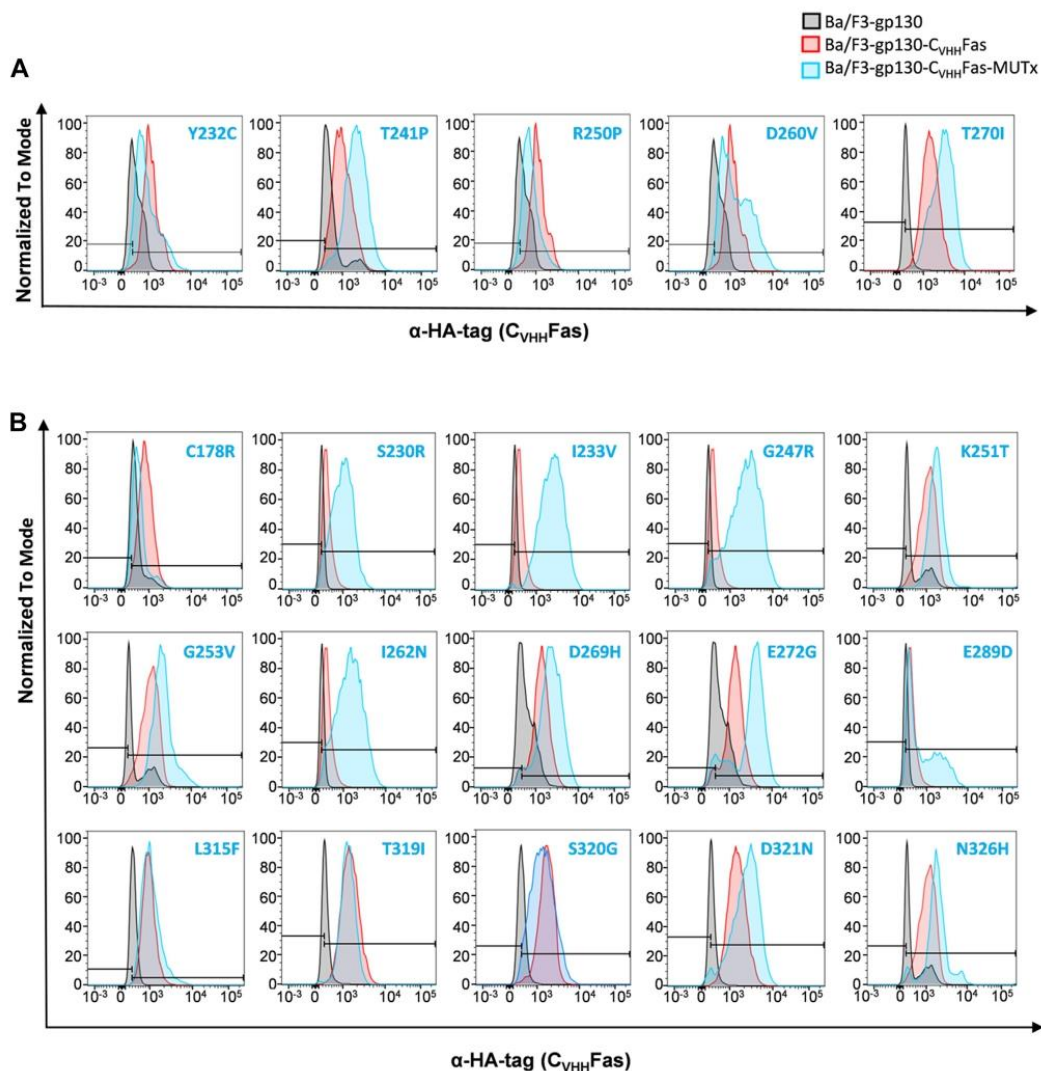


Figure 2. Test expression of WT and mutated C_{VHH} Fas. A, expression of previously published SNPs (Y232C, T241P, R250P, D260V, T270I) by specific detection of surface α -HA-tag through flow cytometry. Black color: Ba/F3-gp130 cells; red color: Ba/F3-gp130- C_{VHH} Fas cells; blue color: Ba/F3-gp130- C_{VHH} Fas with indicated variant. B, test expression of ClinVar reported and Proven predicted SNPs (C178R, S230R, I233V, G247R, K251T, G253V, I262N, D269H, E272G, E289D, L315F, T319I, S320G, D321N, and N326H). Black color: Ba/F3-gp130 cells; red color: Ba/F3-gp130- C_{VHH} Fas cells; blue color: Ba/F3-gp130- C_{VHH} Fas with indicated variant. ClinVar, clinical variant.

Provean prediction (S230R, I233V, K251T) were biologically active. The two variants S230R, L315F showed, however, a reduced IC_{50} of 31 ng/ml and 29.8 ng/ml, respectively. The remaining SNPs K251T, T319I, S320G did not change the biological activity of Fas (IC_{50} of 0.91 ng/ml, 0.95 ng/ml, and 2.64 ng/ml, respectively). Of note, the previously uncharacterized SNPs I233V and D321N were mild GOF mutations with an IC_{50} of 0.11 ng/ml and 0.20 ng/ml, respectively (Fig. 4).

Here, cellular proliferation was used to initially estimate the consequences for the biological activity of the Fas SNP

mutations. In summary, 13 out of 20 SNPs are complete LOFs (Y232C, T241P, R250P, D260V, T270I, C178R, G253V, I262N, E272G, E289D, N326H, G247R, and D269H), two have mild LOFs (S230R, L315F), three have no effect (K251T, T319I, and S320G), and two are GOFs (I233V, D321N).

Structure-predicted mutations within the DD of Fas

Using structure-based prediction, we selected 15 LOF and GOF candidates. All 15 missense mutations were located in

Synthetic Fas receptor platform

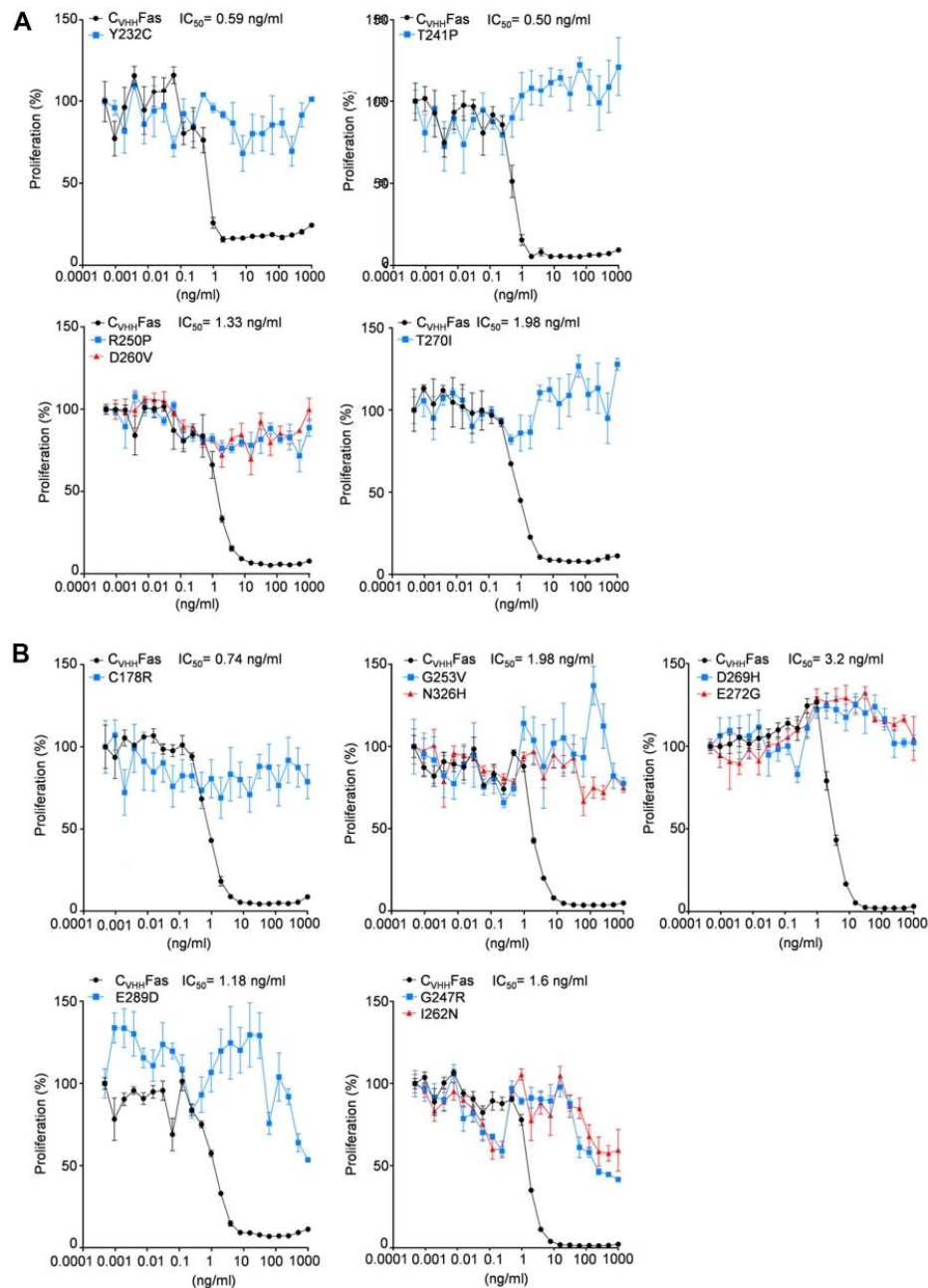


Figure 3. LOF Fas variants failed to inhibit HIL-6-induced cellular proliferation. A, Ba/F3-gp130 cells expressing previously published, LOF SNPs (Y232C, T241P, R250P, D260V, T270I) in $C_{VHH}Fas$ were treated with 20 ng/ml HIL-6 and increasing concentration of 3C (from 1×10^{-4} to 1×10^{-2} ng/ml) for 72 h. Black color: Ba/F3-gp130- $C_{VHH}Fas$ cells; blue color: Ba/F3-gp130- $C_{VHH}Fas$ with indicated variant. B, Ba/F3-gp130 cells expressing up to date uncharacterized, LOF SNPs (C178R, G253V, I262N, D269H, E272G, E289D, and N326H). Cells were treated as described above. Black color: Ba/F3-gp130- $C_{VHH}Fas$ cells; blue or red colors: Ba/F3-gp130- $C_{VHH}Fas$ with indicated variant. Error bars indicate \pm SEM. HIL-6, Hyper-IL-6; LOF, loss-of-function.

Synthetic Fas receptor platform

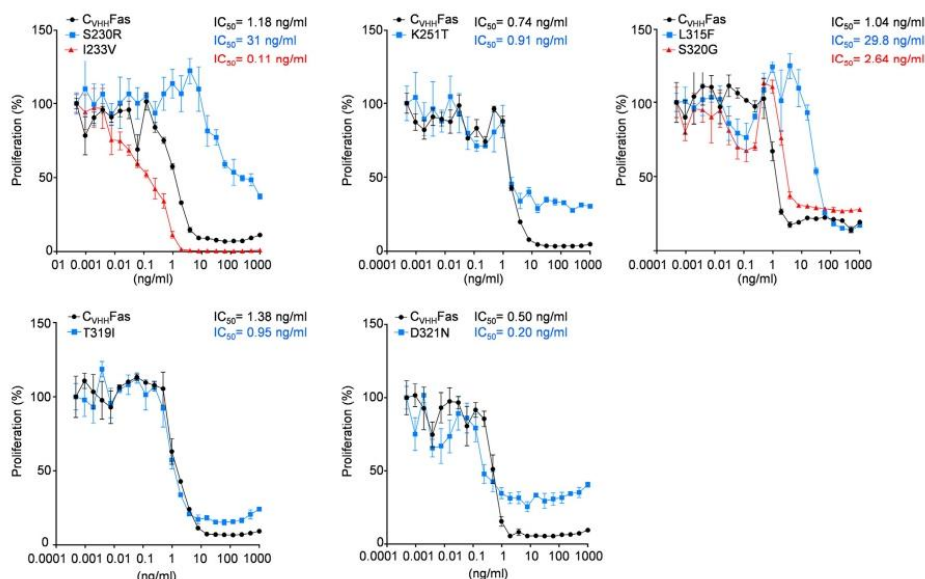


Figure 4. Active SNPs are still able to inhibit HIL-6-induced cellular proliferation upon synthetic ligand stimulation. Ba/F3-gp130 cells expressing previously uncharacterized, active SNPs (S230R, I233V, K251T, L315F, T319I, S320G, and D321N) in $C_{VHH}Fas$ were treated with 20 ng/ml HIL-6 and increasing concentration of 3C (from 1×10^{-4} to 1×10^3 ng/ml) for 72 h. Black color: Ba/F3-gp130- $C_{VHH}Fas$ cells; blue or red color: Ba/F3-gp130- $C_{VHH}Fas$ with indicated variant. Error bars indicate \pm SEM. HIL-6, Hyper-IL-6.

the DD and resulted in substitution into an alanine (ten alanine variants) or an alternative amino acid (five additional variants) to achieve maximal repulsion between the DD and FADD. In detail, D228S causes disruption of a salt bridge with FADD R142, while Y291D leads to loss of hydrophobic interaction with L172, L176, V173, and N107. Figure 5 shows the structural localization of the selected mutations in the Fas/FADD complex structure.

The 15 structure-based mutations were introduced into the cDNA coding for $C_{VHH}Fas$. Ba/F3-gp130 cells expressing the $C_{VHH}Fas$ variants were generated, and cell surface expression

was verified by flow cytometry (Supporting information 1). Ba/F3-gp130- $C_{VHH}Fas$ (variant) cells were stimulated with 3C and HIL-6. The $C_{VHH}Fas$ alanine variants L224A, L229A, K231A, T235A, I236A, G238A, L298A and the two additional variants D228S, Y291D failed to inhibit HIL-6-induced proliferation, suggesting that these mutations cause LOF (Fig. 6A). On the other hand, N223A, I295A, L306A and N302D, Q311E, N329D still prevented cellular proliferation. Of these, I295A and L306A showed reduced inhibitory activity considering that higher concentrations of 3C were needed to abrogate cellular proliferation ($IC_{50} = 9.49$ ng/ml and not to be determined).

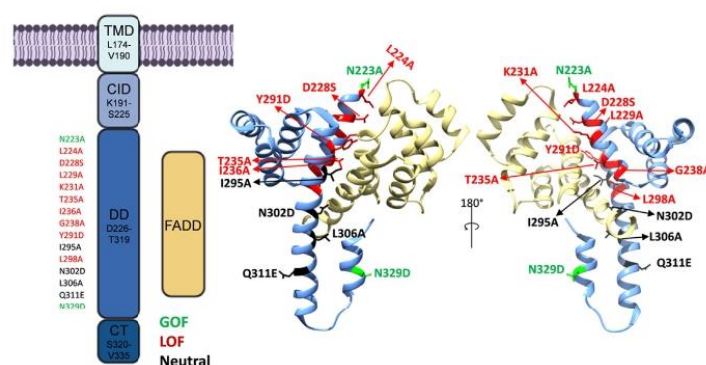


Figure 5. Schematic representation of Fas synthetic receptor and structure-based mutations localization. Fas synthetic receptor's TMD and ICD shown in interaction with FADD (BEZQ). The locations of all the chosen structure-based mutations are highlighted in the DD structure. The following color legend designates the final activity: red, LOF, green, GOF, and black, neutral. GOF, gain-of-function; LOF, loss-of-function.

Synthetic Fas receptor platform

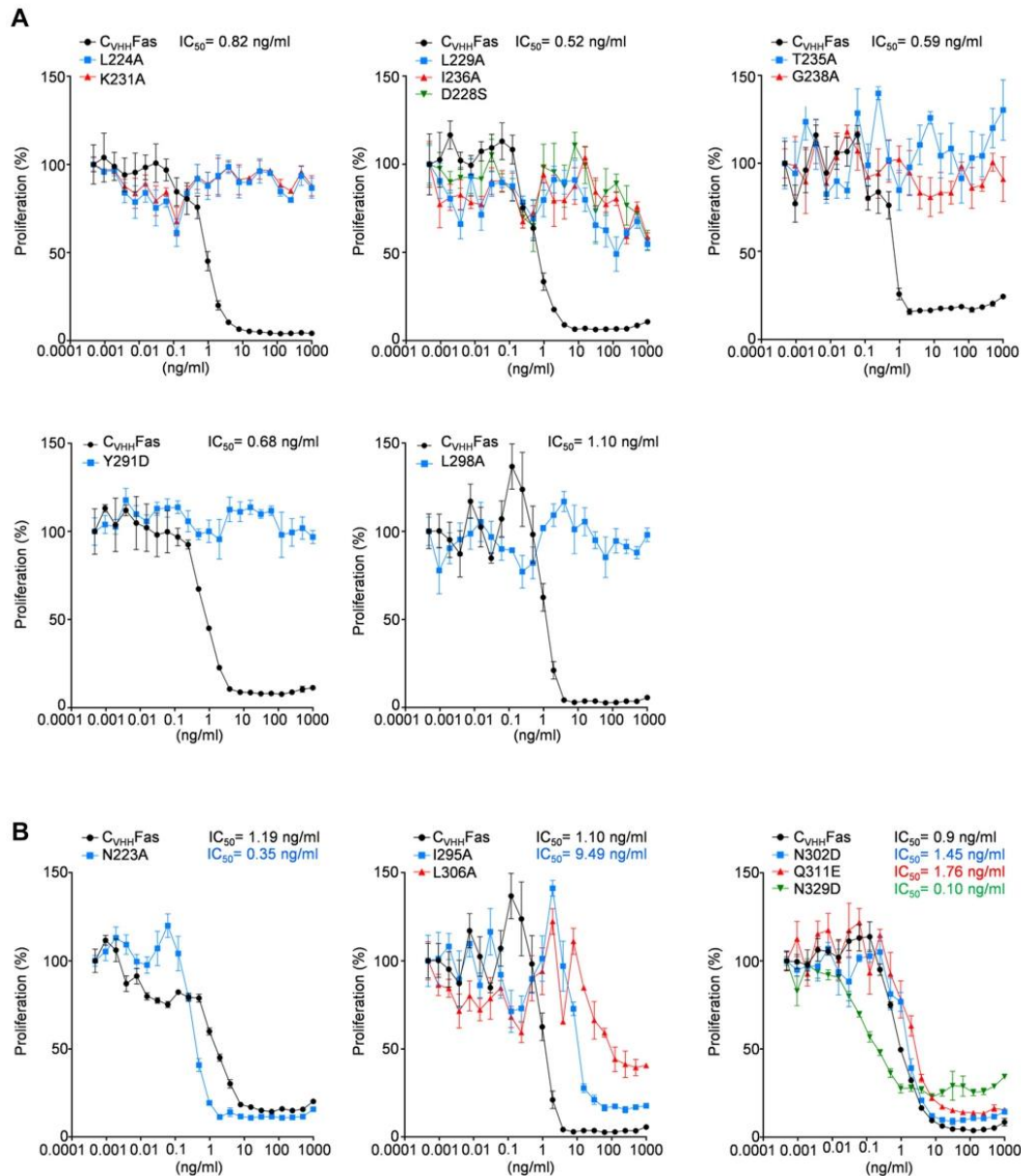


Figure 6. Analysis of Fas structure-based mutations capacity to inhibit HIL-6-induced cellular proliferation. A, Ba/F3-gp130 cells expressing uncharacterized, LOF structure-based mutations (L224A, D228S, L229A, K231A, T235A, I236A, G238A, Y291D, and L298A) in $C_{VHH}Fas$ were treated with 20 ng/ml HIL-6 and increasing concentration of 3C (from 1×10^{-4} to 1×10^3 ng/ml) for 72 h. Black color: Ba/F3-gp130- $C_{VHH}Fas$ cells; blue or red or green color: Ba/F3-gp130- $C_{VHH}Fas$ with indicated mutations. B, Ba/F3-gp130 cells expressing uncharacterized, GOF structure-based mutations (N223A, I295A, N302D, L306A, Q311E, N329D). Cells were treated as described above. Black color: Ba/F3-gp130- $C_{VHH}Fas$ cells; blue or red or green colors: Ba/F3-gp130- $C_{VHH}Fas$ with indicated mutations. Error bars indicate \pm SEM. GOF, gain-of-function; HIL-6, Hyper-IL-6; LOF, loss-of-function.

Moreover, N223A and N329D were more effective ($IC_{50} = 0.35$ ng/ml and $IC_{50} = 0.10$ ng/ml) and might represent mild GOF mutations (Fig. 6B).

In summary, 9 out of 15 SNPs are complete LOFs (L224A, L229A, K231A, T235A, I236A, G238A, L298A, D228S, Y291D), two are mild LOFs (I295A and L306A), two indicated

no effect (N302D, Q311E), and two are proved to be GOFs (N223A and N329D).

LOF SNPs and mutations are unable to induce apoptosis

To analyze apoptosis progression in detail, we performed flow cytometry staining of 7-AAD and Annexin-V of Ba/F3-gp130 cells expressing C_{VHH}Fas variants after 24 h stimulation with HIL-6 alone or in combination with the synthetic Fas ligand 3C. As illustrated in the schematic plots (Fig. 7A), the addition of HIL-6 resulted in 87.7% living Ba/F3-gp130-C_{VHH}Fas cells, whereas co-incubation with 3C resulted in 74% apoptotic cells. The previously characterized SNP variants Y232C, T241P, R250P, D260V, T270I failed to induce apoptosis (Fig. 7B and Supporting information 2). A similar picture was seen for the eight ClinVar and Proven SNPs C178R, G247R, G253V, I262N, D269H, E272G, E289D, N326H (Fig. 7C and Supporting informations 3 and 4) and for the nine structure-based mutants L224A, D228S, L229A, K231A, T235A, I236A, G238A, L298A, Y291D, which all failed to inhibit proliferation with synthetic ligand stimulation and also did not induce apoptosis (Fig. 7D and Supporting informations 5 and 6). K231A was the only partial LOF alanine mutant with still 29% late apoptotic cells after 3C treatment *versus* 5% cells in the late apoptotic state without 3C, albeit this variant was not able to inhibit the proliferation of Ba/F3-gp130 cells.

Four mutations that indicated GOF (I233V, D321N) or with no effect (T319I, S320G) in the proliferation assays efficiently produced late apoptotic cells (82%, 83%, 99%, 99%, respectively). Of note, the remaining three variants (S230R, K251T (no effect), L315F) displayed fewer late apoptotic cells (37%, 36%, 44%, respectively), from which S230R and L315F were also seen in the proliferation assay to be mild LOF variants (Fig. 8, A and B and Supporting information 7).

The proliferation-inhibiting structure-based mutants N223A, I295A, N302D, L306A, Q311E, and N329D all induced cellular apoptosis (Fig. 8C and Supporting information 8). In detail, N223A, I295A, L306A, N302D, Q311E, and N329D induced 71%, 63%, 56%, 33%, 62%, and 67% late apoptotic cells, respectively.

The apoptotic assays generally confirmed LOF phenotypes for the previously described SNPs Y232C, T241P, R250P, D260V, T270I and the ClinVar and Proven predicted SNPs C178R, G247R, G253V, I262N, D269H, E272G, E289D, N326H and the structure-based mutations L224A, D228S, L229A, K231A, T235A, I236A, G238A, L298A, Y291D.

Taken together, a consistent milder LOF phenotype was seen in proliferation and apoptosis assays for the SNPs S230R and L315F and the structure-based mutations I295A, L306A and a comparable to WT Fas phenotype for the SNPs T319I and S320G.

Capacity of Fas-SyCyR variants to activate caspases 3 and 7

An early hallmark of apoptosis is the activation of the effector caspases 3 and 7 (31), which were analyzed by a quantitative, fluorescent caspase-cleavage assay. Ba/F3-gp130 cells expressing C_{VHH}Fas variants were stimulated for

6 h with HIL-6 in the presence and absence of the synthetic Fas ligand 3C. Caspase 3/7 activation after the addition of 3C in Ba/F3-gp130 cells expressing C_{VHH}Fas was set to 100%, and the efficiency of the other C_{VHH}Fas variants was calculated accordingly. As observed for the inhibition of proliferation and determination of late apoptotic cells, the five previously characterized LOF SNPs, Y232C, T241P, R250P, D260V, and T270I completely failed to induce caspase 3/7 activation (Fig. 9A). Likewise, the eight other identified LOF SNPs from ClinVar and Proven C178R, G247R, G253V, I262N, D269H, E272G, E289D, and N326H (Fig. 9B) failed to induce caspase 3/7. Eight out of the nine others identified structure-based LOF mutations L224A, L229A, K231A, T235A, I236A, G238A, Y291D, and L298A (Fig. 9C) were unable to activate the effector caspases, although D228S still resulted in about 20% activation (Fig. 9C). D228S causes the loss of a salt bridge interaction between Fas and FADD. In the D228S, the serine is still within 4.5 Å distance to R142 of FADD and may hence be able to form a H-bond which does not completely abrogate the interaction but significantly weaken it.

Compared to C_{VHH}Fas, induction of caspase 3/7 of the active SNPs S230R, I233V, K251T, L315F, T319I, S320G, D321N was 37%, 134%, 64%, 52.5%, 135%, 39% and 28%, respectively (Fig. 10A).

Similarly, the structure-based mutations N223A, I295A, N302D, L306A, Q311E, and N329D induced caspase 3/7 as well, albeit with different efficiencies compared to stimulation of cells expressing the WT receptor (Fig. 10B). In detail, the effector caspase activation of N223A and N329D mutants supported the previous proliferation and late apoptosis data as them as novel GOF mutants, with a respective percentage equal to 234% and 131% compared to C_{VHH}Fas, respectively. On the contrary, I295A, N302D, L306A, and Q311E induced 32%, 36%, 17%, and 40%, respectively, resulting in mild LOF mutations.

We have summarized all findings in Tables 1 and 2. The five previously described LOF SNPs Y232C, T241P, R250P, D260V, and T270I were also in our experiments unable to inhibit proliferation, to induce cellular apoptosis and to activate effector caspases 3 and 7. The same picture was seen for the ClinVar-reported and Proven-predicted SNPs of the transmembrane and intracellular Fas domain C178R, G247R, G253V, I262N, D269H, E272G, E289D, and N326H and the structure-based L224A, L229A, K231A, T235A, I236A, G238A, Y291D, L298A mutants, with 19% activation for D228S. Contrary, the SNPs S230R, I233V, K251T, L315F, T319I, S320G, D321N and the designed mutations L224A, D228S, L229A, K231A, T235A, I236A, G238A, Y291D, L298A were still able to abrogate proliferation, to induce cellular apoptosis, and to activate effector caspases to some degree.

Combination of mutations to strengthen GOF and LOF

One plausible application for SyCyRs could be to strengthen chimeric antigen receptor (CAR) T-cell therapies, either supporting or suppressing the activity of engineered T-cells. Following this aim, we were curious to test if combining GOF

Synthetic Fas receptor platform

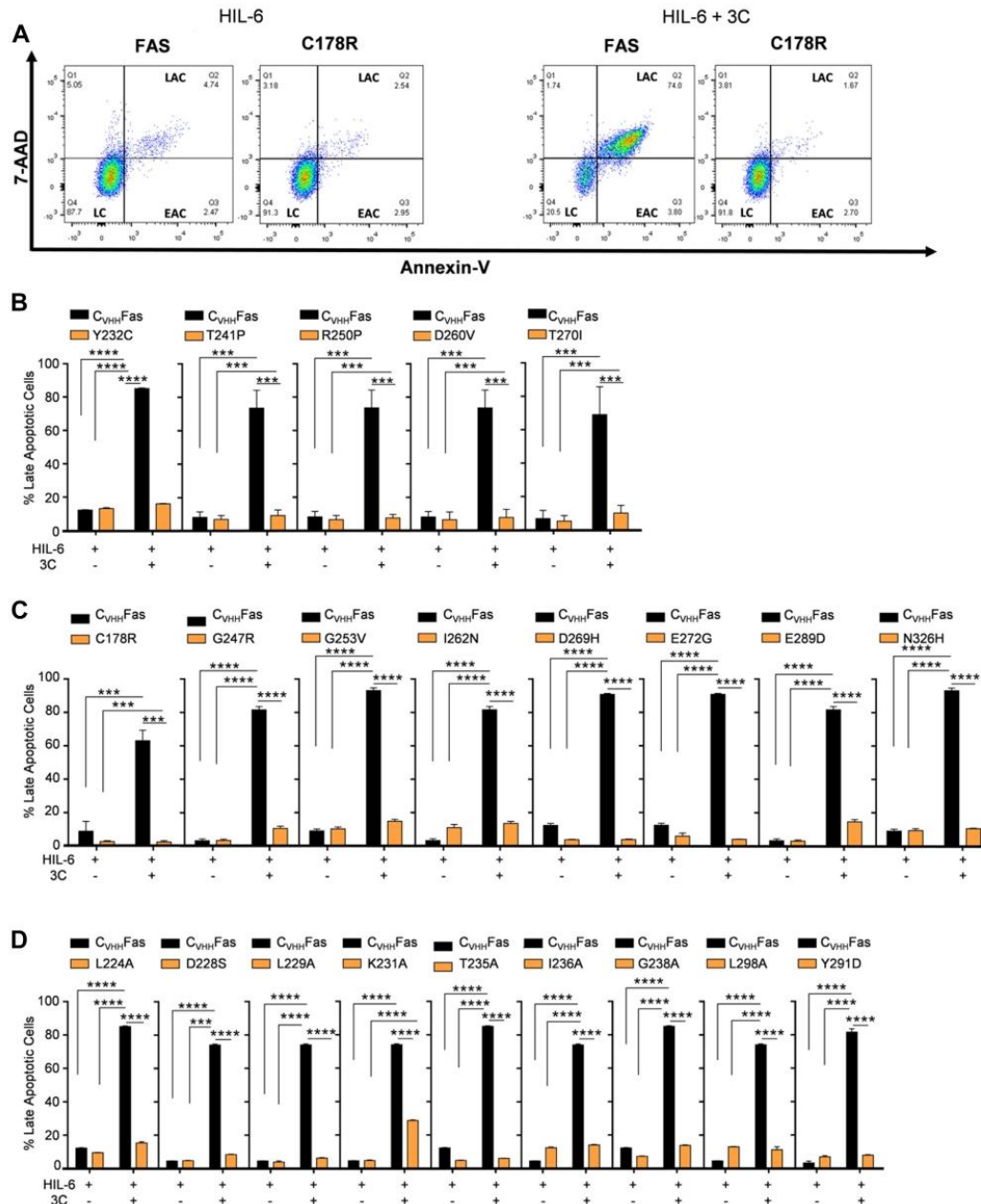


Figure 7. LOF variants failed to induce apoptosis upon synthetic ligand stimulation. A, representative plots of apoptosis progression in Ba/F3-gp130-C_{VH1H}Fas and Ba/F3-gp130-C_{VH1H}Fas-C178R, LOF SNP, stimulated for 24 h with HIL-6 with and without 3C. Cells were stained with 7-AAD and Annexin-V and analyzed by flow cytometry. Graphics of apoptosis progression of Ba/F3-gp130-C_{VH1H}Fas WT compared to (B) previously published SNPs (Y232C, T241P, R250P, D260V, T270I), (C) uncharacterized, LOF SNPs (G247R, G253V, I262N, D269H, E272G, E289D, and N326H), and (D) uncharacterized, LOF structure-based mutations (Y232C, L224A, D228S, L229A, K231A, T235A, I236A, G238A, Y291D, and L298A). Error bars indicate \pm SEM. **** p < 0.0001; *** p < 0.001. EAC, early apoptotic cells; HIL-6, Hyper-IL-6; LAC, late apoptotic cells; LC, living cells.

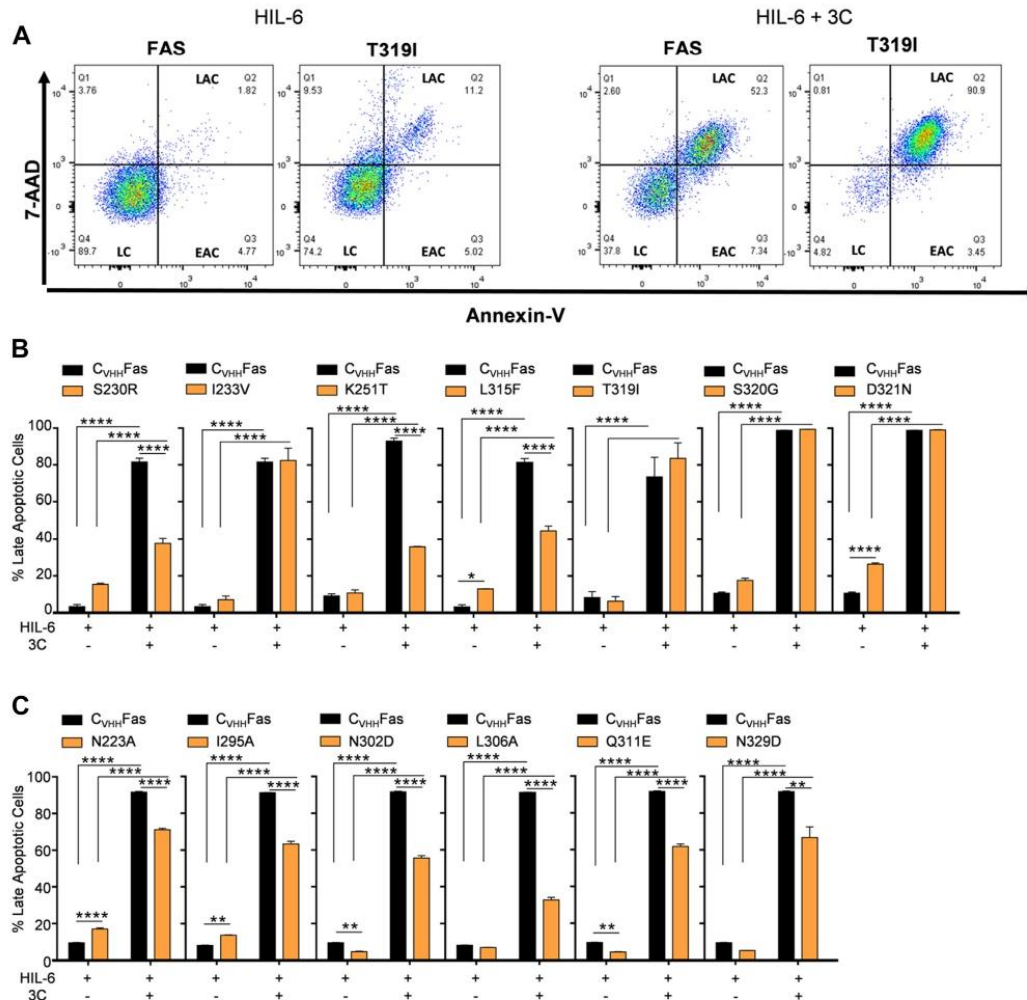


Figure 8. Active variants were still able to induce apoptosis upon synthetic ligand stimulation. A, representative plots of apoptosis progression in Ba/F3-gp130-CvHHFas and Ba/F3-gp130-CvHHFas-T319I, GOF SNP, stimulated for 24 h with HIL-6 with and without 3C. Cells were stained with 7-AAD and Annexin-V and analyzed by flow cytometry. Graphics of apoptosis progression of Ba/F3-gp130-CvHHFas WT compared to (B) uncharacterized, active SNPs (S230R, I233V, K251T, L315F, T319I, S320G, and D321N) and (C) uncharacterized, active structure-based mutations (N223A, I295A, N302D, L306A, Q311E, N329D). Error bars indicate \pm SEM. ** $p < 0.01$; **** $p < 0.0001$. GOF, gain-of-function; HIL-6, Hyper-IL-6; C, living cells; LAC, late apoptotic cells; LEAC, early apoptotic cells.

or LOF mutations would result in stronger and weaker activation of synthetic WT Fas.

The SNP L315F and the alanine mutants I295A and L306A had consistently reduced Fas activity in our assays. Therefore, we combined them in a triple mutant to analyze if this will result in a more severe LOF phenotype. As expected, the combination of the mild LOF L315F, I295A, and L306A in one variant resulted in complete LOF, since this variant was unable to inhibit the proliferation of Ba/F3-gp130 cells (Fig. 11A), did not induce late apoptosis (Fig. 11B and Supporting information 9), and failed to activate caspases 3 and 7 (Fig. 11C).

On the other hand, the mutants N223A and N329D alone conferred a stronger capacity to inhibit proliferation, partially reduced amounts of late apoptotic cells, and significantly higher caspase 3/7 activity compared to WT, after activation with synthetic Fas. Hence, likewise, we combined those two mutants to analyze if this will result in a stronger GOF phenotype. Unexpectedly, the combination of two stronger activated mutations N223A and N329D resulted in a partial LOF variant with a lower capacity to inhibit proliferation ($IC_{50} = 19.01$ ng/ml) (Fig. 11D), to induce apoptosis (38% of late apoptotic cells *versus* 98% for WT Fas) (Fig. 11E and

Synthetic Fas receptor platform

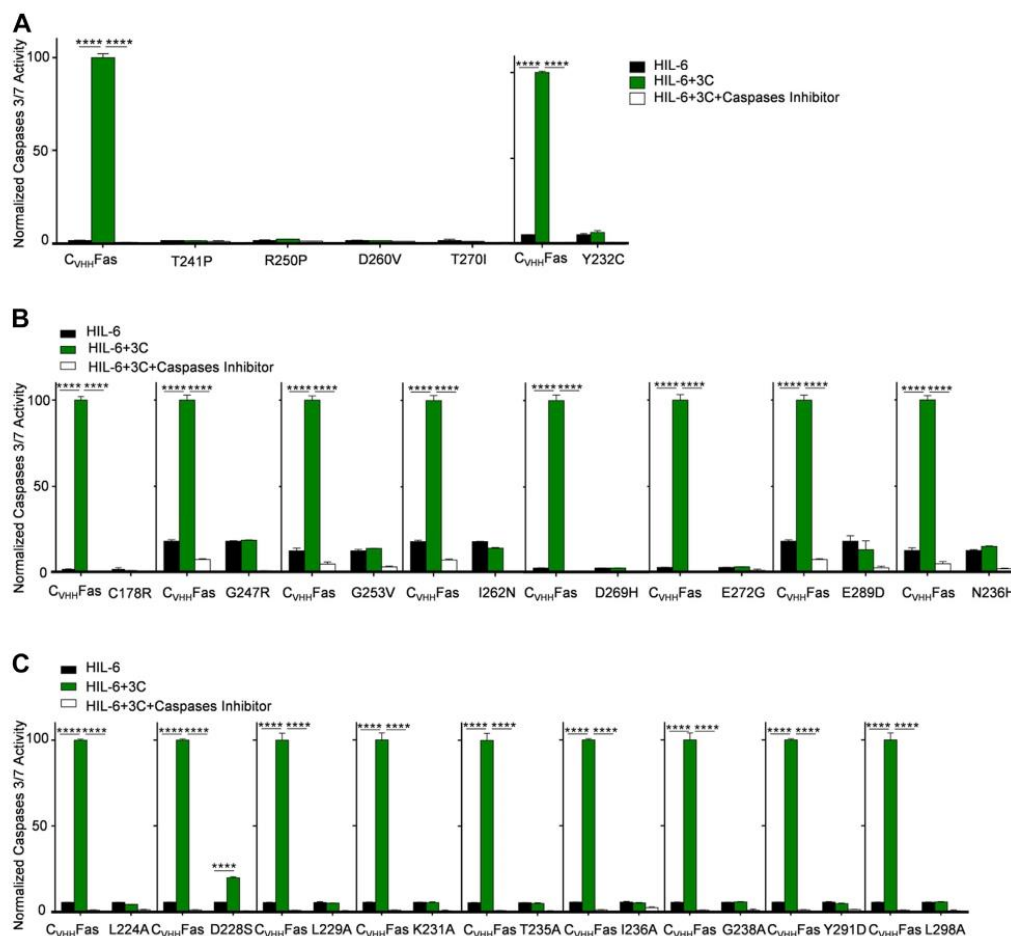


Figure 9. Caspases 3/7 activation was not detected in Ba/F3-gp130 expressing C_{VHH} Fas with LOF mutations. Activation of caspases 3/7 in Ba/F3-gp130- C_{VHH} Fas WT and with (A) LOF, previously published SNPs (Y232C, T241P, R250P, D260V, T270I), (B) uncharacterized, LOF SNPs (C178R, G247R, G253V, I262N, D269H, E272G, E289D, and N326H), and (C) uncharacterized, LOF structure-based mutations (L224A, D228S, L229A, K231A, T235A, I236A, G238A, Y291D, and L298A). Cells were stimulated for 6 h with only HIL-6 (black bars), plus 3C (green bars), plus caspases inhibitor (white bars). Error bars indicate \pm SEM. **** $p < 0.0001$. HIL-6, Hyper-IL-6.

Supporting information 9), and to induce effector caspases activation with a percentage equal to 38% (Fig. 11F).

In conclusion, the combination of three less active mutations (L315F, I295A, L306A) resulted in a complete LOF phenotype, while the combination of two GOF mutations (N223A plus N329D) did not lead to a more active variant.

Dominant-negative effect of selected Fas single nucleotide mutations

ALPS patients have been mainly associated with missense mutations in FAS gene, which cause the disruption of the apoptotic pathway by dominant-negative interference (29). Normally, following endogenous ligand binding, Fas is pre-assembled as homotrimeric receptor. At least one copy of

mutated Fas protein (heterozygous) can cause a dysfunctional trimeric receptor complex (32). In order to test the dominant-negative effect of selected Fas mutations from this study, we retrovirally transduced Ba/F3-gp130- C_{VHH} Fas WT and mutant cells with an additional synthetic G_{VHH} Fas cDNA (Fig. 12A). Cell surface expression of G_{VHH} Fas was verified by flow cytometry using Myc-tag antibodies (Supporting information 10). Next, cells were stimulated for 24 h by synthetic fusion proteins composed of two GFPs and one mCherry (2GC), in order to induce receptor trimerization of two WT and one mutated synthetic Fas receptor (Fig. 12A). We tested the two previously described LOF mutations T241P and D260. As shown in Figure 12B (Supporting information 11), Ba/F3-gp130 cells expressing C_{VHH} Fas T241P or D260 plus G_{VHH} Fas were unable to induce apoptosis by

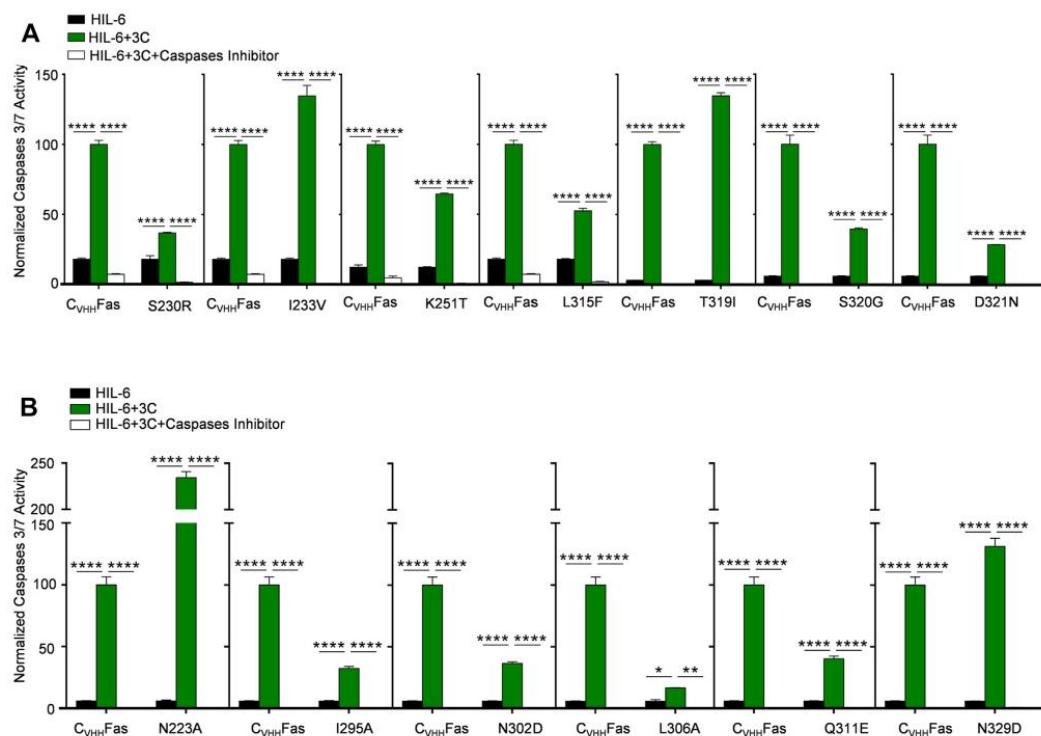


Figure 10. Detection of caspases 3/7 activation in Ba/F3-gp130 expressing C_{VHH}Fas with GOF mutations. Activation of caspases 3/7 in Ba/F3-gp130-C_{VHH}Fas WT and with (A) uncharacterized, active SNPs (S230R, I233V, K251T, L315F, T319I, S320G, and D321N), (B) uncharacterized, active structure-based mutations (N223A, I295A, N302D, L306A, Q311E, N329D). Cells were stimulated for 6 h with only HIL-6 (black bars), plus 3C (green bars), plus caspases inhibitor (white bars). Error bars indicate \pm SEM. * $p < 0.05$; ** $p < 0.01$; **** $p < 0.0001$. GOF, gain-of-function; HIL-6, Hyper-IL-6.

heterotrimerization, confirming the dominant-negative effect of these two variants. We proceeded with testing three previously uncharacterized nonsynonymous SNPs (E289D, N326H, and G253V), which were LOF in our characterization. Interestingly, those mutations still impaired apoptosis compared to normal Fas but with a percentage of apoptotic cells equal to 78%, 49%, and 26%, respectively (Fig. 12C and Supporting information 12), thus having a weaker dominant-negative effect. Finally, we tested the effect of the GOF structure-based mutations that initially resulted in weaker GOF (N329D, N223A, and N329D+N223A). After stimulation, we obtained, respectively, 37.6%, 60%, and 36% of apoptosis (Figs. 12D and S13), also showing reduced Fas function as heterotrimers.

Discussion

Synthetic biology has become an engrossing alternative option to analyze cytokine signal transduction as well as for the development of personalized therapies (5), including the approval of CAR T-cell immunotherapy for acute lymphoblastic leukemia as the first gene therapy (33). Initially, we generated fully synthetic cytokine receptors to phenocopy prototypical dimeric cytokine receptors for IL-6, IL-22, and

IL-23 (10, 11) and recently adopted this system for the activation of trimeric receptors for TNF and FasL (6). The SyCyRs for the death receptor Fas efficiently activated cellular apoptosis as shown by inhibition of cellular proliferation, Annexin-V staining, and caspase 3 cleavage assays (6). The specificity of induced apoptosis due to the synthetic Fas activation was verified by a previously described LOF mutation in the DD (6), which was associated with the development of ALPS (34).

In this study, we used Fas-SyCyR as a systematic tool to characterize the functional and molecular mechanism of LOF or (partial) GOF mutations associated with Fas, with or without a direct immune diseases correlation. We initially predicted relevant SNPs found in the transmembrane and intracellular human Fas domain by in-depth structure-guided analysis (16) or by basic online data processing tools such as Proven (17). Subsequently, we selected 20 SNPs and 15 structure-based mutations. We showed that none of the 35 mutation results in global instability of the protein, since all were normally expressed on the cell surface, confirming previous data reporting expression abnormalities mainly for extracellular Fas mutations (29, 30).

To date, most described LOF SNPs in Fas were found in the transmembrane and intracellular DD and presented a more

Synthetic Fas receptor platform

Table 1
Summary of selected Fas SNPs and activity

	ClinVar rating	ClinVar disease	Provean prediction	Inhibition of proliferation	(%) Late apoptosis	Caspases 3/7	Summary activity (number of criteria fulfilled out of 3)
Previously published SNPs							
Y232C	Pathogenic, uncertain significance	ALPS	Not tested	None	None	None	LOF (3/3)
T241P	Pathogenic	ALPS	Not tested	None	None	None	LOF (3/3)
R250P	Likely pathogenic	ALPS	Not tested	None	None	None	LOF (3/3)
D260V	Pathogenic	ALPS	Not tested	None	None	None	LOF (3/3)
T270I	Pathogenic	ALPS	Not tested	None	None	None	LOF (3/3)
Previously uncharacterized SNPs							
C178R	Pathogenic	SCC	Not tested	None	None	None	LOF (3/3)
S230R	-	-	Yes	IC ₅₀ = 31 ng/ml	37%	37%	Reduced (3/3)
I233V	-	-	Yes	IC ₅₀ = 0.11 ng/ml	82%	134%	GOF (2/3)
G247R	-	-	Yes	None	None	None	LOF (3/3)
K251T	-	-	Yes	IC ₅₀ = 0.91 ng/ml	36%	64%	Reduced (2/3)
G253V	Uncertain significance	ALPS	Not tested	None	None	None	LOF (3/3)
I262N	Likely-pathogenic, uncertain significance	-	Not tested	None	None	None	LOF (3/3)
D269H	-	-	Yes	None	None	None	LOF (3/3)
E272G	Uncertain significance	-	Not tested	None	None	None	LOF (3/3)
E289D	Uncertain significance	ALPS	Not tested	None	None	None	LOF (3/3)
L315F	Uncertain significance	ALPS	Not tested	IC ₅₀ = 29.8 ng/ml	44%	52.5%	Reduced (3/3)
T319I	Uncertain significance	ALPS	Not tested	IC ₅₀ = 0.95 ng/ml	83%	135%	GOF (2/3)
S320G	Likely benign	ALPS	Not tested	IC ₅₀ = 2.64 ng/ml	99%	39%	Reduced (1/3)
D321N	Uncertain significance	ALPS	Not tested	IC ₅₀ = 0.20 ng/ml	99%	28%	GOF (1/3)
N326H	Uncertain significance	-	-	None	None	None	LOF (3/3)

pronounced disrupted phenotype and defective apoptosis in lymphocytes in patients affected by ALPS and SCC, compared to extracellular Fas SNPs (26). Furthermore, patient LOF mutations in the DD of Fas are typically heterozygous because homozygosity would be lethal (25). To validate our system, we selected five SNPs previously associated to ALPS and molecularly described as LOF mutations. Bettinardi *et al.* showed how two ALPS-affected siblings were carrying the same mutation Y232C in Fas gene causing a defect in apoptosis (23), while patients carrying Fas SNPs T241P, R250P, and D260V showed reduced apoptosis (26, 28), reduced T-cell loss (25), and altered death-inducing-signaling complex formation (29). Lastly, the SNP T270I exhibited inhibition of Fas-mediated apoptosis deduced by higher cell viability and absence of FADD recruitment (30). Our results confirmed and completed the previous studies with additional structural analysis, apoptosis, and caspases 3 and 7 cleavage assays. We further shed light on the molecular mechanism of 15 additional new

SNPs reported in ClinVar as (likely) pathogenic or with uncertain significance or predicted by Provean. From our analysis, eight SNPs resulted in complete LOF, four showed a partially reduced Fas activity, while three conferred a milder GOF. We widely demonstrated that prediction by in-depth structure-guided analysis or by basic online data processing tools such as Provean may be useful as preliminary screening but need to be experimentally and systematically validated. We predicted 15 further LOF candidates using structure-based modeling. To design LOF variants, DD residues within the DD-FADD interface were substituted by alanine (ten alanine variants) or an alternative amino acid (five rational designed variants). N223A and N329D did not negatively affect Fas-induced inhibition of proliferation, apoptosis, and caspase activation, while I295A, N302D, L306A, and Q311E only partially diminished the WT activity.

SyCyRs might potentially be used to boost CAR T-cell therapy (6). Despite the significant clinical success of CAR

Table 2
Summary of Fas structure-based mutations activity

Structure-based mutations	Inhibition of proliferation	(%) Late apoptosis	(%) Caspases 3/7	Summary activity (number of criteria fulfilled out of 3)
N223A	IC ₅₀ = 0.35 ng/ml	71%	234%	GOF (2/3)
L224A	None	None	None	LOF (3/3)
D228S	None	None	19%	LOF (2/3)
L229A	None	None	None	LOF (3/3)
K231A	None	29%	None	LOF (2/3)
T235A	None	None	None	LOF (3/3)
I236A	None	None	None	LOF (3/3)
G238A	None	None	None	LOF (3/3)
Y291D	None	None	None	LOF (3/3)
I295A	IC ₅₀ = 9.49 ng/ml	63%	32%	Reduced (3/3)
L298A	None	None	None	LOF (3/3)
N302D	IC ₅₀ = 1.45 ng/ml	56%	36%	Reduced (2/3)
L306A	Not detectable IC ₅₀	33%	17%	Reduced (3/3)
Q311E	IC ₅₀ = 1.76 ng/ml	62%	40%	Reduced (2/3)
N329D	IC ₅₀ = 0.10 ng/ml	67%	131%	GOF (2/3)

Synthetic Fas receptor platform

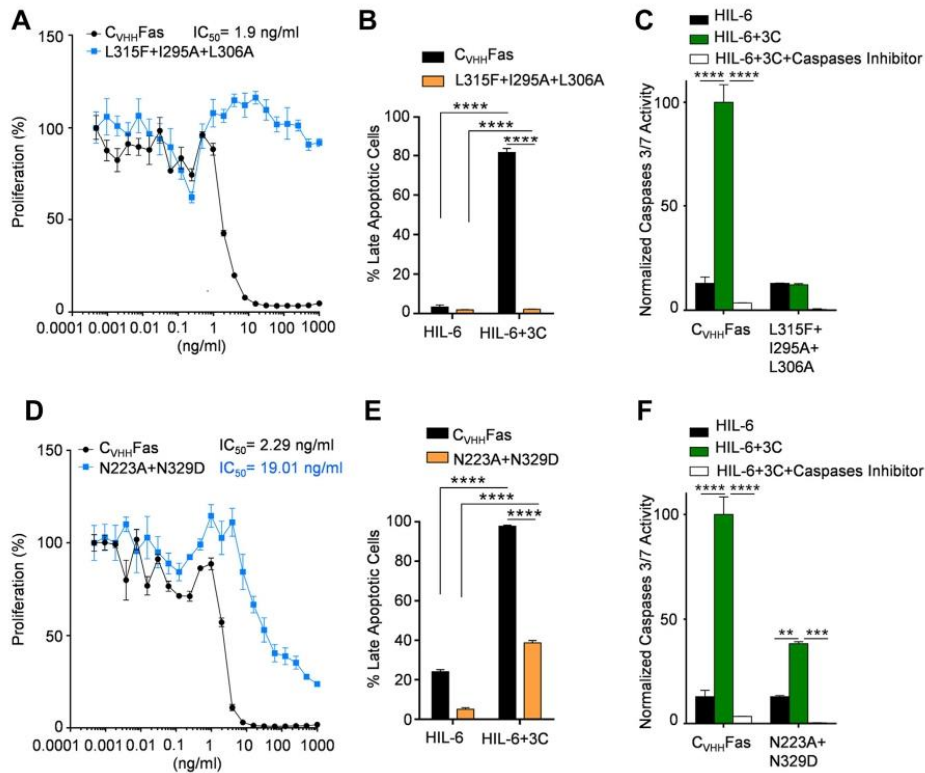


Figure 11. Combination of selected mutations to achieve more severe phenotypes. Proliferation assay of (A) Ba/F3-gp130- C_{VHH} Fas-L315F+I295A+L306A and (D) Ba/F3-gp130- C_{VHH} Fas-N223A+N329D. Cells were treated with 20 ng/ml HIL-6 and increasing concentration of 3C (from 1×10^{-4} to 1×10^3 ng/ml) for 72 h. Apoptosis progression in (B) Ba/F3-gp130- C_{VHH} Fas-L315F+I295A+L306A and (E) Ba/F3-gp130- C_{VHH} Fas-N223A+N329D. Cells were stimulated for 24 h with HIL-6 with and without 3C. Cells were stained with 7-AAD and Annexin-V and analyzed by flow cytometry. Activation of caspases 3/7 in (C) Ba/F3-gp130- C_{VHH} Fas-L315F+I295A+L306A and (F) Ba/F3-gp130- C_{VHH} Fas-N223A+N329D. Cells were stimulated for 6 h with only HIL-6 (black bars), plus 3C (green bars), plus caspases inhibitor (white bars). Error bars indicate \pm SEM. ** $p < 0.01$; *** $p < 0.001$; **** $p < 0.0001$. HIL-6, Hyper-IL-6.

T-cells in treating patients with leukemia and lymphoma, two primary clinical side effects have been encountered: cytokine release syndrome and neurotoxicity (35). We propose a plausible innovative approach to overcome the side effects by promoting or repressing the activity of transgenic T-cells, respectively activating gp130 and synthetic Fas. In line with this aim, we were interested to test if combining GOF or LOF mutations would produce greater or weaker activation of synthetic WT Fas, in order to induce an improved (stronger or weaker) synthetic Fas activation in primary T-cells and consequent suppression of the deadly pro-inflammatory response.

We observed that two more intensely activated mutations, N223A and N329D, were combined to create a stronger active variant; however, the combination was unfavorable and resulted in a mild LOF phenotype. N223 is in close proximity to N136 and R135 of FADD, but in the structure, it seems to not be in contact with FADD. N329 is far away from FADD. Looking at the structure, we cannot explain the LOF

phenotype of the N223A and N329D combination. Possibly, the exchange of both amino acids might lead to a decreased stability of the Fas, since these two amino acids contribute to the overall protein stability with -9.7 KJ/mol (N223) and -32.1 KJ/mol (N329) in the closed conformation (PDB: 1DDF) and -86.3 KJ/mol (N329) in the open conformation (PDB: 3EZQ) (36).

To conclude, we aimed at testing the dominant-negative effect of some selected SNPs and mutations that was confirmed for two ALPS-associated LOF SNPs and partially showed for three additional uncharacterized nonsynonymous SNPs and two GOF structure-based mutations, as well as the combination of the two.

Indubitably, following this initial screening, one possible prospective analysis is to test the selected disease-related SNPs and mutations in primary immune cells that co-express endogenous Fas activated by FasL.

In summary, defining the specific molecular mechanism that cause defective apoptotic pathway using a systematic and

Synthetic Fas receptor platform

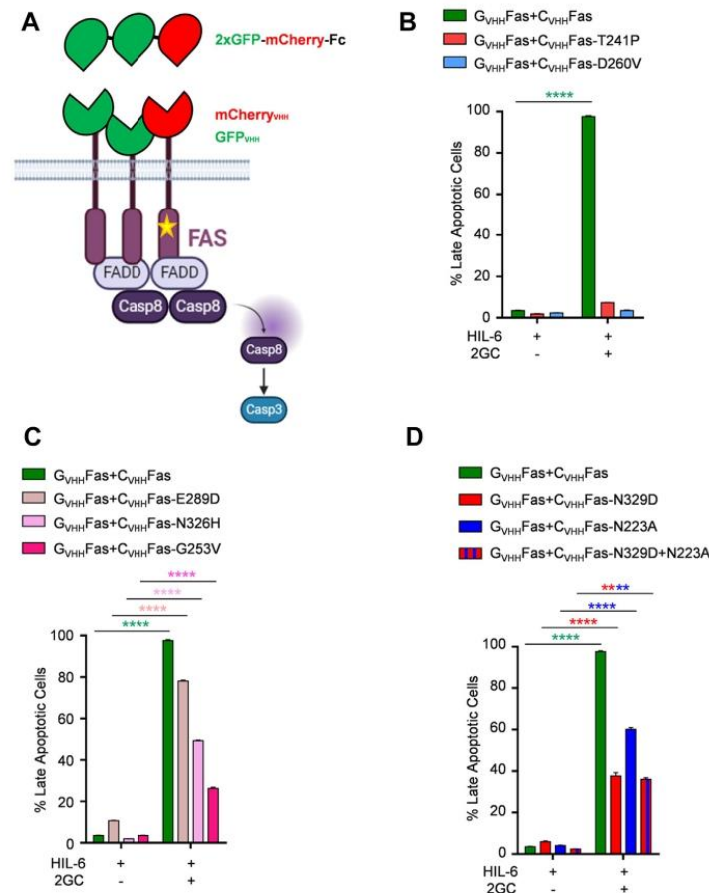


Figure 12. Verification of the dominant-negative effect of Fas selected mutation. A, schematic representation of synthetic C_{VHH} Fas-mutated and G_{VHH} Fas complex formation and activation by synthetic ligand 2GC. Apoptosis progression in (B) Ba/F3-gp130- G_{VHH} Fas- C_{VHH} Fas wt, Ba/F3-gp130- G_{VHH} Fas- C_{VHH} Fas-T241P, and Ba/F3-gp130- G_{VHH} Fas- C_{VHH} Fas-D260V; (C) Ba/F3-gp130- G_{VHH} Fas- C_{VHH} Fas wt, Ba/F3-gp130- G_{VHH} Fas- C_{VHH} Fas-E289D, Ba/F3-gp130- G_{VHH} Fas- C_{VHH} Fas-N326H, and Ba/F3-gp130- G_{VHH} Fas- C_{VHH} Fas-G253V; and in (D) Ba/F3-gp130- G_{VHH} Fas- C_{VHH} Fas wt, Ba/F3-gp130- G_{VHH} Fas- C_{VHH} Fas-N329D, Ba/F3-gp130- G_{VHH} Fas- C_{VHH} Fas-N223A, and Ba/F3-gp130- G_{VHH} Fas- C_{VHH} Fas-N329D+N223A. Cells were stimulated for 24 h with HIL-6 with and without 2GC. Cells were stained with 7-AAD and Annexin-V and analyzed by flow cytometry. Error bars indicate \pm SEM. **** p < 0.0001. HIL-6, Hyper-IL-6.

rapid tool such as Fas-SyCyR that supports *in silico* analysis can help to better understand Fas pathological roles and to establish suitable therapeutic strategies. Moreover, our Fas-SyCyR system may have a useful role in enhancing the application of synthetic biology for personalized therapies.

Experimental procedures

Cell culture

Murine Ba/F3-gp130 cells were obtained from Immunex. Ba/F3-gp130 and Ba/F3-gp130- C_{VHH} Fas cells were cultured at 37 °C with 5% CO_2 in a water-saturated atmosphere in Dulbecco's modified Eagle's Medium high glucose culture medium (GIBCO, Life Technologies) with 10% fetal calf serum (GIBCO, Life Technologies.), 60 mg/l penicillin, and 100 mg/l streptomycin (Genaxxon Bioscience GmbH), and supplemented with Hyper-IL-6, a fusion protein of IL-6 and soluble

IL-6 receptor (37). In detail, 0.2% (10 ng/ml) of conditioned medium was used from a stable clone of CHO-K1 cells secreting Hyper-IL-6 in the supernatant (stock solution approximately 10 μ g/ml as determined by ELISA).

Transduction and selection of cells

According to a prior description (38), Fas-SyCyR-coding pMOWS plasmids were used to retrovirally transduce Ba/F3-gp130 cells. The packing cell line was Phoenix-Eco cells (received from Ursula Klingmüller (DKFZ)). After transduction, cells were expanded as above described plus hygromycin B (1 mg/ml) (Carl Roth).

Cell surface detection of synthetic cytokine receptors

α -HA-tag mAb (C29F4; cat. #S724S; Cell Signaling Technology; dilution 1:1000) was used to identify the expression of

Fas-SyCyR (WT and all variants) in the transfected Ba/F3-gp130 cells. The cells were resuspended in 50 μ l of fluorescence-activated cell sorting (FACS) solution plus primary antibody HA after being washed in FACS buffer (PBS, 1% bovine serum albumin). Cells were washed and resuspended in 50 μ l FACS buffer with secondary antibody Alexa Fluor 488–conjugated Fab goat anti-rabbit IgG (cat. # A11070; 1:500) before being incubated for at least 1 h at room temperature. Cells were washed, resuspended in 200 μ l of FACS buffer, and the fluorescence signal was acquired by flow cytometry (BD FACSCanto II flow-cytometer, BD Biosciences). Data were analyzed with FlowJo V10 (<https://www.flowjo.com/solutions/flowjo/downloads>) (FlowJo LLC).

Proliferation assay

Ba/F3-gp130 cells were washed three times with PBS. 5×10^4 cells were suspended in Dulbecco's modified Eagle's Medium containing 10% FCS, 60 mg/l penicillin, and 100 mg/ml streptomycin. Cells were stimulated for 72 h in a volume of 100 μ l with Hyper-IL-6 and increasing concentration of synthetic ligand 3xmCherry-Fc (from 1×10^{-4} to 1×10^3 ng/ml). As previously described (6), the Cell Titer Blue Viability Assay (Promega) was used to determine the approximate number of viable cells by measuring the fluorescence (excitation 560 nm, emission 590 nm) using the Infinite M200 Pro plate reader (Tecan). After adding 20 μ l per well of Cell Titer Blue reagent (point 0), fluorescence was measured approximately every 20 min for up to 2 h. For each condition of an experiment, four wells were measured. All values were normalized by subtracting time point 0 values from the final measurement. Average of values of Ba/F3-gp130- C_{VHH} Fas WT cells stimulated with lowest concentration of 3xmCherry-Fc (1×10^{-4} ng/ml) was set as 100%, and the efficiency of the other C_{VHH} Fas variants was calculated accordingly.

Apoptosis assay

Ba/F3-gp130 cell lines were washed three times with PBS. 2.5×10^5 cells were seeded and stimulated for 24 h with HIL-6 (20 ng/ml) with and without 3xmCherry-Fc (100 ng/ml). Afterward, cells were washed twice with ice-cold PBS and resuspended in 50 μ l Annexin-V-binding buffer (BD Bioscience) and Annexin-V (1:600) (ImmunoTools). Following incubation at room temperature for 15 min in the dark, 1 μ l 7-AAD (R&D Systems) was added and diluted in 200 μ l of Annexin-V-binding buffer. Analysis was carried out by flow cytometry (BD FACSCanto II flow-cytometer, BD Biosciences). Data were evaluated using FlowJo V10 (FlowJo LLC).

Caspases 3/7 activation assay

Effector caspases 3 and 7 activation was detected using Amplitude Fluorimetric Caspase 3/7 Assay Kit *Green Fluorescence* (AAT Bioquest, cat. #13503). Briefly, Ba/F3-gp130 cell lines were washed three times with PBS. 1×10^5 cells were seeded in 100 μ l/well in 96 wells/plate and stimulated with 20 ng/ml HIL-6 with and without 100 ng/ml 3xmCherry-Fc.

After 6 h stimulation, 1 μ l of 1 mM caspase 3/7 inhibitor Ac-DEVD-CHO stock solution was added only in the selected samples for 10 min at room temperature, and subsequently, 100 μ l of caspase 3/7 working solution was added for at least 1 h at room temperature. Fluorescence intensity was measured at Ex/Em = 490/525 nm. For each condition of an experiment, three wells were measured. All values were normalized by subtracting background values from the final measurement. Caspase 3/7 activation after addition of 3xmCherry-Fc in Ba/F3-gp130 cells expressing C_{VHH} Fas was set to 100%, and the efficiency of the other C_{VHH} Fas variants was calculated accordingly.

Statistical analysis

Data are shown as mean \pm SEM. Multiple comparisons were determined with GraphPad Prism 6 (GraphPad Software) using one-way ANOVA column analyses. Statistical significance was set to $p < 0.05$ (**** $p < 0.0001$, *** $p < 0.001$, ** $p < 0.01$, * $p < 0.05$).

Structural analysis

Structural analysis of FAS and FADD was performed using UCSF Chimera (39) based on PDB 3EZQ.

Data availability

Lead contact

Further information and requests for resources and reagents should be directed to and will be fulfilled by the lead contact, Jürgen Scheller (jscheller@uni-duesseldorf.de).

Materials availability

This study did not generate new unique reagents. All cDNAs are available upon request.

Limitation of study

As shown and discussed before, this study shows early research upon the usage of a new synthetic cytokine system. Further studies are necessary to verify these findings *in vivo* and to analyze the potential combination with the CAR T-cell treatment.

Supporting information—This article contains supporting information.

Acknowledgments—We thank Petra Oprée and Yvonne Arlt for assistance. This work was funded by a grant from the Deutsche Forschungsgemeinschaft, Graduiertenkolleg VIVID.

Author contributions—A. R. M., P. R., S. M., D. M. F., and J. S. methodology; A. R. M. and F. B. investigation; A. R. M. and J. M. M. formal analysis; A. R. M. and J. S. writing—original draft; S. M., F. B., D. M. F., and J. S. supervision.

Conflict of interest—The authors declare that they have no conflicts of interest with the contents of this article.

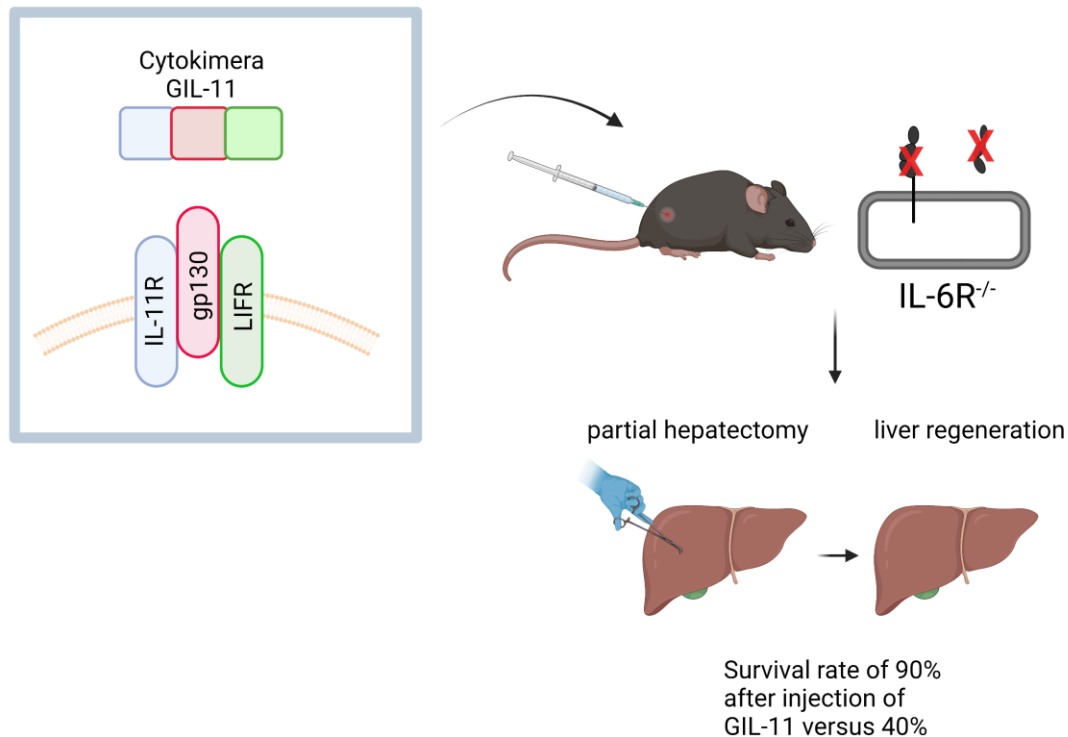
Synthetic Fas receptor platform

Abbreviations—The abbreviations used are: ALPS, autoimmune lymphoproliferative syndrome; CAR, chimeric antigen receptor; cDNA, complementary DNA; ClinVar, clinical variant; dbSNP, SNP database; FADD, fas-associated death domain; FACS, fluorescence-activated cell sorting; Fas-SyCyR, Fas synthetic cytokines receptor; GOF, gain-of-function; HA, human influenza hemagglutinin; HIL-6, Hyper-IL-6; LOF, loss-of-function; SCC, squamous cell carcinoma; TNF, tumor necrosis factor.

References

- Yi, F., Frazzette, N., Cruz, A., Klebanoff, C., and Siegel, R. (2018) Beyond cell death: new functions for TNF family cytokines in autoimmunity and tumor immunotherapy. *Trends Mol. Med.* **24**, 642–653
- Chinnaiyan, A. M., O'Rourke, K., Tewari, M., and Dixit, V. M. (1995) FADD, a novel death domain-containing protein, interacts with the death domain of Fas and initiates apoptosis. *Cell* **81**, 505–512
- Scott, F., Stec, B., Pop, C., Dobaczewska, M., Lee, J., Monosov, E., et al. (2009) The Fas-FADD death domain complex structure unravels signaling by receptor clustering. *Nature* **457**, 1019–1022
- Dostert, C., Grusdat, M., Letellier, E., and Brenner, D. (2019) The TNF family of ligands and receptors: communication modules in the immune system and beyond. *Physiol. Rev.* **99**, 115–160
- Chakravarti, D., and Wong, W. (2015) Synthetic biology in cell-based cancer immunotherapy. *Trends Biotechnol.* **33**, 449–461
- Mossner, S., Floss, D., and Scheller, J. (2021) Pro- and anti-apoptotic fate decisions induced by di- and trimeric synthetic cytokine receptors. *iScience* **24**, 102471
- Fridy, P. C., Li, Y., Keegan, S., Thompson, M. K., Nudelman, I., Scheid, J. F., et al. (2014) A robust pipeline for rapid production of versatile nanobody repertoires. *Nat. Met.* **11**, 1253–1260
- Rothbauer, U., Zolghadr, K., Muyldermans, S., Schepers, A., Cardoso, M. C., and Leonhardt, H. (2008) A versatile nanotrap for biochemical and functional studies with fluorescent fusion proteins. *Mol. Cell Proteomics* **7**, 282–289
- Mossner, S., Phan, H., Triller, S., Moll, J., Conrad, U., and Scheller, J. (2020) Multimerization strategies for efficient production and purification of highly active synthetic cytokine receptor ligands. *PLoS One* **15**, e0230804
- Engelowski, E., Schneider, A., Franke, M., Xu, H., Clemen, R., Lang, A., et al. (2018) Synthetic cytokine receptors transmit biological signals using artificial ligands. *Nat. Commun.* **9**, 2034
- Mossner, S., Kuchner, M., Fazel Modares, N., Knebel, B., Al-Hasani, H., Floss, D. M., et al. (2020) Synthetic interleukin 22 (IL-22) signaling reveals biological activity of homodimeric IL-10 receptor 2 and functional cross-talk with the IL-6 receptor gp130. *J. Biol. Chem.* **295**, 12378–12397
- Rieux-Laucat, F. (2017) What's up in the ALPS. *Curr. Opin. Immunol.* **49**, 79–86
- de Carvalho-Neto, P., dos Santos, M., de Carvalho, M., Mercante, A., dos Santos, V., Severino, P., et al. (2013) FAS/FASL expression profile as a prognostic marker in squamous cell carcinoma of the oral cavity. *PLoS One* **8**, e69024
- Robert, F., and Pelletier, J. (2018) Exploring the impact of single-nucleotide polymorphisms on translation. *Front. Genet.* **9**, 507
- Rauscher, R., and Ignatova, Z. (2018) Timing during translation matters: synonymous mutations in human pathologies influence protein folding and function. *Biochem. Soc. Trans.* **46**, 937–944
- Pettersen, E., Goddard, T., Huang, C., Meng, E., Couch, G., Croll, T., et al. (2021) UCSF ChimeraX: structure visualization for researchers, educators, and developers. *Protein Sci.* **30**, 70–82
- Kumar, P., Henikoff, S., and Ng, P. (2009) Predicting the effects of coding non-synonymous variants on protein function using the SIFT algorithm. *Nat. Protoc.* **4**, 1073–1081
- Service, R. (2021) AI reveals structures of protein complexes. *Science* **374**, 804
- Baek, M., DiMaio, F., Anishchenko, I., Dauparas, J., Ovchinnikov, S., Lee, G., et al. (2021) Accurate prediction of protein structures and interactions using a three-track neural network. *Science* **373**, 871–876
- Jumper, J., Evans, R., Pritzel, A., Green, T., Figurnov, M., Ronneberger, O., et al. (2021) Highly accurate protein structure prediction with AlphaFold. *Nature* **596**, 583–589
- Tauzin, S., Debure, L., Moreau, J.-F., and Legembre, P. (2012) CD95-mediated cell signaling in cancer: mutations and post-translational modulations. *Cell Mol. Life Sci.* **69**, 1261–1277
- Price, S., Shaw, P. A., Seitz, A., Joshi, G., Davis, J., Niemela, J. E., et al. (2014) Natural history of autoimmune lymphoproliferative syndrome associated with FAS gene mutations. *Blood* **123**, 1989–1999
- Bettinardi, A., Brugnani, D., Quiros-Roldan, E., Malagoli, A., La Grutta, S., Corraa, A., et al. (1997) Missense mutations in the Fas gene resulting in autoimmune lymphoproliferative syndrome: a molecular and immunological analysis. *Blood J. Am. Soc. Hematol.* **89**, 902–909
- Bodian, D. L., McCutcheon, J. N., Kothiyal, P., Huddleston, K. C., Iyer, R. K., Vockley, J. G., et al. (2014) Germline variation in cancer-susceptibility genes in a healthy, ancestrally diverse cohort: implications for individual genome sequencing. *PLoS One* **9**, e94554
- Fisher, C. R. (1995) *Toward an appreciation of hydrothermal-vent animals: Their environment, physiological ecology, and tissue stable isotope values* **91**. American Geophysical Union Geophysical Monograph Series, Washington DC: 297–316
- Jackson, C. E., Fischer, R. E., Hsu, A. P., Anderson, S. M., Choi, Y., Wang, J., et al. (1999) Autoimmune lymphoproliferative syndrome with defective Fas: genotype influences penetrance. *Am. J. Hum. Genet.* **64**, 1002–1014
- Martin-Villalba, A., Herr, I., Jeremias, I., Hahne, M., Brandt, R., Vogel, J., et al. (1999) CD95 ligand (Fas-L/APO-1L) and tumor necrosis factor-related apoptosis-inducing ligand mediate ischemia-induced apoptosis in neurons. *J. Neurosci.* **19**, 3809–3817
- Martin, D. A., Zheng, L., Siegel, R. M., Huang, B., Fisher, G. H., Wang, J., et al. (1999) Defective CD95/APO-1/Fas signal complex formation in the human autoimmune lymphoproliferative syndrome, type Ia. *Proc. Natl. Acad. Sci. U. S. A.* **96**, 4552–4557
- Kuehn, H. S., Caminha, I., Niemela, J. E., Rao, V. K., Davis, J., Fleisher, T. A., et al. (2011) FAS haploinsufficiency is a common disease mechanism in the human autoimmune lymphoproliferative syndrome. *J. Immunol.* **186**, 6035–6043
- Vaishnav, A. K., Orlinick, J. R., Chu, J.-L., Krammer, P. H., Chao, M. V., and Elkon, K. B. (1999) The molecular basis for apoptotic defects in patients with CD95 (Fas/Apo-1) mutations. *J. Clin. Invest.* **103**, 355–363
- Matsuura, K., Canfield, K., Feng, W., and Kurokawa, M. (2016) Metabolic regulation of apoptosis in cancer. *Int. Rev. Cell Mol. Biol.* **327**, 43–87
- Fu, Q., Fu, T. M., Cruz, A. C., Sengupta, P., Thomas, S. K., Wang, S., et al. (2016) Structural basis and functional role of intramembrane trimerization of the Fas/CD95 death receptor. *Mol. Cell* **61**, 602–613
- Si, W., Li, C., and Wei, P. (2018) Synthetic immunology: T-cell engineering and adoptive immunotherapy. *Synth. Syst. Biotechnol.* **3**, 179–185
- Rieux-Laucat, F., Le Deist, F., Hivroz, C., Roberts, I. A., Debatin, K. M., Fischer, A., et al. (1995) Mutations in Fas associated with human lymphoproliferative syndrome and autoimmunity. *Science* **268**, 1347–1349
- Larson, R. C., and Maus, M. V. (2021) Recent advances and discoveries in the mechanisms and functions of CAR T cells. *Nat. Rev. Cancer* **21**, 145–161
- Galgonek, J., Vymetal, J., Jakubec, D., and Vondrášek, J. (2017) Amino acid interaction (INTAA) web server. *Nucl. Acids Res.* **45**, W388–W392
- Fischer, M., Goldschmitt, J., Peschel, C., Brakenhoff, J. P., Kallen, K. J., and Wollmer, A. (1997) A bioactive designer cytokine for human hematopoietic progenitor cell expansion. *Nat. Biotechnol.* **15**, 142–145
- Floss, D. M., Mrotzek, S., Klöcker, T., Schröder, J., Grötzinger, J., Rose-John, S., and Scheller, J. (2013) Identification of canonical tyrosine-dependent and non-canonical tyrosine-independent STAT3 activation sites in the intracellular domain of the interleukin 23 receptor. *J. Biol. Chem.* **288**, 19386–19400
- Pettersen EF, G. T., Huang, C. C., Couch, G. S., Greenblatt, D. M., Meng, E. C., and Ferrin, T. E. (2004) UCSF Chimera—a visualization system for exploratory research and analysis. *J. Comput. Chem.* **25**, 1605–1612

4. Cytokimera GIL-11 rescued IL-6R deficient mice from partial hepatectomy-induced death by signaling via non-natural gp130:LIFR:IL-11R complexes.



Status: published in Commun Biol. 2023 Apr 15; 6(1):418.


doi: 10.1038/s42003-023-04768-4.

Impact factor: 6.5

Contribution: 10%

Contribute to formal analysis, validation, investigation, methodology, and correction of manuscript.

Cytokimera GIL-11 rescued IL-6R deficient mice from partial hepatectomy-induced death by signaling via non-natural gp130:LIFR:IL-11R complexes

Puyan Rafii¹, Christiane Seibel¹, Hendrik T. Weitz¹, Julia Ettich¹, Anna Rita Minafra¹, Patrick Petzsch², Alexander Lang³, Doreen M. Floss¹, Kristina Behnke¹, Karl Köhrer³, Jens M. Moll¹ & Jürgen Scheller¹  [✉]

All except one cytokine of the Interleukin (IL)-6 family share glycoprotein (gp) 130 as the common β receptor chain. Whereas Interleukin (IL)-11 signal via the non-signaling IL-11 receptor (IL-11R) and gp130 homodimers, leukemia inhibitory factor (LIF) recruits gp130:LIF receptor (LIFR) heterodimers. Using IL-11 as a framework, we exchange the gp130-binding site III of IL-11 with the LIFR binding site III of LIF. The resulting synthetic cytokimera GIL-11 efficiently recruits the non-natural receptor signaling complex consisting of gp130, IL-11R and LIFR resulting in signal transduction and proliferation of factor-dependent Ba/F3 cells. Besides LIF and IL-11, GIL-11 does not activate receptor complexes consisting of gp130:LIFR or gp130:IL-11R, respectively. Human GIL-11 shows cross-reactivity to mouse and rescued *IL-6R^{-/-}* mice following partial hepatectomy, demonstrating gp130:IL-11R:LIFR signaling efficiently induced liver regeneration. With the development of the cytokimera GIL-11, we devise the functional assembly of the non-natural cytokine receptor complex of gp130:IL-11R:LIFR.

¹Institute of Biochemistry and Molecular Biology II, Medical Faculty, Heinrich-Heine-University, 40225 Düsseldorf, Germany. ²Biological and Medical Research Center (BMFZ), Medical Faculty, Heinrich-Heine-University, Universitätsstraße 1, 40225 Düsseldorf, Germany. ³Cardiovascular Research Laboratory, Medical Faculty, University Hospital Düsseldorf, 40225 Düsseldorf, Germany. [✉]email: jscheller@uni-duesseldorf.de

Progress made in our understanding of cytokine receptor complex formation has enabled the implementation of various of approaches to assemble non-natural cytokine receptor complexes by designer cytokines. These include syntheleukins¹, neoleukins² and chimeric cytokines (cytokimeras)³ but also fully synthetic cytokine systems⁴. Syntheleukins are fusions of two dominant negative cytokine variants in which each variant binds only one receptor subunit¹. Neoleukins recapitulate some aspects of the natural cytokines but have a completely unrelated overall design and amino acid sequence². Cytokimeras are based on the framework of a natural cytokine with at least one receptor recognition site exchanged from a closely related cytokine³, a concept that has yet specifically been applied for the IL-6 type cytokines Interleukin (IL)-6 and ciliary neurotrophic factor (CNTF) in cytokine IC7³.

IL-6-type cytokines comprise IL-6, IL-11, IL-27, IL-30, IL-31, leukemia inhibitory factor (LIF), oncostatin M (OSM), CNTF, cardiotrophin-1 (CT-1), cardiotrophin-like cytokine (CLC) and neuropoietin^{5,6}. Apart from IL-31, all IL-6-type cytokines induce signal transduction via the common gp130 β -receptor^{7,8}, which activates signaling cascades including the JAK/STAT, Ras/Map kinase and phosphatidylinositol 3-kinase pathways^{8,9}. Whereas IL-6 and IL-11 signal via gp130 homodimers, the other cytokines signal via gp130 heterodimers. For instance, CNTF and LIF recruit gp130:LIF receptor (LIFR)^{10–12}. Moreover, the IL-6-type cytokines IL-6, IL-11 and CNTF have to interact with specific α -receptors (IL-6R, IL-11R, CNTFR, respectively) to allow binding to β -receptors^{10,11,13–15}.

In the landmark paper from 1999³, Kallen et al. suggested that the receptor recognition sites of cytokines have evolved as discontinuous modules which should principally be freely exchangeable between different cytokines. In general IL-6 type cytokines have in the case of LIF two or the case of IL-11 or CNTF three receptor binding sites, the site I for the α -receptor, site II and site III for the two β -receptors^{10–12}. Through the transfer of the LIFR binding site III of CNTF¹⁶ to binding site III of IL-6 the first of its kind cytokimera IC7 was described more than 20 years ago³. The abbreviation IC7 originates from the seventh tested chimeric Interleukin/CNTF variant. The module swap created a mash-up cytokine with IL-6R dependent activity on cells expressing gp130, IL-6R, and LIFR, instead of being dependent on IL-6R and gp130 in case of IL-6 or on gp130, CNTFR and LIFR in case of CNTF³. IC7 was recently shown to improve glucose tolerance and hyperglycemia, thereby preventing weight gain and liver steatosis in mice¹⁷. Apart from IC7 also other cytokines of the IL-6 cytokine family showed protective effects against obesity and insulin, including IL-6¹⁸, IL-27¹⁹ and CNTF²⁰. However, any therapeutic use of IL-6 is, however, out of the question because of its pronounced pro-inflammatory effects. The CNTF variant Axokine failed because of the early development of neutralizing CNTF antibodies²¹. IC7 combined the best of both worlds and showed no safety issues in non-human primates¹⁷.

Here, we developed the cytokimera GIL-11 which binds the non-natural receptor complex consisting of gp130:IL-11R:LIFR. We used IL-11 as a backbone for the transfer of site III from LIF, resulting in the cytokimera GIL-11. The highly active GIL-11 combines the activities of LIF^{22,23} and IL-11²⁴ in one molecule. Of note, a protective contribution of IL-11 in liver diseases has recently been challenged^{25,26}, making the therapeutic application of IL-11 undesirable. To demonstrate the therapeutic potential of GIL-11, we made use of IL-6R^{-/-} mice challenged in partial hepatectomy (PHX). IL-6R^{-/-} mice showed a high mortality rate of up to 80% versus 10% in wild-type mice following PHX²⁷. Here, we showed that GIL-11 rescued mice from death following partial hepatectomy.

Results

Cytokimera GIL-11: generation of chimeric IL-11:LIF synthetic cytokine. The IL-6 type cytokines share a common four-helix bundle structure consisting of four anti-parallel α -helices (A, B, C, and D) connected by two long cross-over loops (AB, CD) and one short loop (BC)²⁸. IL-6, IL-11 and CNTF bind to their α -receptor via binding site I which includes residues of the C-terminal AB loop and the C-terminal D-helix^{10,11,13–15}. Residues of the A- and C-helices of CNTF, LIF, and IL-6 constitute a gp130-binding site which is called site II^{10–12}. In IL-6 and IL-11 a second gp130-binding site III consists of amino acids residues of the N-terminal AB loop, the C-terminal CD loop, and the N-terminal D-helix^{10,11}. Site III in CNTF and LIF renders the contact to LIFR, whereas site II is in contact with gp130¹². For IL-11, site II and site III are in contact with gp130, whereas a third site (site I) recruits IL-11R¹¹. Of Notably, primary binding of IL-11 to IL-11R is mandatory for secondary binding to gp130^{11,29}. The site I,II,III paradigm for IL-11 and LIF is illustrated in Fig. 1a, b.

Of note IL-6 and IL-11 can form tetrameric and hexameric receptor complexes, consisting of one cytokine, one α -receptors and two gp130 or two cytokines, two α -receptors and two gp130^{10,30} (Fig. 1a). Albeit the tetrameric receptor complex is principally biologically active³¹, the structures of receptor complexes showed only hexameric assemblies^{10,11}. However, LIF exclusively signals via a trimeric receptor complex consisting of LIF engaged with one gp130 via site II and one LIFR via site III^{12,32} (Fig. 1b). Of note, LIF does not require an α -receptor to bind to its β -receptor combination of gp130 and LIFR¹². The binding of LIF to LIFR is, however, facilitated by an identically located binding site III in IL-11 to gp130 (Fig. 1b)¹². We hypothesized that the structure-based exchange of the partitioned binding site III of human IL-11 with site III of human LIF will render the resulting chimeric cytokine into a binder of the non-natural cytokine receptor composition gp130:IL-11R:LIFR, a cytokine class which we called cytokimera GIL-11. Since β -receptor binding of LIF is α -receptor independent¹², we were undecided if gp130:LIFR recruitment of the chimeric cytokine GIL-11 will be IL-11R dependent (Fig. 1c, d). Structural inspection of site III in IL-11 and LIF guided the design of the cytokimera GIL-11 with the framework of IL-11 and an exchange of site III from LIF^{11,33}. IL-11 consists of 199 amino acids, we pinpointed the partitioned site III from amino acids 58–72 for IIa, 111–128 for IIb and 162–179 for IIc. LIF has 202 amino acids with partitioned site III located from amino acids 64–88 for IIa, 119–138 for IIb and 172–189 for IIc (Fig. 1d–f, Supplementary Fig. 1A). We decided to transfer the complete binding site from LIF to IL-11, albeit this resulted in somewhat longer GIL-11 cytokimera with 211 amino acids than the original IL-11. Molecular modeling suggested that the transfer of the entire site III amino acid stretches should not interfere with the overall architecture and folding of the cytokimera GIL-11 (Fig. 1d, e)^{11,12}. Comparable to trimeric LIF:gp130:LIFR complexes, GIL-11 will only form tetrameric GIL-11:IL-11R:gp130:LIFR receptor complexes. The tetrameric assembly will be based on the requirement of GIL-11 for the LIFR. Whereas gp130 has two cytokine binding sites in one receptor molecule, LIFR has only one cytokine binding site. The LIFR interacts only with site III of LIF/GIL-11, whereas gp130 contacts site II of LIF/GIL-11. In this setting, the second contact site in gp130 remains free, because site III of LIF/GIL-11 cannot interact with gp130 (Fig. 1c) and the formation of hexameric 2xGIL-11:2xIL-11R:1xLIFR:1xgp130 complexes can be excluded.

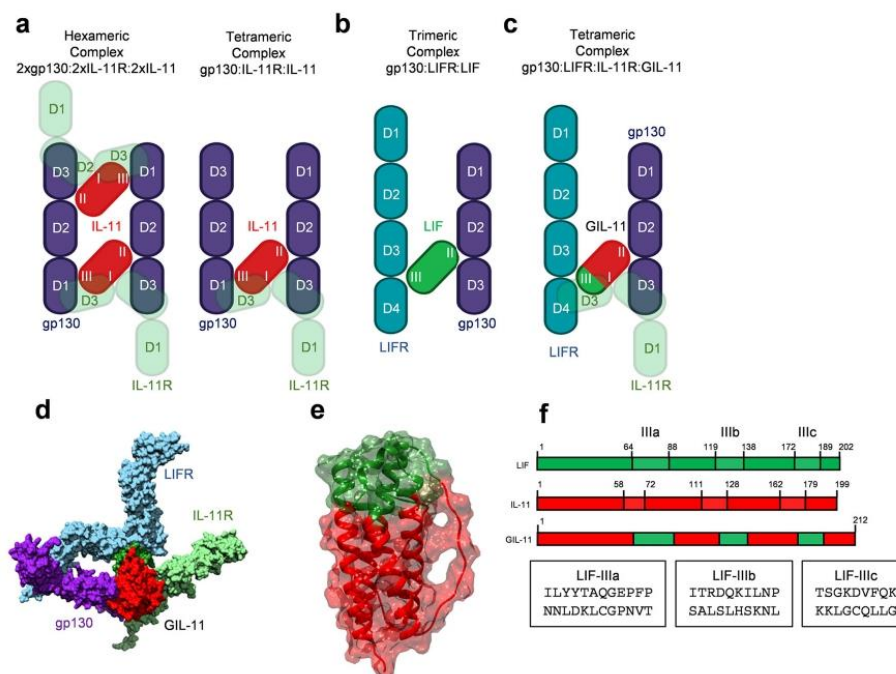


Fig. 1 Design of the cytokinera GIL-11. **a** schematic illustration of the tetrameric and hexameric IL-11:IL-11R:gp130 receptor complex possibilities. IL-11 initially binds to IL-11R via site I. gp130 is recruited into this complex via major interactions between site III of IL-11 and D1 (Ig-like) of gp130 and site II of IL-11 and D2/D3 (cytokine binding module (CBM)) of gp130. **b** schematic illustration of the trimeric LIF:gp130:LIFR complex. LIF binds via site III to D3/D4 of LIFR and via site II to D2/D3 of gp130. **c** schematic illustration of the tetrameric GIL-11:IL-11R:gp130:LIFR complex. GIL-11 binds via site III to D3/D4 of LIFR, via site II to D2/D3 of gp130 and via site I to D2/D3 of IL-11R. **d** schematic illustration (left) and space fill model (right) of the tetrameric GIL-11:IL-11R:gp130 (PDB 6O4P¹¹, 2Q7N⁸³, 1P9M¹⁰). GIL-11 binds via site I to IL-11R, via site II to gp130 and via site III to LIFR. **e** Combined transparent space fill/band model of GIL-11, red: IL-11, green: exchanged region by LIF. **f** Structure-based schematic sequence alignment of hIL-11 (PDB 6O4O¹¹), hLIF (PDB 1PVH³³) and the resulting GIL-11. Site IIIa, b, c residues are highlighted in green and red boxes.

GIL-11 induce JAK/STAT signaling and cellular proliferation via the non-natural gp130:IL-11R:LIFR cytokine receptor complex. The proliferation of the murine pre-B cell line Ba/F3 is IL-3 dependent³⁴. After the introduction of human gp130 plus additional family receptors (IL-6R, IL-11R^{35,36}, OSMR and LIFR (Supplementary Fig. 1B, C)), proliferation shifted to the respective IL-6 type cytokine receptor combination. In case of Ba/F3-gp130 cells, proliferation is induced by IL-11 and the soluble IL-11R or by the corresponding fusion protein Hyper IL-11 (HIL-11)³⁷, additional introduction of IL-11R renders these cells IL-11 dependent. Co-expression of gp130 and IL-6R renders these cells responsive to IL-6. Ba/F3 cells expressing gp130 and LIFR proliferate with LIF and OSM, whereas gp130 and OSMR expressing Ba/F3 cells are responsive to OSM. Using our Ba/F3 cell repertoire with the eight different receptor combinations gp130, gp130:IL-11R, gp130:LIFR, gp130:OSMR, gp130:IL-11R:OSMR, gp130:IL-6R:LIFR and gp130:IL-11R:LIFR, we determined the qualitative proliferation properties after addition of IL-11, HIL-11, OSM, LIF and GIL-11. Using a rather high concentration of 500 ng/ml to initially assess possible receptor cross-activation. GIL-11 specifically only induced proliferation of Ba/F3-gp130:IL-11R:LIFR cells but not of any other tested cell line, suggesting that GIL-11 signals via gp130:IL-11R:LIFR (Fig. 2a, Supplementary Data). As expected, only HIL-11 induced proliferation of all Ba/F3 cells lines, since they all express gp130. All Ba/F3 cells expressing gp130 and IL-11R proliferated with IL-11. Expression

of gp130 and LIFR resulted in LIF and OSM-induced proliferation, whereas cells expressing gp130 and OSMR cells were OSM selective. Next, we analyzed the phosphorylation of STAT3 which is the major hallmark of IL-6 type cytokine JAK/STAT signaling in our Ba/F3 cell portfolio. As expected from the cytokine-induced Ba/F3 cell proliferation assays (Fig. 2a), STAT3 phosphorylation in Ba/F3 cells was induced by the following cytokine:cytokine receptor combinations: HIL-11 via gp130; IL-11 via gp130:IL-11R; OSM via gp130:OSMR; OSM and LIF via gp130:LIFR (Fig. 2b; Supplementary Figs. 2, 3). Importantly, sustained STAT3 phosphorylation for GIL-11 was only observed in Ba/F3 cells expressing the receptor combination gp130, IL-11R and LIFR (Fig. 2b; Supplementary Figs. 2, 3). Taken together, our data also showed that GIL-11 specifically activated signaling via the non-natural receptor complex consisting of gp130:IL-11R:LIFR.

GIL-11 transcriptome pattern differs from IL-11 and LIF. To evaluate the transcription profile of GIL-11, Ba/F3-gp130:IL-11R:LIFR cells were stimulated for 40 min with GIL-11, IL-11 or LIF with 100-fold EC₅₀ concentrations to ensure maximum signal transduction and comparability for transcriptome analysis. Venn diagram shows 37 genes were at least 1.5-fold upregulated by GIL-11, IL-11 and LIF (Fig. 3a, b). Interestingly, 31 genes were at least 1.5-fold upregulated by IL-11 and LIF but not by GIL-11.

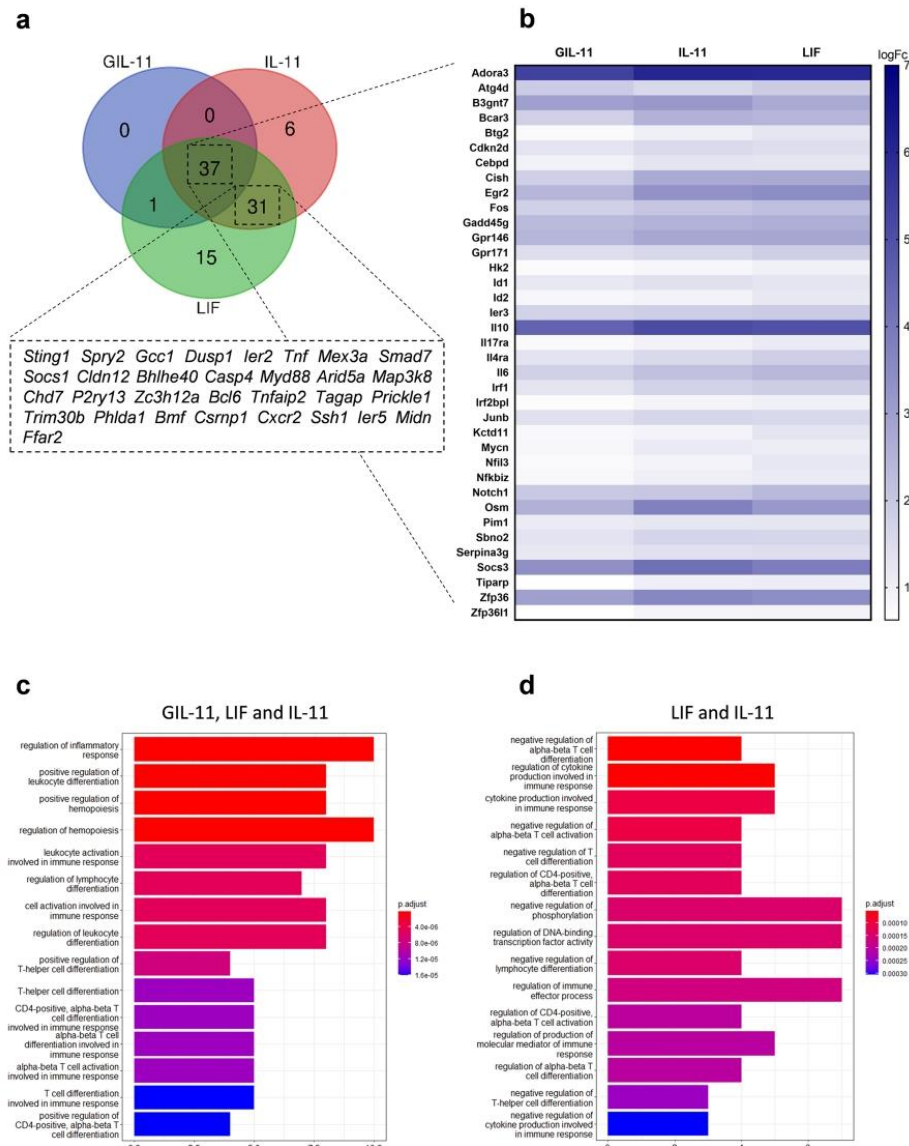
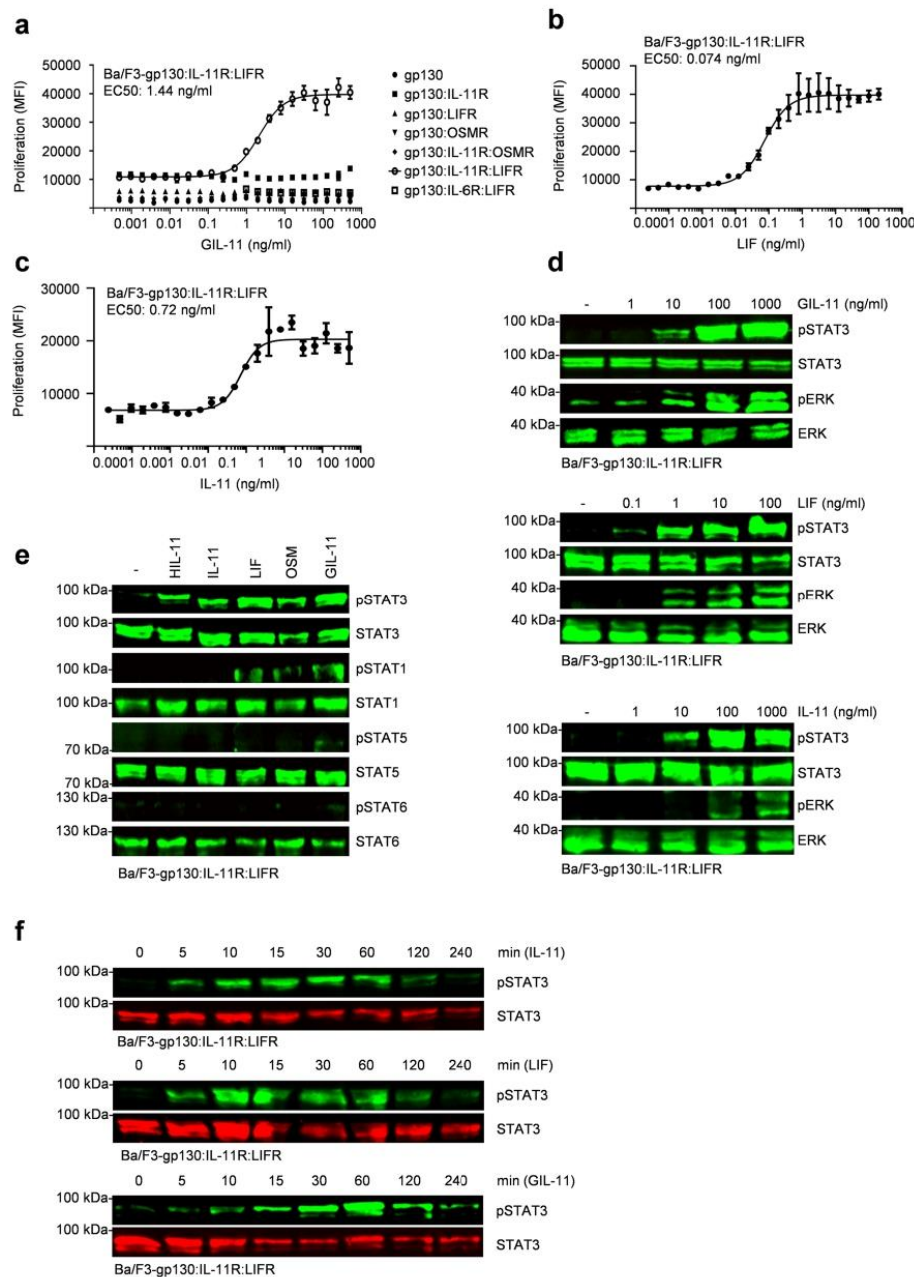


Fig. 3 Transcriptome profiling of Ba/F3-gp130:IL-11R:LIFR cells demonstrate attenuated gene activation by GIL-11. **a** Venn Diagram shows overlap of genes that are activated by natural or synthetic cytokines. Filter: $p < 0.05$ including false discovery rate correction; $|FC| \geq 1.5$. **b** Heat map shows genes that are significant increased by GIL-11 vs untreated, IL-11 vs untreated and LIF vs untreated. Scale bar shows log fold change. Filter: $p < 0.05$ including false discovery rate correction; $|FC| \geq 1.5$. **c** Gene ontology analysis of common gene pathways that are activated by GIL-11, LIF and IL-11 (**c**) and by the natural cytokines only (**d**). Filter: $p < 0.05$ including false discovery rate correction; $|FC| \geq 1.5$. X-axis: number of genes involved in common gene pathway. Gene expression accession code: GSE226064.

STAT1, as well as STAT5, activation was observed³⁸. Here, all cytokines induced sustained STAT3 phosphorylation. Interestingly, IL-11 and IL-11 did not induce STAT1 and STAT5 phosphorylation, whereas LIF, OSM, and GIL-11 also induced STAT1 phosphorylation (Fig. 4e, Supplementary Fig. 6; 2c, d). STAT5 phosphorylation was only seen for GIL-11. As expected, none of the cytokines induced STAT6 phosphorylation. Next, we stimulated

Ba/F3-gp130:LIFR:IL-11R cells with IL-11, LIF, and GIL-11 for 5–240 min. STAT3 phosphorylation begins 5 min after cytokine stimulation, with a peak after 30–60 min. As typically seen for IL-11 and LIF, STAT3 phosphorylation declines after 120–240 min, which is likely due to SOCS3 upregulation³⁹ (compare Fig. 3b, transcriptomic analysis, SOCS3 upregulation by 10.5-fold GIL-11, 18.4-fold IL-11, 14.5-fold LIF), the same regulation of STAT3



phosphorylation was seen for the cytokine GIL-11 (Fig. 4f, Supplementary Fig. 7). Taken together, the activity of GIL-11 is in the same concentration range as the precursor cytokine IL-11, demonstrating that the expansion of the receptor requirement by site III transfer did not affect the overall biological cytokine activity.

GIL-11:soluble IL-11R complexes are poor inducer of trans-signaling via gp130:LIFR. The α -receptor dependent cytokines

IL-6 and IL-11 activate cells via the signal transducing receptor gp130 and the non-signaling membrane-bound IL-6R or IL-11R, respectively^{37,40}. Here, we showed GIL-11 signals via the membrane-bound IL-11R in complex with the heterodimeric gp130:LIFR complex. Signaling via the membrane-bound IL-11R is called classic-signaling. The IL-11R also exists as a soluble receptor that in complex with IL-11 activates cells lacking membrane-bound α -receptor expression in a process called trans-

Fig. 4 Biological activity of GIL-11 is comparable to IL-11 and LIF. **a** Proliferation of Ba/F3, Ba/F3-gp130, Ba/F3-gp130:IL-11R, Ba/F3-gp130:LIFR, Ba/F3-gp130:OSMR, Ba/F3-gp130:IL-11R:OSMR, Ba/F3-gp130:IL-6R:LIFR, Ba/F3-gp130:LIFR:IL-11R cells in the presence and absence of increasing concentrations of GIL-11 (0.0005–500 ng/ml). **b** Proliferation of Ba/F3-gp130:IL-11R:LIFR cells in the presence and absence of increasing concentrations of LIF (0.000025–200 ng/ml). **c** Proliferation of Ba/F3-gp130:IL-11R:LIFR cells in the presence and absence of increasing concentrations of IL-11 (0.000025–500 ng/ml). **a–c** Error bars define \pm SEM. One representative experiment with three biological replicates out of three is shown. **d** STAT3 and ERK activation in Ba/F3-gp130:LIFR:IL-11R cells without cytokine (–) and after stimulation with increasing amounts of GIL-11 (1, 10, 100, 1000 ng/ml), LIF (0.1, 1, 10, 100 ng/ml) and IL-11 (1, 10, 100, 1000 ng/ml) for 15 min. Equal amounts of proteins (50 μ g/lane) were analyzed via specific antibodies detecting phospho-STAT3, STAT3, ERK and phospho-ERK. Western blot data shows one representative experiment out of three. **e** STAT1,3,5,6 activation in Ba/F3-gp130:IL-11R:LIFR cells without cytokine (–) and after stimulation with 50 ng/ml HIL-11, 50 ng/ml IL-11, 10 ng/ml LIF, 10 ng/ml OSM, 500 ng/ml GIL-11 for 15 min. Equal amounts of proteins (50 μ g/lane) were analyzed via specific antibodies detecting phospho-STATs and STATs. Western blot data shows one representative experiment out of three. **f** Time-dependent STAT3 activation of Ba/F3-gp130:IL-11R:LIFR cells with the cytokines IL-11 (200 ng/ml), LIF (20 ng/ml) and GIL-11 (200 ng/ml) for the indicated time. Equal amounts of proteins (50 μ g/lane) were analyzed via specific antibodies detecting phospho-STAT3 and STAT3.

signaling^{37,40}. Here, we analyzed to what extent GIL-11 induced trans-signaling in complex with soluble IL-11R (sIL-11R) on cells expressing gp130 and LIFR. Ba/F3-gp130:LIFR cells were stimulated with a fixed concentration of 100 ng/ml sIL-11R and increasing concentrations of GIL-11 (2–2000 ng/ml). For comparison, we used the same fixed concentration of sIL-11R and increasing cytokine concentrations for IL-11. Whereas the EC50 for IL-11 was 71.6 ng/ml for 100 ng/ml sIL-11R (Fig. 5a; Supplementary Data), GIL-11 hardly induced proliferation via sIL-11R. It was not possible to calculate an EC50 value, because even the concentration of 2000 ng/ml GIL-11 was not sufficient to reach maximal cellular proliferation (Fig. 5b; Supplementary Data). Therefore, we evaluated the intracellular signal transduction in Ba/F3-gp130:LIFR cells stimulated with comparably high concentrations of 1 μ g/ml GIL-11 and 2 μ g/ml sIL-11R. Here, GIL-11:sIL-11R complexes resulted in sustained STAT3 activation. sgp130Fc is a selective IL-6/IL-11 trans-signaling inhibitor, which inhibits LIF signaling at least 100–1000-fold less efficiently than IL-6/IL-11 trans-signaling^{40,41}. Next, we tested if sgp130Fc inhibits GIL-11 trans-signaling. As shown in Fig. 5c, Supplementary Fig. 8, sgp130Fc (10 μ g/ml) did not inhibit STAT3 phosphorylation induced by GIL-11 (1 μ g/ml):sIL-11R (2 μ g/ml) trans-signaling in Ba/F3-gp130:LIFR cells (Fig. 5c, Supplementary Fig. 8). For Ba/F3-gp130:LIFR cells, concentrations for GIL-11 (0.5 μ g/ml) or IL-11 (0.5 μ g/ml) plus sIL-11R (1 μ g/ml) were chosen to allow cellular proliferation via trans-signaling. Titration of increasing concentrations of sgp130Fc resulted in the inhibition of IL-11 trans-signaling (IC50 = 22.5 ng/ml, Fig. 5d; Supplementary Data), whereas even the highest concentration of 10 μ g/ml sgp130Fc was not able to inhibit GIL-11 trans-signaling. In principle, GIL-11 is able to signal via trans-signaling, albeit with a much lesser efficiency compared to IL-11. Like LIF, GIL-11 trans-signaling is not inhibited by sgp130Fc at least under conditions that are sufficient to block IL-11 trans-signaling^{37,40,41}. As shown in Fig. 2a, the proliferation of Ba/F3-gp130:LIFR and Ba/F3-gp130:IL-11R was induced by LIF and IL-11, respectively, but not by GIL-11. We could, however, not exclude that GIL-11 binds to IL-11R:gp130 on Ba/F3-gp130:IL-11R cells and blocks IL-11 signaling or to LIFR on Ba/F3-gp130:LIFR cells and blocks LIF signaling. Using cytokine co-incubation for Ba/F3-gp130:IL-11R with IL-11 and GIL-11 and for Ba/F3-gp130:LIFR with LIF and GIL-11 did not result in inhibition of cellular proliferation even at a 20-fold mass concentration excess of GIL-11 over IL-11 and a 200-fold GIL-11 excess over LIF (Fig. 5e; Supplementary Data). We conclude that GIL-11 did not interfere with IL-11 and LIF signaling at least for the concentration range tested.

Human GIL-11 activates signal transduction via the murine gp130:IL-11R:LIFR cytokine receptor complex. Human IL-11 and LIF are cross-reactive between mice and men^{42–44}. We

analyzed if human GIL-11 also activates murine cells expressing murine gp130:IL-11R:LIFR chains. We chose the murine myoblast cell line C2C12. C2C12 cells were stimulated with human HIL-11 (200 ng/ml), human IL-11 (200 ng/ml), human LIF (10 ng/ml) and GIL-11 (200 ng/ml). HIL-11 and LIF induced sustained STAT3 phosphorylation whereas IL-11 and GIL-11 did not, suggesting that C2C12 cells express gp130 and LIFR but lack the expression of IL-11R (Fig. 6a, Supplementary Fig. 9). We transfected C2C12 cells with a plasmid coding for murine IL-11R cDNA. Resulting in mIL-11R expression, which makes these cells responsive to IL-11 and GIL-11 as shown by STAT3 phosphorylation (Fig. 6a, Supplementary Fig. 9). We also stimulated murine embryonic fibroblast cells line NIH/3T3 with 1, 10, 100 and 1000 ng/ml human GIL-11, IL-11 and 0.1, 1, 10 and 100 ng/ml LIF. LIF and IL-11 induced STAT3 phosphorylation in NIH/3T3 as shown by Western blotting (Fig. 6b, Supplementary Fig. 10), because these cells express gp130, LIFR and IL-11R⁴⁵. Dose-dependent cellular stimulation showed 10–100 ng/ml of GIL-11 and IL-11 were needed to achieve sustained STAT3 phosphorylation in murine NIH/3T3. Next, we injected 5, 10 and 20 μ g GIL-11 intraperitoneally into wild-type mice. 30 min after injection mice were sacrificed and heart, liver and spleen tissue were removed. Analysis of STAT3 phosphorylation by Western blotting showed that at least 10 μ g/mouse GIL-11 was sufficient to induce sustained STAT3 phosphorylation in the heart, liver and spleen (Fig. 6c, Supplementary Fig. 11). Taken together, our data demonstrated that human GIL-11 activates the murine receptor combination gp130:IL-11R:LIFR.

GIL-11 rescued IL-6R^{−/−} mice from death following partial hepatectomy. Interleukin-6 (IL-6) is critically involved in liver regeneration following partial hepatectomy (PHX). IL-6^{−/−} and IL-6R^{−/−} mice have a high mortality rate of 40–80% versus 10% in wild-type mice accompanied by decreased STAT3 phosphorylation and diminished proliferation of hepatocytes^{27,46–50} following PHX. We have previously shown that Hyper IL-6 (HIL-6) injection 24 h before and directly after surgery rescued mice from death following partial hepatectomy⁵¹. Here, 10 μ g/mouse GIL-11 was injected 24 h before and directly after PHX in IL-6R^{−/−} mice. The overall survival rate of IL-6R^{−/−} mice 9 days after PHX was about 40%, whereas IL-6R^{−/−} mice injected with two doses of GIL-11 had a survival rate of 90% (Fig. 7a; Supplementary Data). As seen before²⁷, body weight 9 days after PHX was not different in surviving IL-6R^{−/−} mice, irrespective if injected with GIL-11 or PBS, whereas liver weight to body weight ratio was slightly decreased (Fig. 7b, c; Supplementary Data). However, we noticed that untreated IL-6R^{−/−} mice had a bigger spleen weight compared to GIL-11 treated IL-6R^{−/−} mice (Fig. 7d; Supplementary Data). Gene expression analysis showed increased expression of fibrotic marker α SMA and acute phase response gene SAA1 in IL-

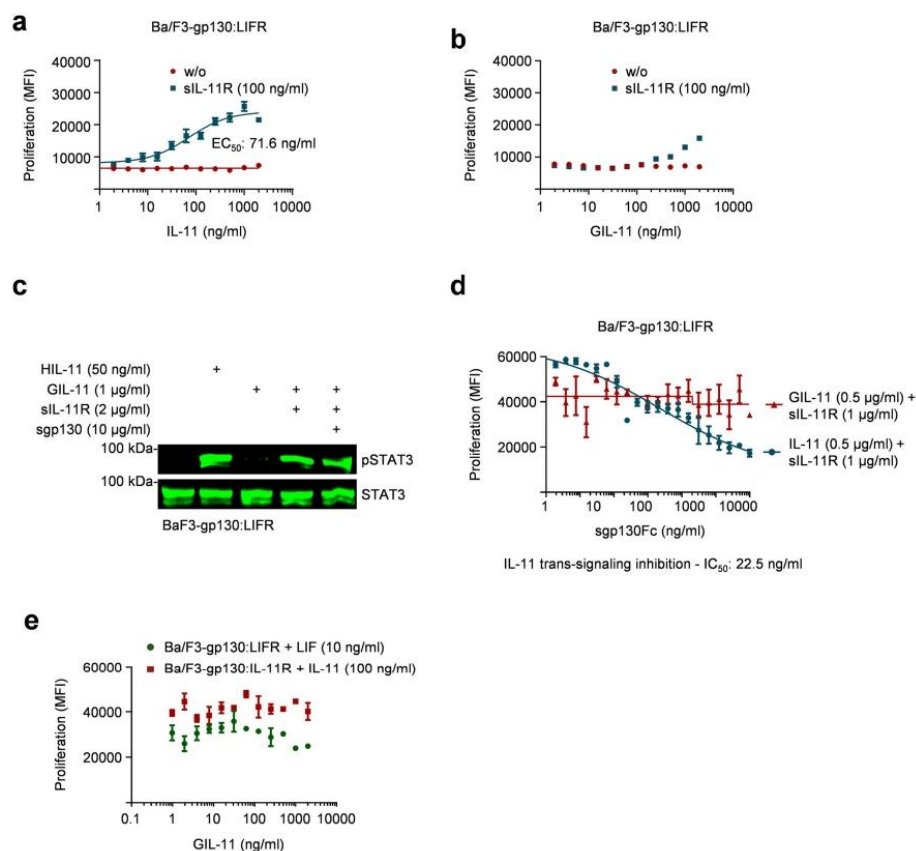


Fig. 5 GIL-11:IL-11 complexes induce trans-signaling via gp130:LIFR. **a** Proliferation of Ba/F3-gp130:LIFR cells in the presence and absence of fixed concentrations of sIL-11R (0 or 100 ng/ml) and increasing concentrations of IL-11 (1–2000 ng/ml). One representative experiment out of three is shown. **b** Proliferation of Ba/F3-gp130:LIFR cells in the presence and absence of fixed concentrations of sIL-11R (0 or 100 ng/ml) and increasing concentrations of GIL-11 (1–2000 ng/ml). One representative experiment out of three is shown. **c** STAT3 activation in Ba/F3-gp130:LIFR cells without cytokine (-) and after stimulation with HIL-11 (50 ng/ml), GIL-11 (1 µg/ml), GIL-11 (1 µg/ml):sIL-11R (2 µg/ml), GIL-11 (1 µg/ml):sIL-11R (2 µg/ml):sgp130Fc (10 µg/ml) for 15 min. Equal amounts of proteins (50 µg/lane) were analyzed via specific antibodies detecting phospho-STAT3 and STAT3. Western blot data shows one representative experiment out of three. **d** Proliferation of Ba/F3-gp130:LIFR cells in the presence and absence of fixed concentrations of IL-11 (0.5 µg/ml):sIL-11R (1 µg/ml) or GIL-11 (0.5 µg/ml):sIL-11R (1 µg/ml) and increasing concentrations of sgp130Fc (1–10,000 ng/ml). One representative experiment out of three is shown. **e** Proliferation of Ba/F3-gp130:LIFR cells in the presence and absence of fixed concentrations of LIF (10 ng/ml) and increasing concentrations of GIL-11 (1–2000 ng/ml) (green). Proliferation of Ba/F3-gp130:IL-11R cells in the presence and absence of fixed concentrations of IL-11 (100 ng/ml) and increasing concentrations of GIL-11 (1–2000 ng/ml) (red). Error bars define \pm SEM. One representative experiment with three biological replicates out of three is shown.

6R^{-/-} mice treated with GIL-11 compared to untreated IL-6R^{-/-} mice directly following PHX (Fig. 7e; Supplementary Data). Taken together, our data showed that GIL-11 rescued IL-6R^{-/-} mice from death following partial hepatectomy.

Discussion

Our experiments define a human chimeric designer cytokine that induces family-typical JAK/STAT signaling and cellular proliferation via the non-natural gp130:IL-11R:LIFR complex with cross-species specificity from mouse to man. The exchange of site III from LIF to IL-11 results in the cytokimera GIL-11 with receptor binding properties thus far not found in nature. The prototype cytokimera IC7, based on the IL-6 scaffold with site III from CNTF, served as a blueprint for GIL-11³, IC7 and GIL-11

revealed that the overall scaffold within the IL-6 type cytokine family is exchangeable due to a general modular architecture. Since the transfer is restricted to site III, it remains to be seen whether the transfer of site I and site II will also be feasible. With the second of its kind, GIL-11 has unique features which separates it from IC7. First of all, IC7 recruits the receptor complex gp130:IL-6R:LIFR, whereas GIL-11 assembles gp130:IL-11R:LIFR, meaning that only those cells expressing IL-11R are targeted by GIL-11. This might be an important issue with respect to cellular specificity in vivo. Whereas the common β -receptor gp130 is ubiquitously expressed, expression of LIFR and also the α -receptors is restricted and therefore more cell type specific. Unlike IL-6R, which is mainly found on immune cells and hepatocytes^{52,53}, the distribution of membrane-bound IL-11R

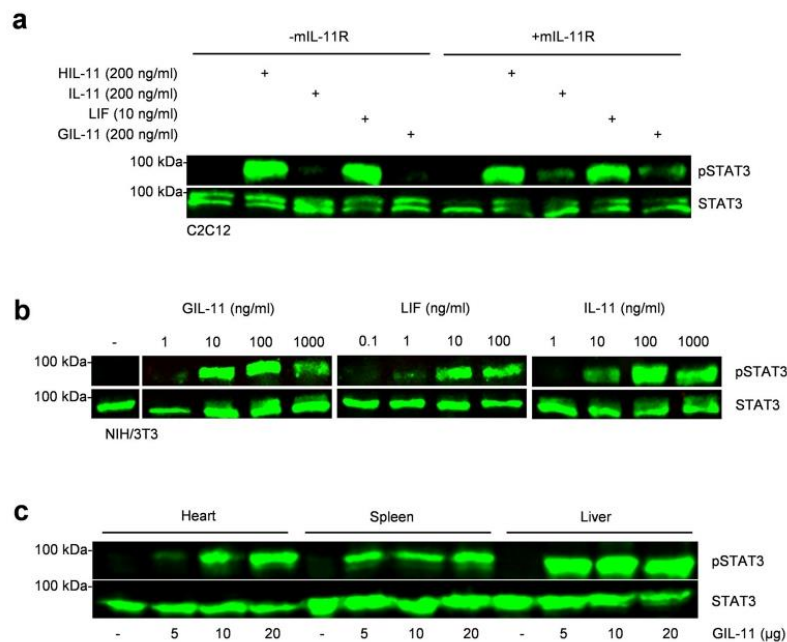


Fig. 6 Human GIL-11 transmits signal transduction via the non-natural murine gp130:IL-11R:LIFR cytokine receptor complex. **a** STAT3 activation in untransfected and transfected with a cDNA coding for murine IL-11R murine myoblasts (C2C12) without cytokine (-) and after stimulation with HIL-11 (200 ng/ml), IL-11 (200 ng/ml), LIF (10 ng/ml), GIL-11 (200 ng/ml) for 15 min. Equal amounts of proteins (50 μg/lane) were analyzed via specific antibodies detecting phospho-STAT3 and STAT3. Western blot data shows one representative experiment out of three. **b** STAT3 activation in murine fibroblast NIH/3T3 without cytokine (-) and after stimulation with increasing amounts of GIL-11 (1, 10, 100, 1000 ng/ml), LIF (0.1, 1, 10, 100 ng/ml) and IL-11 (1, 10, 100, 1000 ng/ml) for 20 min. Equal amounts of proteins (50 μg/lane) were analyzed via specific antibodies detecting phospho-STAT3 and STAT3. Western blot data shows one representative experiment out of three. **c** STAT3 activation in heart, liver and spleen after injection of 5, 10 or 20 μg/ml GIL-11. Mice were sacrificed 30 min after intraperitoneal cytokine injection. Equal amounts of proteins (50 μg/lane) were analyzed via specific antibodies detecting phospho-STAT3 and STAT3. Western blot data shows one representative experiment out of three.

appears to be more balanced⁵⁴ including cardiomyocytes⁵⁵, fibroblasts⁵⁶ and epithelial cells⁵⁷.

Due to their limited expression profile, the α-receptors IL-6R, IL-11R and CNTFR confer a second layer of cellular specificity⁶. We hypothesize that the recruitment of synthetic complexes eventually results in a gain-of-function in cellular specificity and thereby might promote beneficially and reduce negative effects during in vivo applications of designer cytokines in synthetic biology. Of note, IC7Fc selectively activates metabolic pathways resulting in increased fatty acid oxidation accompanied by prevented steatosis, increased energy dissipation accompanied by weight loss, muscle hypertrophy and preserved lean mass with improved bone stability in mice¹⁷. In contrast to IL-6 and CNTF, IC7 injection has proven to be safe in both, mice and non-human primate macaques without promoting excess inflammatory responses^{3,17,58}.

Moreover, it was assumed the transcriptomic profile of GIL-11 could cover with LIF, since both recruit and activate the gp130 and LIFR heterodimers, whereas IL-11 recruits gp130 homodimers. Interestingly, GIL-11 acted more in between of IL-11 and LIF but with an attenuated extent. It has been proposed that the geometry and affinity of the ligand-receptor complex may account for functional diversity of particular IL-6 type cytokines⁵⁹. The lack of GIL-11s ability for some gene expression might be beneficial. *Smad7* is a negative regulator of TGF-β signaling and seems to be involved in pathogenesis of inflammatory bowel diseases (IBDs), including Crohn's disease (CD) and ulcerative colitis (UC) and

mediates intestinal inflammation⁶⁰. Overexpression of *MyD88* has been showed to decrease cardiac function and contributes to cardiovascular autoimmune diseases^{61–63}. *Arid5a* is assumed to contribute to cytokine storm. Apart from that *Arid5a*^{-/-} mice are refractory to endotoxin shock, bleomycin-induced lung injury, and inflammatory autoimmune disease⁶⁴.

Secondly, the natural cytokines IC7, IL-6 and CNTF are dependent on α-receptor binding before binding to gp130 and LIFR³, meaning that shaping of the CNTF-derived binding site III in IC7 is a direct consequence of IL-6R binding, as after binding of CNTF to CNTFR. This situation is different for GIL-11. Here, we introduced the α-receptor independent binding site III from LIF into the α-receptor dependent IL-11. As shown here, GIL-11 activates the gp130:LIFR receptor complex only after binding to the non-signal transducing IL-11R. Moreover, GIL-11 was not able to inhibit LIF signaling on Ba/F3-gp130:LIFR cells, which should have been the case, if GIL-11 can bind to LIFR in the absence of the IL-11R. Taken together our experiments showed that albeit the original binding site context of LIF-site III to LIFR is α-receptor independent, re-formatting of LIF-site III into the IL-11 scaffold makes the LIF-site III binding α-receptor dependent. Therefore, not the exact binding site III amino acid composition but rather the interconnection mediated by α-helical shifts of site I with site III defines whether a cytokine is α-receptor dependent or independent⁶⁵.

With respect to biological activity, GIL-11 (EC50: 1.44 ng/ml) is comparable to IL-11 (EC50: 0.72 ng/ml) but less effective than

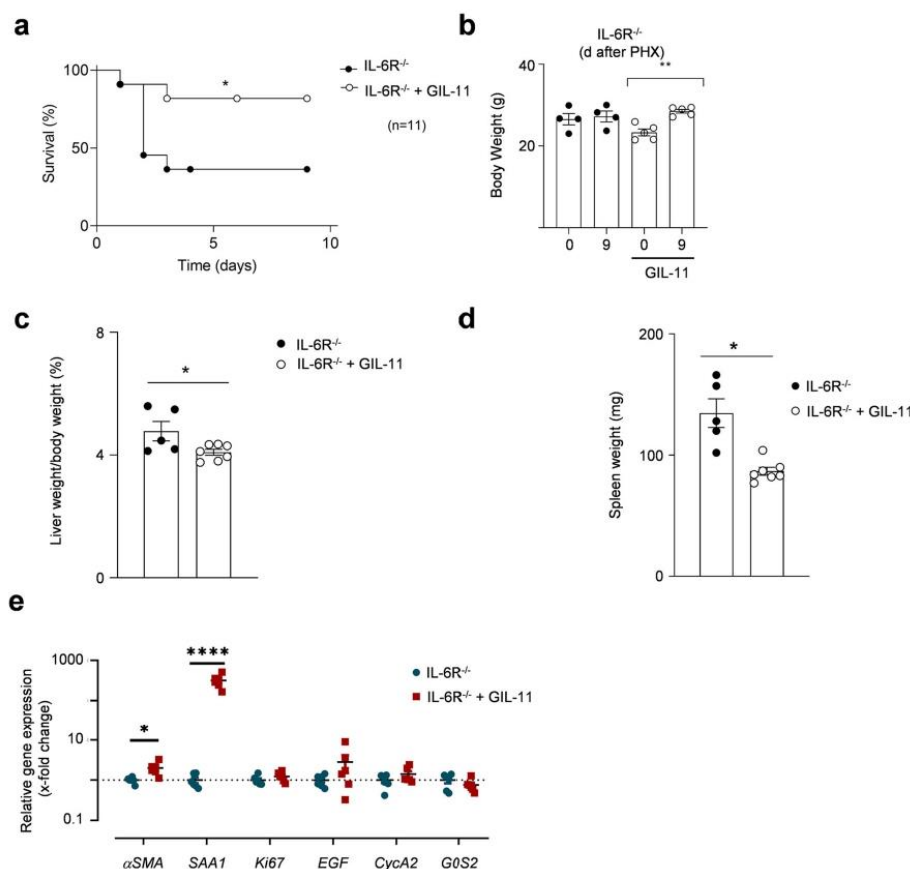


Fig. 7 Human GIL-11 rescued IL-6R^{-/-} mice from death following partial hepatectomy. **a** IL-6R^{-/-} mice were subjected to 70% PHX, injected with PBS (n = 11) or GIL-11 (n = 11), 20 μ g each, 24 h before and directly after surgery and survival was monitored for 9 days. **b** Body weight of IL-6R^{-/-} mice treated with and without GIL-11 after 70% PHX was determined 12 days after PHX (n = 4 untreated, n = 5 GIL-11). **c** Liver/body weight ratio of IL-6R^{-/-} mice treated with and without GIL-11 after 70% PHX was determined at 9 days after PHX (n = 5 untreated, n = 7 GIL-11). **d** Spleen weight of IL-6R^{-/-} mice treated with and without GIL-11 after 70% PHX was determined at 9 days after PHX (n = 5 untreated, n = 7 GIL-11). **e** Total RNA was extracted from the liver directly after PHX from IL-6R^{-/-} mice previously treated with and without GIL-11 and mRNA level of α SMA, SAA1, Ki67, EGF, CycA2 and G0S2 were determined by quantitative PCR (n = 6). **b–e** Each dot represent data derived from one mouse. Error bars are \pm SEM.

LIF (EC50: 0.074 ng/ml). This might be based on the dominant scaffold effect of IL-11 rather than the minor site III exchange effect from LIF. Biological activity of GIL-11 might, however, be increased by site I D186A mutation, since this amino acid exchange is known to increase the affinity of IL-11 to IL-11R⁶⁶. Improving cytokine binding to the α -receptor is a common strategy to improve overall activity in this cytokine family, as has also been shown for CNTF to CNTFR⁶⁷ and IL-6 to IL-6R⁶⁸.

After having characterized the biological activity and the unique receptor composition of GIL-11, we have investigated the ability of GIL-11 to functionally substitute IL-6 during liver regeneration following PHX in IL-6R^{-/-} mice. We and others have previously shown that IL-6 and IL-6R are critically involved in liver regeneration after PHX, resulting in higher mortality in IL-6R^{-/-} mice^{27,46–50}. Importantly, HIL-6 rescued mice from death following partial hepatectomy⁵¹. Moreover, in wild-type mice the combined injection of IL-6 and soluble IL-6R (sIL-6R), but not of IL-6 alone, accelerates liver regeneration after PHX⁶⁹. Likely because hepatocytes express much more gp130 than IL-6R,

the increased presence of IL-6 and sIL-6R result in more gp130 activation and stronger IL-6 signaling compared to IL-6 alone⁷⁰. Finally, blockade of IL-6 trans-signaling by sgp130Fc results in increased mortality following PHX²⁷. Mechanistically, IL-6 trans-signaling induced hepatocyte growth factor (HGF) production by hepatic stellate cells directly contributed to liver regeneration following PHX²⁷. Since, the IL-6R^{-/-} mice used in this work lack in the expression of IL-6R, both classic- and trans-signaling are disabled. Thus, they exhibit a mortality rate of 90% versus 10% in wild-type mice²⁷. A crucial difference between GIL-11 treatment and HIL-6 is that GIL-11 targets only cells expressing gp130:IL-11R:LIFR, which limits the scope of potential targeted cells in the body, whereas HIL-6 targets almost all cells, because unlike IL-11R and LIFR, gp130 is considered to be ubiquitously expressed⁷¹. However, since IL-11R, LIFR as well as gp130 are expressed on hepatocytes, GIL-11 was able to compensate for IL-6 trans-signaling and rescued IL-6R^{-/-} mice from death following PHX. Interestingly, most parameters including body, liver and spleen weight were not changed in surviving GIL-11-treated

and untreated mice. GIL-11, however, increases *SAA1* more than 300-fold even nine days following PHX. *SAA1* induces the proliferation of hepatic stellate cells⁷², which might contribute to liver regeneration following GIL-11 application.

Having shown the general in vitro and in vivo activity, we believe that GIL-11 will be of common interest for conditions in which IL-6 type cytokines including IC7 show beneficial effects⁷³. Recently, the originally described beneficial effects of human IL-11⁶ in murine models of human diseases has been challenged. It was stated that the mode of action of injected human IL-11 into mice actually relies on competitive inhibition of endogenous IL-11 signaling²⁶. It was concluded that IL-11 has rather detrimental than beneficial effects in a variety of murine disease models, including non-alcoholic steatohepatitis, cardiovascular fibrosis, idiopathic pulmonary fibrosis and fibrotic lung disease²⁶. Interestingly, IL-11 was considered to preferentially induce ERK signaling and not, like IL-6, which acts via the same gp130 homodimer, STAT3 phosphorylation²⁶. Therefore, we treated murine myoblasts (C2C12 cells) with recombinant hIL-11, IL-11 and GIL-11 in the presence and absence of murine IL-11R, which, however, resulted in sustained IL-11R-dependent STAT3 phosphorylation. Injection of GIL-11 into mice also resulted in sustained STAT3 phosphorylation in heart, liver and spleen tissue, demonstrating that our human cytokines and GIL-11 activate canonical gp130 and gp130:LIFR signaling pathways characterized by STAT3 phosphorylation. For unknown reasons and unlike IL-11, GIL-11 is only poorly inducing trans-signaling via GIL-11:sIL-11R complexes and is not inhibited by sgp130Fc. It will be interesting to see, what will be the consequence of GIL-11 application for murine models of fibrotic diseases.

Although LIF is related to fertility and a series of neurological disorders including multiple sclerosis, recombinant LIF is not used as therapeutic^{74,75}. GIL-11s ability to induce LIF-like signaling via gp130:LIFR complexes might open LIF-like applications as a potential surrogate for recombinant hLIF. Since GIL-11 activity need cells not only expressing LIFR but also the IL-11R, GIL-11s activity is restricted to a lower limited number of target cells compared to LIF which might alleviate potential unwanted negative side effects.

In conclusion, our study defines GIL-11 as a to the best of our knowledge novel promising cytokimera with specific high-affinity activation of the non-natural receptor gp130:LIFR:IL-11R complex. The modular architecture of cytokimeras in general enables a wide range of targeted receptor combinations and directed cell targeting.

Methods

Cloning. The cDNA coding for GIL-11 was ordered by BioCat GmbH, which was codon optimized and based on human IL-11 and LIF. The GIL-11 cDNA was then inserted into pcDNA3.1 expression vector including 5' signal peptide for human IL-11R (Q14626, aa 1–24) followed by sequences for myc tag (EQKLISEEDL) and the fragment encoding for GIL-11, Gly4Ser linker, a TEV recognition site and a twin-strep-tag.

Molecular modeling. Protein models were generated via the Phyre2 web portal⁷⁶. Complex models and structure-based sequence alignments were generated using UCSF Chimera version 1.13.1, developed by the Resource for Biocomputing, Visualization, and Informatics at the University of California, San Francisco, with support from NIH P41-GM103311⁷⁷.

Cells, reagents and recombinant proteins. The generation of Ba/F3-gp130, Ba/F3-gp130:IL-6R and Ba/F3-gp130:IL-11R cells was described elsewhere^{33,36}. The packaging cell line Phoenix-Eco was received from Ursula Klingmüller (DKFZ, Heidelberg, Germany). NIH/3T3 cells were purchased from the Leibniz Institute DSMZ-German Collection of Microorganisms and Cell Culture (Braunschweig, Germany). All cells were grown at 37 °C with 5% CO₂ in a water-saturated atmosphere in Dulbecco's modified Eagle's medium (DMEM) high-glucose culture medium (GIBCO[®], Life Technologies, Darmstadt, Germany) with 10% fetal calf serum (GIBCO[®], Life Technologies) and 60 mg/l penicillin and 100 mg/l

streptomycin (Genaxxon Bioscience GmbH, Ulm, Germany). Murine Ba/F3-gp130 cells were obtained from Immunex (Seattle, WA, USA) and grown in the presence of hIL-6. 0.2% (10 ng/ml) conditioned medium from a stable clone of CHO-K1 cells secreting hIL-6 in the supernatant⁷⁸. Expi-293F[™] cells (ThermoFisher Scientific) were cultured in Expi293[™] expression medium without antibiotics until they reached a density of 3–5 × 10⁶ c/ml in a 37 °C incubator with 8% CO₂ on an orbital shaker at 125 rpm. Synthetic ligands were expressed and purified as described⁷⁹. Recombinant human OSM (catalog no. 295-OM) and recombinant human LIF (catalog no. 7734-LF) were purchased from R&D Systems (Minneapolis, MN, USA). An expression plasmid for IL-11 pET22-IL-11-His6 was used for the expression of IL-11. IL-11 was expressed as a soluble protein in *Escherichia coli* and purified via immobilized metal affinity chromatography. Sgp130Fc was expressed in ExpiCHO[™] cells (ThermoFisher Scientific). Cells were cultured in ExpiCHO[™] Medium and transfected according to vendor manual (Catalog Number: A29133). The protein was purified as previous described⁸⁰.

Stimulation assay. Ba/F3-gp130 cell lines were washed three times with PBS to remove cytokines and starved in serum-free DMEM for 3 h. Inhibitor sgp130Fc or sIL-11R were added 5 min prior to stimulation. Cells were stimulated for 15 min (or as indicated) with purified protein (concentration as indicated), harvested, frozen in liquid nitrogen and then lysed. In case of the C2C12 and NIH/3T3 cells, the cells were washed after the stimulation with PBS once before they were detached by 0.05% trypsin, 0.1% EDTA (Genaxxon, catalog. C4261.0100) treatment for 5 min and washed again. Cells were lysed for 45 min with buffer containing 10 mM Tris-HCl, pH 7.5, 150 mM NaCl, 0.5 mM MgCl₂ and a cComplete, EDTA-free protease inhibitor mixture tablet (Roche Diagnostics, Mannheim, Germany). Protein concentration was determined by a BCA protein assay (Thermo Fisher Scientific) according to the manufacturer's instruction. Protein expression and pathway activation was then analyzed by western blotting.

Western blotting. Fifty micrograms total protein were loaded each lane and separated by SDS-PAGE under reducing conditions and transferred to a nitrocellulose membrane (Amersham Protran; Cytiva; LC, UK; catalog no. 10600016). Blocking of membrane was performed with blocking buffer (Intercept[®] Blocking Buffer; LI-COR; USA; catalog no. 927-60001) diluted 1:3 in TBS (10 mM Tris-HCl pH 7.6, 150 mM NaCl) for 1 h. Primary antibodies (Phospho-STAT3; Tyr-705; D3A7; catalog no. 9145, STAT3; 124H6; catalog no. 9139, Erk1/2; 134F12; catalog no. 4696, Phospho-Erk1/2; D13.14.4E; catalog no. 4370, Cell Signaling Technology, USA were diluted 1:1000 in blocking buffer containing 0.2% Tween-20 (Sigma-Aldrich; USA; catalog no. P1379-1L) for at least 90 min at ambient temperature or overnight at 4 °C. Membranes were washed with TBS-T (0.1% Tween-20) and then incubated with secondary fluorophore-conjugated antibodies 1:10,000 (IRDye[®] 800CW Donkey anti-Rabbit; catalog no. 926-32213 and IRDye[®] 680RD Donkey anti-Mouse; catalog no. 926-68072, LI-COR; USA) for 1 h. Signal detection was achieved using LI-COR Odyssey; USA; Model 2800). Secondary antibodies were detected simultaneously on different channels. Data analysis was conducted using Image Studio Lite 5.2. Liver, spleen and heart tissue were lysed in lysis buffer (50 mM Tris-HCl pH 7.5, 150 mM NaCl, 2 mM EDTA pH 8.0, 2 mM NaF, 1 mM Na₂VO₄, 1% NP-40, 1% Triton X-100, 1 cComplete protease inhibitor cocktail tablet). After lysis, the protein content was measured by BCA assay. Fifty micrograms total protein amount was then loaded each line followed by immunoblotting. Antibodies used for blotting of lysed animal organs were as follows: anti-p-STAT3 (catalog no. 9145), anti-total-STAT3 (catalog no. 9139).

Cell viability assay. Ba/F3-gp130 cell lines were washed three times with PBS to remove cytokines from the medium. Cells with a density of 5 × 10⁴ cells/ml were suspended in DMEM containing 10% fetal calf serum, 60 mg/l penicillin and 100 mg/ml streptomycin. Cells were cultured for 3 days in a volume of 100 µl with or without cytokines or inhibitor in the indicated concentrations. The CellTiter Blue Viability Assay (Promega, Karlsruhe, Germany) was used to determine the approximate number of viable cells by measuring the fluorescence (λ_{ex} 560 nm/λ_{em} 590 nm) using the Infinite M200 Pro plate reader (Tecan, Crailsheim, Germany). After adding 20 µl/well of CellTiter Blue reagent (time point 0), fluorescence was measured after 60 min every 20 min for up to 2 h. For each condition of an experiment, 3 wells were measured. All values were normalized by subtracting time point 0 values from the final measurement.

Transfection of cells. Ba/F3-gp130 cell lines were retrovirally transduced with the pMOWS expression plasmids as described³⁴. Transduced cells were grown in DMEM medium as described above supplemented with 10 ng/ml hIL-6. Selection of transduced Ba/F3-gp130 cells was performed with puromycin (1.5 µg/ml) or hygromycin B (1 mg/ml) (Carl Roth, Karlsruhe, Germany) for at least 2 weeks. Afterwards, the generated Ba/F3-gp130 cell lines were analyzed for receptor cell surface expression via flow cytometry. C2C12 cells were transfected by 7.5 µg pcDNA3.1 plamid encoding for mL-11R cDNA and 15 µl TurboFect and incubated for 48 h.

Cell surface detection of cytokine receptors via flow cytometry. Cell surface expression of stably transfected Ba/F3-gp130 cell lines was detected by specific

antibodies. 5×10^5 cells were washed in FACS buffer (PBS, 1% BSA) and then incubated in 50 μ l of FACS buffer containing the indicated specific primary antibody (anti-LIFR or α -OSMR; 1:20; catalog no. BAF249 and BAF4389, R&D Systems; MN, USA). After incubation of at least 1 h at room temperature, cells were washed and resuspended in 50 μ l of FACS buffer containing secondary antibody (NothernLights 493-conjugated anti-goat IgG 1:200) and incubated for 30 min at room temperature. Cells were washed and resuspended in 500 μ l of FACS buffer and analyzed by flow cytometry (BD FACSCanto II flow cytometer using the FACSDiva software, BD Biosciences). Data analysis was conducted using FlowJo Version 10 (Tree Star Inc, USA).

Animals and ethics statement. C57BL/6 and IL-6R^{-/-} mice⁵² were obtained from the Jackson Laboratory and the animal facility of the Heinrich-Heine University of Düsseldorf, respectively. The experiments of this study were carried out according to the requirements of LANUV-NRW, Germany with the approval number 84-02.04.2019.A303.

3'-RNA-Seq analyses. Ba/F3-gp130-IL-11R:LIFR cells were stimulated with GIL-11, IL-11 or LIF for 40 min at 37 °C. mRNA was isolated with NucleoSpin RNA (Macherey-Nagel, Düren, Germany, cat. no. 740955.250) according to vendor's manual. DNase digested total RNA samples used for 3'-RNA-Seq analyses were quantified (Qubit RNA HS Assay, Thermo Fisher Scientific) and quality measured by capillary electrophoresis using the Fragment Analyzer and the 'Total RNA standard Sensitivity Assay' (Agilent Technologies, Inc. Santa Clara, USA). All samples in this study showed very high quality RNA Quality Numbers (RQN; mean = 10.0). The library preparation was performed according to the manufacturer's protocol using the QuantSeq 3' mRNA-Seq Library Prep Kit FWD from Lexogen[®]. Input amount was 200 ng total RNA. Bead purified libraries were normalized and finally sequenced on the NextSeq2000 system (Illumina Inc. San Diego, USA) with a read setup of SR 1 \times 100 bp. The Illumina DRAGEN FASTQ Generation tool (version 3.8.4) was used to convert the bd files to fastq files as well for adapter trimming and demultiplexing. The gene ontology analysis was performed with the r package clusterProfiler and r version 4.1.3.

Animals. All mice were kept under specific pathogen-free conditions and handled according to regulations defined by FELASA and the national animal welfare body GV-SOLAS (www.gv-solas.de). All transgenic animals were on C57BL/6N background. Mice were fed with a standard laboratory diet and given autoclaved tap water *ad libitum*. They were kept in an air-conditioned room with controlled temperature (20–24 °C), humidity (45–65%), and day/night cycle (12 h light, 12 h dark). Laparotomy was performed predominantly on male mice at least at 10–12 weeks of age using isoflurane inhalation narcosis 1.5–2% isoflurane with 1 l/min oxygen⁸¹. In order to perform 70% partial hepatectomy, the right upper lobe, left upper lobe and left lower lobe of liver together with the gallbladder was resected via one-staple ligation using 5-0 polyester suture tie (B. Braun Surgical, S.A., Rubi, Spain). Thereafter, the abdominal cavity and outer layer of skin was closed by 5-0 polyglycolic acid (HR13, B. Braun Surgical, S.A., Rubi, Spain) and 4-0 polypropylene monofilament (DS16, B. Braun Surgical, S.A., Rubi, Spain) respectively. In order to reduce the mild pain from operation mice were treated with 5 mg/kg Carprofen (Rimadyl; Pfizer, Wurselen, Germany) after surgery. IL-6R^{-/-} mice were subjected to 70% partial hepatectomy. At specific time points (0, 12, and 24 h) after surgery mice were weighed and anesthetized (100 mg/kg ketamine, 10 mg/kg xylazine; Vetquinol GmbH, Ravensburg, Germany). Upon anesthesia mice were bled in order to generate the serum for further analysis. For the liver tissue, liver was rinsed with phosphate-buffered saline (PBS) and weighed to calculate liver weight to body weight ratio and tissue samples were stored at –80 °C for histology and RNA and protein extraction.

GIL-11 expression, purification and injection into mice. GIL-11 was produced and secreted by Expi293 cells (Thermo Fisher) and purified by Strep-Tag affinity chromatography (Strep-TactinXT 4flow; IBA, catalog no. 2-5023-001) according to the manufacturer's manual. In order to force cytokine signaling, mice were injected intraperitoneal (i.p.) with 20 μ g GIL-11 24 h before and directly after surgery.

Gene expression analysis. Total RNA was extracted from liver and spleen using Trizol (Thermo Fisher Scientific, Waltham, MA, USA). RNA concentration was measured with NanoDrop 2000c spectrophotometer (Thermo Scientific, Waltham, MA, USA, cat. #172-5140) and adjusted to 100 ng/ μ l for all samples. To determine the expression of specific genes, iTaq[™] Universal SYBR green One-Step Kit (BioRad, California, USA, catalog no. 1725151) was used. Master Mix was prepared according to the manufacturer's instructions. 5 μ l of iTaq universal probe reaction mix (2 \times), 0.125 μ l of iScript advanced reverse transcriptase, 0.125 μ l of primers and 200 ng of RNA was used. The total volume of the mixture was then adjusted to 10 μ l by adding Nuclease-free H₂O. For analysis, the expression levels of all target genes were normalized to glyceraldehyde 3-phosphate dehydrogenase (*gapdh*) expression (Δ CT). Gene expression values were calculated based on the $\Delta\Delta$ CT method. Relative quantities⁸² were determined using the equation: $RQ = 2^{-\Delta\Delta CT}$. The expression level of target genes was determined by ABI 7500 real-time PCR System (Thermo Fisher Scientific, Waltham, MA, USA). The following primer

pairs were used in this study: *GAPDH* fw 5' TCCCACTCTTCCACCTTCGA, *GAPDH* rev 5' AGTTGGGATAGGGCTCTCTT, *SAA1* fw 5' GACACCAATT GCTGAGCAGGAA, *SAA1* rev 5' GGGAGTCCAGGAGCTCTGTAG, *Ki67* fw 5' GCCGAGTCTGGCATTGAA, *Ki67* rev 5' TTTTCTTTCTTTCTTTGCTGAGG, *EGF* fw 5' TTCTCACAGGAAAGAGCATCTC, *EGF* rev 5' GTCCTGTCCC GTTAAGGAAAAC, *Cyclin A2* fw 5' GAGGTGGGAGAAGAATATA, *Cyclin A2* rev 5' ACTAGGTGCTCCATTCTCAG, *G0S2* fw 5' TCTCTTCCCACTGCACC CTA, *G0S2* rev 5' TCCTGCACACTTTCCATCTG, *aSMA* fw 5' CTGACAGAG GCACCACTGAA, *aSMA* rev 5' CATCTCCAGAGTCCAGACA.

Statistics and reproducibility

Statistical analysis. Data are provided as arithmetic means \pm SEM using GraphPad Prism, Version 8. Statistically significant differences between two groups were determined with a Student's *t*-test, including Welch's correction if indicated. Statistically analysis between several groups were determined using a two-way ANOVA, including Tukey or Dunnett's correction. Significance was calculated as follows $p > 0.05$: n.s.; $p < 0.05$: *; $p < 0.01$: **; $p < 0.001$: ***; $p < 0.0001$: ****. In vitro assays were performed at least in three independent experiments. For in vivo experiments littermate mice were used as independent individual specimens.

Statistical analysis of RNA-Seq. Data analyses on fastq files were conducted with CLC Genomics Workbench (version 22.0.2, QIAGEN, Venlo, NL). After UMI (Unique Molecular Identifier) filtering, all remaining reads of all probes were adapter trimmed and quality trimmed (using the default parameters: bases below Q13 were trimmed from the end of the reads, ambiguous nucleotides maximal 2). Mapping was done against the *Mus musculus* (mm39; GRChm39.107) (July 20, 2022) genome sequence. After grouping of samples (for biological replicates each) according to their respective experimental condition, the statistical differential expression was determined using the Differential Expression for RNA-Seq tool (version 2.7). The Resulting *P* values were corrected for multiple testing by FDR correction. A *P* value of ≤ 0.05 was considered significant. The Gene Set Enrichment Test (version 1.2) was done with default parameters and based on the GO term 'biological process' (*M. musculus*; December 16, 2021). For each group $n = 4$ biological independent samples were used.

Reporting summary. Further information on research design is available in the Nature Portfolio Reporting Summary linked to this article.

Data availability

The authors declare that the data supporting the findings of this study are available within the manuscript and from the authors on request. Gene expression data of 3'-RNA-Seq are available at NCBI Gene Expression Omnibus; accession code: GSE226064. The plasmid coding for GIL-11 has been deposited at Addgene; Plasmid ID: 199627 and will be provided upon request.

Received: 30 June 2022; Accepted: 27 March 2023;

Published online: 15 April 2023

References

- Moraga, I. et al. Synthekines are surrogate cytokine and growth factor agonists that compel signaling through non-natural receptor dimers. *Elife* **6**, e22882 (2017).
- Silva, D. et al. De novo design of potent and selective mimics of IL-2 and IL-15. *Nature* **565**, 186–191 (2019).
- Kallen, K. et al. Receptor recognition sites of cytokines are organized as exchangeable modules. Transfer of the leukemia inhibitory factor receptor-binding site from ciliary neurotrophic factor to interleukin-6. *J. Biol. Chem.* **274**, 11859–11867 (1999).
- Engelowski, E. et al. Synthetic cytokine receptors transmit biological signals using artificial ligands. *Nat. Commun.* **9**, 2034 (2018).
- Garbers, C. et al. Plasticity and cross-talk of interleukin 6-type cytokines. *Cytokine Growth Factor Rev.* **23**, 85–97 (2012).
- Garbers, C. & Scheller, J. Interleukin-6 and interleukin-11: same same but different. *Biol. Chem.* **394**, 1145–61 (2013).
- Grötzinger, J., Kernebeck, T., Kallen, K. J. & Rose-John, S. IL-6 type cytokine receptor complexes: hexamer, tetramer or both? *Biol. Chem.* **380**, 803–813 (1999).
- Heinrich, P. C., Behrmann, I., Müller-Newen, G., Schaper, F. & Graeve, L. Interleukin-6-type cytokine signalling through the gp130/Jak/STAT pathway. *Biochem. J.* **334**, 297–314 (1998).
- Taga, T. & Kishimoto, T. Gp130 and the interleukin-6 family of cytokines. *Ann. Rev. Immunol.* **15**, 797–819 (1997).

10. Boulanger, M., Chow, D., Brevnova, E. & Garcia, K. Hexameric structure and assembly of the interleukin-6/IL-6 alpha-receptor/gp130 complex. *Science* **300**, 2101–2104 (2007).
11. Metcalfe, R. et al. The structure of the extracellular domains of human interleukin 11a receptor reveals mechanisms of cytokine engagement. *J. Biol. Chem.* **295**, 8285–8301 (2020).
12. Skiniotis, G., Lupardus, P., Martick, M., Walz, T. & Garcia, K. Structural organization of a full-length gp130/LIF-R cytokine receptor transmembrane complex. *Mol. Cell.* **31**, 737–748 (2008).
13. McDonald, N., Panayotatos, N. & Hendrickson, W. Crystal structure of dimeric human ciliary neurotrophic factor determined by MAD phasing. *EMBO J.* **14**, 2689–2699 (1995).
14. Saggio, I., Gloguen, I., Poiana, G. & Laufer, R. CNTF variants with increased biological potency and receptor selectivity define a functional site of receptor interaction. *EMBO J.* **14**, 3045–3054 (1995).
15. Wagener, E. et al. The amino acid exchange R28E in ciliary neurotrophic factor (CNTF) abrogates interleukin-6 receptor-dependent but retains CNTF receptor-dependent signaling via glycoprotein 130 (gp130)/leukemia inhibitory factor receptor (LIFR). *J. Biol. Chem.* **289**, 18442–18450 (2014).
16. Li, Y. et al. gp130 Controls cardiomyocyte proliferation and heart regeneration. *Circulation* **142**, 967–982 (2020).
17. Findeisen, M. et al. Treatment of type 2 diabetes with the designer cytokine IC7Fc. *Nature* **574**, 63–68 (2019).
18. Carey, A. et al. Interleukin-6 increases insulin-stimulated glucose disposal in humans and glucose uptake and fatty acid oxidation in vitro via AMP-activated protein kinase. *Diabetes* **55**, 2688–2697 (2006).
19. Wang, Q. et al. IL-27 signalling promotes adipocyte thermogenesis and energy expenditure. *Nature* **600**, 314–318 (2021).
20. Watt, M. et al. CNTF reverses obesity-induced insulin resistance by activating skeletal muscle AMPK. *Nat. Med.* **12**, 541–548 (2006).
21. Ettinger, M. et al. Recombinant variant of ciliary neurotrophic factor for weight loss in obese adults: a randomized, dose-ranging study. *JAMA* **289**, 1826–1832 (2003).
22. Arora, G. et al. Cachexia-associated adipose loss induced by tumor-secreted leukemia inhibitory factor is counterbalanced by decreased leptin. *JCI Insight* **3**, e121221 (2018).
23. Guo, T. et al. LIFR- α -dependent adipocyte signaling in obesity limits adipose expansion contributing to fatty liver disease. *iScience* **24**, 102227 (2021).
24. Obana, M. et al. Therapeutic activation of signal transducer and activator of transcription 3 by interleukin-11 ameliorates cardiac fibrosis after myocardial infarction. *Circulation* **121**, 684–691 (2010).
25. Viswanathan, S. et al. Critical conditions for studying interleukin-11 signaling in vitro and avoiding experimental artefacts. *Curr. Protoc.* **1**, e251 (2021).
26. Widjaja, A., Chothani, S. & Cook, S. Different roles of interleukin 6 and interleukin 11 in the liver: implications for therapy. *Hum. Vaccin. Immunother.* **16**, 2357–2362 (2020).
27. Modares, N. et al. IL-6 trans-signaling controls liver regeneration after partial hepatectomy. *Hepatology* **70**, 2075–2091 (2019).
28. Bazan, J. Haemopoietic receptors and helical cytokines. *Immunol. Today* **11**, 350–354 (1990).
29. Hilton, D. et al. Cloning of a murine IL-11 receptor alpha-chain; requirement for gp130 for high affinity binding and signal transduction. *EMBO J.* **13**, 4765–4775 (1994).
30. Barton, V., MA, H., Hudson, K. & Heath, J. Interleukin-11 signals through the formation of a hexameric receptor complex. *J. Biol. Chem.* **275**, 36197–36203 (2000).
31. Pflanz, S., Kurth, I., Grötzinger, J., Heinrich, P. & Müller-Newen, G. Two different epitopes of the signal transducer gp130 sequentially cooperate on IL-6-induced receptor activation. *J. Immunol.* **165**, 7042–7049 (2000).
32. Zhang, J. et al. Evidence for the formation of a heterotrimeric complex of leukaemia inhibitory factor with its receptor subunits in solution. *Biochem. J.* **325**, 693–700 (1997).
33. Boulanger, M., Bankovich, A., Kortemme, T., Baker, D. & Garcia, K. Convergent mechanisms for recognition of divergent cytokines by the shared signaling receptor gp130. *Mol. Cell.* **12**, 577–589 (2003).
34. Baran, P. et al. The balance of interleukin (IL)-6, IL-6-soluble IL-6 receptor (sIL-6R), and IL-6-sIL-6R-sgp130 complexes allows simultaneous classic and trans-signaling. *J. Biol. Chem.* **293**, 6762–6775 (2018).
35. Monhasery, N. et al. Transcytosis of IL-11 and apical redirection of gp130 is mediated by IL-11a receptor. *Cell Rep.* **16**, 1067–1081 (2016).
36. Chalaris, A. et al. Apoptosis is a natural stimulus of IL6R shedding and contributes to the pro-inflammatory trans-signaling function of neutrophils. *Blood* **110**, 1748–1755 (2007).
37. Lokau, J. et al. Proteolytic cleavage governs interleukin-11 trans-signaling. *Cell Rep.* **14**, 1761–1773 (2016).
38. Heinrich, P. et al. Principles of interleukin (IL)-6-type cytokine signalling and its regulation. *Biochem. J.* **374**, 1–20 (2003).
39. CA, W. & NA, N. SOCS3: an essential physiological inhibitor of signaling by interleukin-6 and G-CSF family cytokines. *JAKSTAT* **2**, e25045 (2013).
40. Jostock, T. et al. Soluble gp130 is the natural inhibitor of soluble interleukin-6 receptor transsignaling responses. *Eur. J. Biochem.* **268**, 160–167 (2001).
41. Scheller, J., Schuster, B., Hölscher, C., Yoshimoto, T. & Rose-John, S. No inhibition of IL-27 signaling by soluble gp130. *Biochem. Biophys. Res. Commun.* **326**, 724–728 (2005).
42. Wang, X., Fuhrer, D., Marshall, M. & Yang, Y. Interleukin-11 induces complex formation of Grb2, Fyn, and JAK2 in 3T3L1 cells. *J. Biol. Chem.* **270**, 27999–28002 (1995).
43. Owczarek, C. et al. The unusual species cross-reactivity of the leukemia inhibitory factor receptor alpha-chain is determined primarily by the immunoglobulin-like domain. *J. Biol. Chem.* **272**, 23976–23985 (1997).
44. Ernst, M. et al. STAT3 and STAT1 mediate IL-11-dependent and inflammation-associated gastric tumorigenesis in gp130 receptor mutant mice. *J. Clin. Invest.* **118**, 1727–1738 (2008).
45. Jakob, L. et al. Murine Oncostatin M has opposing effects on the proliferation of OP9 Bone Marrow Stromal Cells and NIH/3T3 fibroblasts signaling through the OSMR. *Int. J. Mol. Sci.* **22**, 11649 (2021).
46. Cressman, D. E. et al. Liver failure and defective hepatocyte regeneration in interleukin-6-deficient mice. *Science* **274**, 1379–1383 (1996).
47. Peters, M. et al. Combined Interleukin-6 and soluble Interleukin-6 receptor accelerates murine liver regeneration. *Gastroenterology* **119**, 1663–1671 (2000).
48. Blindenbacher, A. et al. Interleukin 6 is important for survival after partial hepatectomy in mice. *Hepatology* **38**, 674–682 (2003).
49. Nechemia-Arbely, Y. et al. Early hepatocyte DNA synthetic response posthepatectomy is modulated by IL-6 trans-signaling and PI3K/AKT activation. *J. Hepatol.* **54**, 922–929 (2011).
50. Tachibana, S. et al. Interleukin-6 is required for cell cycle arrest and activation of DNA repair enzymes after partial hepatectomy in mice. *Cell Biosci.* **4**, 6 (2014).
51. Behnke, K. et al. B cell-mediated maintenance of CD169+ cells is critical for liver regeneration. *Hepatology*. <https://doi.org/10.1002/hep.30088> (2018).
52. McFarland-Mancini, M. M. et al. Differences in wound healing in mice with deficiency of IL-6 versus IL-6 receptor. *J. Immunol.* **184**, 7219–7228 (2010).
53. Schumertl, T., Lokau, J., Rose-John, S. & Garbers, C. Function and proteolytic generation of the soluble interleukin-6 receptor in health and disease. *Biochim. Biophys. Acta Mol. Cell. Res.* **1869**, 119143 (2022).
54. Uhlén, M. et al. Proteomics. Tissue-based map of the human proteome. *Science* **347**, 1260419 (2015).
55. Kimura, R. et al. Identification of cardiac myocytes as the target of interleukin 11, a cardioprotective cytokine. *Cytokine* **38**, 107–115 (2007).
56. Schafer, S. et al. IL-11 is a crucial determinant of cardiovascular fibrosis. *Nature* **552**, 110–115 (2017).
57. Ropeleski, M., Tang, J., Walsh-Reitz, M., Musch, M. & Chang, E. Interleukin-11-induced heat shock protein 25 confers intestinal epithelial-specific cytoprotection from oxidant stress. *Gastroenterology* **124**, 1358–1368 (2003).
58. Donath, M. Y. Designer cytokine for the treatment of diabetes. *Nat. Metab.* **1**, 933–934 (2019).
59. Moraga, I., Spangler, J., Mendoza, J. & Garcia, K. Multifarious determinants of cytokine receptor signaling specificity. *Adv. Immunol.* **121**, 1–39 (2014).
60. Garo, L. et al. Smad7 controls immunoregulatory PDL2/1-PD1 signaling in intestinal inflammation and autoimmunity. *Cell Rep.* **28**, 3353–3366 (2019).
61. Marty, R. et al. MyD88 signaling controls autoimmune myocarditis induction. *Circulation* **113**, 258–265 (2006).
62. Popovic, Z. et al. The proteoglycan biglycan enhances antigen-specific T cell activation potentially via MyD88 and TRIF pathways and triggers autoimmune perimyocarditis. *J. Immunol.* **187**, 6217–6226 (2011).
63. Blyszczuk, P. et al. Myeloid differentiation factor-88/interleukin-1 signaling controls cardiac fibrosis and heart failure progression in inflammatory dilated cardiomyopathy. *Circ. Res.* **105**, 912–920 (2009).
64. Masuda, K. & Kishimoto, T. A potential therapeutic target RNA-binding protein, Arid5a for the treatment of inflammatory disease associated with aberrant cytokine expression. *Curr. Pharm. Des.* **24**, 1766–1771 (2018).
65. Bobby, R. et al. Functional implications of large backbone amplitude motions of the glycoprotein 130-binding epitope of interleukin-6. *FEBS J.* **281**, 2471–2483 (2014).
66. Harmegnies, D. et al. Characterization of a potent human interleukin-11 agonist. *Biochem. J.* **375**, 23–32 (2003).
67. Battista, M. R. et al. Efficacy of PEGylated ciliary neurotrophic factor superagonist variant in diet-induced obesity mice. *PLoS ONE* **17**, e0265749 (2022).
68. Toniatti, C. et al. Engineering human interleukin-6 to obtain variants with strongly enhanced bioactivity. *EMBO J.* **15**, 2726–2737 (1996).
69. Peters, M. et al. Combined interleukin 6 and soluble interleukin 6 receptor accelerates murine liver regeneration. *Gastroenterology* **119** 1663–71 (2000).

70. Fazel Modares, N. et al. IL-6 trans-signaling controls liver regeneration after partial hepatectomy. *Hepatology* **70**, 2075–2091 (2019).
71. Garbers, C. & Rose-John, S. Dissecting interleukin-6 classic- and trans-signaling in inflammation and cancer. *Methods Mol. Biol.* **1725**, 127–140 (2018).
72. Siegmund, S. V. et al. Serum Amyloid A induces inflammation, proliferation and cell death in activated hepatic stellate cells. *PLoS ONE* **11**, e0150893 (2016).
73. Giraldez, M., Carneros, D., Garbers, C., Rose-John, S. & Bustos, M. New insights into IL-6 family cytokines in metabolism, hepatology and gastroenterology. *Nat. Rev. Gastroenterol. Hepatol.* **18**, 787–803 (2021).
74. Gunawardana, D. H. et al. A phase I study of recombinant human leukemia inhibitory factor in patients with advanced cancer. *Clin. Cancer Res.* **9**, 2056–2065 (2003).
75. Pinho, V., Fernandes, M., da Costa, A., Machado, R. & Gomes, A. C. Leukemia inhibitory factor: recent advances and implications in biotechnology. *Cytokine Growth Factor Rev.* **52**, 25–33 (2020).
76. Kelley, L., Mezulis, S., Yates, C., Wass, M. & Sternberg, M. The Phyre2 web portal for protein modeling, prediction and analysis. *Nat. Protoc.* **10**, 845–858 (2015).
77. Pettersen, E. et al. UCSF Chimera—a visualization system for exploratory research and analysis. *J. Comput. Chem.* **25**, 1605–1612 (2004).
78. Fischer, M. et al. I. A bioactive designer cytokine for human hematopoietic progenitor cell expansion. *Nat. Biotechnol.* **15**, 142–145 (1997).
79. Mossner, S. et al. Multimerization strategies for efficient production and purification of highly active synthetic cytokine receptor ligands. *PLoS ONE* **15**, e0230804 (2020).
80. Jostock, T. et al. Immunoadhesins of interleukin-6 and the IL-6/soluble IL-6R fusion protein hyper-IL-6. *J. Immunol. Methods* **223**, 171–183 (1999).
81. Greene, A. K. & Puder, M. Partial hepatectomy in the mouse: technique and perioperative management. *J. Invest. Surg.* **16**, 99–102 (2003).
82. Kim, J. W. et al. Engineering a potent receptor superagonist or antagonist from a novel IL-6 family cytokine ligand. *Proc. Natl Acad. Sci. USA* **117**, 14110–14118 (2020).
83. Huyton, T. et al. An unusual cytokine:Ig-domain interaction revealed in the crystal structure of leukemia inhibitory factor (LIF) in complex with the LIF receptor. *PNAS* **104**, 12737–12742 (2007).

Acknowledgements

We thank Yvonne Arlt for technical assistance. Computational infrastructure and support were provided by the Centre for Information and Media Technology at Heinrich Heine University Düsseldorf. This work was funded by a grant from the Deutsche Forschungsgemeinschaft (SFB1116).

Author contributions

P.R. performed most experiments, data curation, P.R., C.S., A.M., H.T.W., D.M.F., K.B., J.M., J.S. formal analysis, validation, investigation, methodology, correcting manuscript; K.B. and H.T.W. performed partial hepatectomy. J.E. supported cloning and cell culture. C.S. expressed and purified the sgp130Fc; P.P. and K.K. helped with the transcriptomic analysis; A.L. helped with Venn diagram and gene ontology; P.R. and J.S. writing-original draft; J.S. project administration, funding acquisition.

Funding

Open Access funding enabled and organized by Projekt DEAL.

Competing interests

J.S., P.R. and J.M. are inventors of GIL-11 and hold patents for this molecule (EP22214005.5). All other authors declare no competing interests.

Additional information

Supplementary information The online version contains supplementary material available at <https://doi.org/10.1038/s42003-023-04768-4>.

Correspondence and requests for materials should be addressed to Jürgen Scheller.

Peer review information *Communications Biology* thanks the anonymous reviewers for their contribution to the peer review of this work. Primary handling editor: Joao Valente.

Reprints and permission information is available at <http://www.nature.com/reprints>

Publisher's note Springer Nature remains neutral with regard to jurisdictional claims in published maps and institutional affiliations.



Open Access This article is licensed under a Creative Commons Attribution 4.0 International License, which permits use, sharing, adaptation, distribution and reproduction in any medium or format, as long as you give appropriate credit to the original author(s) and the source, provide a link to the Creative Commons license, and indicate if changes were made. The images or other third party material in this article are included in the article's Creative Commons license, unless indicated otherwise in a credit line to the material. If material is not included in the article's Creative Commons license and your intended use is not permitted by statutory regulation or exceeds the permitted use, you will need to obtain permission directly from the copyright holder. To view a copy of this license, visit <http://creativecommons.org/licenses/by/4.0/>.

© The Author(s) 2023

5. DISCUSSION

Synthetic cytokine biology is currently a thriving field of study, aiming at elucidate the intricate mechanisms by which cytokines control immune responses and discover new therapeutic targets to develop novel treatments for various diseases, such as metabolic and autoimmune diseases, and cancer.

Following these goals, I have been investigating the controversial role of the immune cytokine IL-6 in obesity-induced inflammation and its anti-diabetogenic functions after physical exercise, using engineered sIL-6R and IL-6R KO mouse model. According to the initial hypothesis, IL-6 trans-signaling was a potential and valid therapeutic target for type 2 diabetes and obesity, since it hypothetically involved body weight increase, impaired glucose tolerance, and insulin resistance.

Furthermore, during my doctoral studies, synthetic biology has been adopted as a tool to investigate cytokine receptor-effector interactions and signaling pathways in an immunological context to develop cutting-edge future therapies. In detail, I have established the previously described synthetic Fas receptor (Mossner, Floss et al. 2021) as a tool to systematically analyze missense SNPs and single nucleotide mutations within the natural Fas transmembrane and intracellular domain. Those mutations, indeed, were (potentially) associated with autoimmune lymphoproliferative syndrome or squamous cell carcinoma, but the exact molecular mechanism behind them was not yet known. Moreover, I aimed to further use this tool to boost the clinically approved CAR T-cells therapy, in particular, to overcome the described side effects, such as cytokine release syndrome (CRS) and neurotoxicity (Larson and Maus 2021).

5.1 Revealing the role of IL-6 classic and trans-signaling in diet-induced obesity and physical exercise.

To uncover the unknown mechanisms behind the role of IL-6 in meta-inflammation in adipose tissue in an obesity context and its beneficial effects associated with physical exercise, IL-6R deficient and sIL-6R^{+/+} trans-signaling mice have been metabolically characterized.

Body weight, body fat, and lean mass was monitored following the standard carbohydrate (CHO) diet and high-fat diet (HFD), with and without treadmill exercise, as well as glucose and insulin tolerance test, and indirect calorimetry.

The sIL-6R^{+/+} mice fed with the CHO diet displayed a modest increase in body weight compared to controls, which was primarily attributed to higher body lean mass. To support this observation, the

fatty acid utilization during light and dark periods were indeed augmented, which may explain why adipose tissue did not increase. Furthermore, after 9 weeks of HFD, neither the wild-type control group nor the IL-6R deficient mice showed any signs of altered blood glucose levels. Finally, the positive effects of exercise on body weight, body composition, glucose, and insulin tolerance, as well as basal metabolism, were not significantly affected by IL-6R absence.

In summary, the data suggested that neither classic nor trans-signaling have a significant impact on the phenotype, in contrast to what was proposed in the literature, but important to consider that other studies mostly focused on IL-6 KO mouse models (Wueest and Konrad 2020).

We introduced the trans-signaling mouse model for the first time in the context of obesity. As previously described (Fazel Modares, Polz et al. 2019), Cre-mediated deletion of the genetic sequence coding for IL-6R transmembrane and intracellular domains simulates the natural activation of the metalloproteases ADAM10/17 to constantly cleave membrane-bound IL-6R resulting in the availability of the soluble form only. This mechanism subsequently leads to specific trans-signaling execution, being, thus, a unique approach to study only IL-6 trans-signaling, without the classic signaling activation. It is a valid method to reveal IL-6 mechanism during pathophysiological settings, such as, in liver regeneration after partial hepatectomy (Fazel Modares, Polz et al. 2019), or, in this instance, obesity linked with insulin signaling and glucose metabolism distortion, as well as in physical activity as the therapeutic approach.

Our findings confirmed the specificity of our model since, after a high-fat diet, circulating sIL-6R was up to 48-fold higher in sIL-6R^{+/+} mice compared to littermate controls. Furthermore, we have previously demonstrated that there were no differences between the IL-6R mRNA expression in sIL-6R^{fl/fl} and IL-6R^{fl/fl} animals and wild-type littermate controls, whereas sIL-6R^{+/+} mice showed a significant increase. Immunohistochemistry findings also corroborated this claim by showing that IL-6R was expressed in wild-type mice but not in IL-6R deficient and sIL-6R^{+/+} animals, emphasizing how membrane-bound IL-6R is converted to sIL-6R and quickly released (Fazel Modares, Polz et al. 2019). Together, these factors account for the sIL-6R levels noticeably rising in our mouse model.

The goal of the current investigation was to determine whether IL-6R deficient animals phenocopy IL-6 deficient mice in response to diet-induced obesity and exercise exposure. The majority of studies linked IL-6 deficiency to development of obesity, glucose intolerance, and insulin resistance. In the pioneer study conducted by Wallenius et al., the researchers explored the role of IL-6 in the development of obesity and its impact on carbohydrate and lipid metabolism, utilizing mice

deficient for IL-6. The findings of Wallenius et al. revealed that mice lacking IL-6 exhibited mature-onset obesity, indicating that IL-6 is essential for controlling body weight and adiposity. However, those results were a few years later challenged by Di Gregorio et al., who reported no differences in obesity in 8 months old mice and after three months of high-fat diet (Di Gregorio, Hensley et al. 2004), speculating that the discrepancies between the two beforehand mentioned are unclear or perhaps due to different genetic backgrounds.

Furthermore, any changes in body weight and fat content, and decreased insulin sensitivity have been observed in mice with specific deletion of IL-6R in hepatocytes, as well as elevated production of pro-inflammatory IL-6, TNF-, and IL-10 (Wunderlich, Ströhle et al. 2010).

Despite some contentious IL-6-related findings, the bulk of the research showed abnormalities in the metabolism of carbohydrates, the emergence of insulin resistance, and the development of obesity. It should be noted that we adopted a novel mechanistic model and that the hypothesised phenotype of increased body weight and fat content, decreased insulin, and glucose tolerance were not confirmed.

McFarland-Mancini et al. found a comparable scenario in which, despite some parallels in inflammatory deficiencies, mice lacking IL-6R displayed a distinct phenotype in the delayed wound healing process compared to mice deficient in IL-6, while the combined phenotype of IL-6 and IL-6R deficit was identical to IL-6R. Due to the large number of studies that have already been published in the literature, in our study a direct comparison with IL-6 KO mice is missing. However, based on those evidences, we concluded that IL-6R KO contributes less to the phenotypic development than IL-6 KO.

Interestingly, we concur with the theory given by McFarland-Mancini et al. that IL-6 might exert its effects through alternative receptors, that might compensate the lack of IL-6R and induce same pathway's activation. To support this statement, it is known that IL-6-type cytokines, sharing structural and functional similarities, can engage in cross-talk with each other, leading to complex signaling interactions and diverse biological effects. For instance, in addition to IL-6, the IL-6R was demonstrated to bind to CNTF, but with a lower affinity than the CNTF/CNTFR interaction. In order to activate signal transduction, the gp130/LIFR heterodimer was formed by the CNTF/IL-6R complex (Schuster, Kovaleva et al. 2003). Moreover, an additional cytokine able to bind IL-6R is IL-30, p28 subunit of IL-27, leading to STAT1 and STAT3 activation after gp130 recruitment (Crabé, Guay-Giroux et al. 2009).

To explain the divergent results, another plausible explanation could be the differences in genetic backgrounds, such as different strains of mice, that can significantly influence the outcome of experiments and metabolic processes.

Genetic background refers to the collection of genetic variations that can affect the expression of genes, protein function, and overall metabolism, leading to variations in experimental outcomes and metabolic phenotypes. Genetic variations can influence the expression and activity of enzymes involved in metabolic pathways, the regulation of hormones and signaling molecules, and the response to dietary and environmental factors. These variations can contribute to differences in energy metabolism, nutrient utilization, and susceptibility to metabolic disorders such as obesity, diabetes, and cardiovascular diseases (Abou Ziki and Mani 2016).

For instance, there are other cases when genetic background can have opposing impacts on metabolism, such as when distinct mouse strains exhibit conflicting effects on insulin sensitivity in the muscles and the liver (Colombo, Haluzik et al. 2003). In detail, in this study, transgenic A-ZIP/F-1, which lacks completely of white adipose tissue and partially of brown adipose tissue, have been metabolically characterized comparing two different murine strains: FVB and B6. The results showed that AZIP phenotype, mainly characterized by strong insulin resistance, high serum levels of glucose and triglycerides, is milder with a B6 genetic background compared to FVB.

Other elements include the adoption of various breeding techniques and/or different controls, such as general wild-type or littermate controls. Notably, regardless of IL-6R genotype, using the same C57/BL6 background and identical experimental techniques, we found unexpected differences between the two control strains, IL-6R^{f/f} and sIL-6R^{f/f}, in terms of body weight and body composition, as well as blood glucose levels and preferred metabolic substrate, both under standard conditions and following a high-fat diet and physical activity. This emphasizes the importance of using littermate controls rather than general wild-type mice when conducting experiments.

Furthermore, one should carefully consider parameters such as age, methodology that may vary from one lab to another, ambient conditions, or different types of food, and microbiota. In particular, this last area of study has grown significantly over the past few years. It has been demonstrated that the metabolic profile of diet-induced obese mice differs in the proportion of the two prominent bacterial divisions, the Bacteroidetes and the Firmicutes, which affects the ability for dietary energy harvesting and results in larger body fat contents (Urnbauh, Ley et al. 2006).

In conclusion, despite previous studies defining IL-6 as the primary initiator of inflammation in adipose tissue in obese conditions and subsequent glucose and insulin intolerance in peripheral tissues, membrane-bound IL-6R and sIL-6R do not appear to be involved in regulating glucose and insulin metabolism in diet-induced obesity. These research findings contributed important new data to the well-known complex picture surrounding the function of IL-6 signaling in the processes mentioned above. This opens the door to addressing new issues that demand additional research in regard to a probable novel IL-6R mechanism in adipocytes and skeletal muscles.

5.2 Implementation of a synthetic receptor platform underlines loss-of-function single nucleotide variants and novel functionally diverse mutants in the death receptor Fas/CD95

Analysing cytokine signal transduction and creating individualized treatments are now both made possible by the captivating alternative of synthetic biology. It is a method that integrates concepts from biology, engineering, and computational science to create new biological systems or modify those that already exist to serve practical needs.

On this base, the aim of this project was to adopt a specific synthetic cytokine receptor, such as synthetic Fas, to identify and consequentially characterise loss-of-function mutations within the transmembrane and intracellular domain that are linked to the onset of diseases like cancer and the autoimmune lymphoproliferative syndrome (ALPS), as well as to reveal the mechanism that results in distorted apoptosis.

Synthetic cytokine receptors have been previously established in our research group to phenocopy dimeric receptors for IL-6, IL-22, and IL-23 (Engelowski, Schneider et al. 2018, Mossner, Kuchner et al. 2020) and, recently, also trimeric receptors, such as TNFR1, TNFR2, and Fas/CD95 receptors, belonging to the subgroup of death receptors of the tumor necrosis factor superfamily (TNFS). Mossner et al. demonstrated the efficiency of the system by effective activation of the apoptotic pathway, shown through different experimental approaches, such as proliferation, apoptosis assays, and detection of effector caspases 3 and 7. A previously identified loss-of-function mutation in the death domain, which was associated to the onset of ALPS, served as proof of the specificity of induced apoptosis caused by synthetic Fas activation (Mossner, Floss et al. 2021).

During my doctoral studies, I implemented the synthetic Fas receptor as a tool to functionally and systematically characterize new single nucleotide polymorphisms (SNPs) discovered in the clinic and new candidate loss-of-function mutations proposed in our laboratory. In detail, among the total

17,889 SNPs discovered in the Fas gene, we examined the 337 non-synonymous missense SNPs of the transmembrane and intracellular domain, of which 39 were mentioned in ClinVar. Of note, of the 337 missense SNPs, 23 were published in peer-reviewed articles, 19 had a direct clinical link, but only 13 were experimentally verified. Among all non-synonymous SNPs, we chose Provean predicted (Kumar, Henikoff et al. 2009) and previously uncharacterized non-synonymous SNPs from ClinVar, in addition to LOF SNPs previously identified in the intracellular death domain, linked to ALPS and squamous cell carcinoma (SCC), to prove the validity of our model. By using comprehensive structure-guided analysis (Pettersen, Goddard et al. 2021), we then selected additional structure-based mutations.

We demonstrated that none of the 35 mutations cause the protein to be globally unstable because all variants were normally expressed on the cell surface, supporting earlier studies that reported aberrant expression patterns primarily for extracellular Fas mutations (Vaishnaw, Orlinick et al. 1999, Kuehn, Caminha et al. 2011).

In contrast to extracellular Fas SNPs, the most common LOF SNPs in Fas were located in the transmembrane and intracellular death domain (DD) and showed a more significant disturbed phenotype and faulty apoptosis in lymphocytes in patients with ALPS and SCC (Jackson, Fischer et al. 1999). Furthermore, because homozygosity would be fatal, patient LOF mutations in the death domain of Fas are often heterozygous (Fisher, Rosenberg et al. 1995).

Bettinardi et al. demonstrated that two ALPS-affected siblings had the identical Fas gene mutation Y232C that resulted in apoptotic disruption (Bettinardi, Brugnani et al. 1997), whereas patients bearing the Fas SNPs T241P, R250P, and D260V displayed reduced apoptosis (Jackson, Fischer et al. 1999, Martin, Zheng et al. 1999), reduced T-cell loss (Fisher, Rosenberg et al. 1995), and altered DISC formation (Kuehn, Caminha et al. 2011). Last but not least, the SNP T270I showed suppression of Fas-mediated apoptosis as indicated by increased cell survival and absence of FADD recruitment (Vaishnaw, Orlinick et al. 1999).

Our findings, which included further structural analysis, apoptosis, and caspases 3 and 7 cleavage assays, supported and completed the conclusions of the earlier investigations.

15 novel SNPs listed as non-functional in ClinVar as (presumably) pathogenic, of unknown significance, or predicted by Provean were also further clarified in terms of their molecular mechanisms.

According to my research, four SNPs exhibited partially reduced Fas activity, three SNPs conferred a milder GOF, and eight SNPs caused total LOF.

Using structure-based modelling, 15 additional LOF candidates were predicted. Ten alanine variations and five rationally designed variants of an alternative amino acid were used to design LOF variants by replacing death domain residues within the DD-FADD interface. I295A, N302D, L306A, and Q311E only partially decreased the wild-type activity, while N223A and N329D had no detrimental effects on Fas-induced suppression of proliferation, apoptosis, and caspase activation.

Another crucial factor that requires consideration and is worth testing is the dominant-negative effect that Fas-mutations could result in. Dominant-negative effects occur when a mutant protein interferes with the function of the normal protein, even in the presence of the wild-type allele. In the case of Fas mutations, at least one mutant Fas receptor can interact with the wild-type Fas receptor to form complexes on the cell surface, which might interfere with the function of the wild-type receptor. As a result of their dominant-negative effects, Fas mutations may disrupt or decrease the apoptotic signaling system (Kuehn, Caminha et al. 2011, Fu, Fu et al. 2016). With a novel synthetic strategy, characterized by co-expression of synthetic wild-type or mutated mCherry-VHH Fas with wild-type GFP-VHH Fas in a cell-based system, the goal was to test the heterotrimerization and, thus, the dominant-negative effects of a few selected SNPs and mutations. To sum up, this effect was confirmed for two ALPS-associated LOF SNPs, which were unable to induce apoptosis by heterotrimerization, and were partially demonstrated for three additional uncharacterized non-synonymous SNPs and two GOF structure-based mutations, therefore having a milder dominant-negative effect.

To conclude, we extensively elucidated the requirement for experimental and systematic validation of SNPs and mutations (potentially) associated with diseases, following in silico prediction using in-depth structure-guided analysis or basic online data processing tools like Provean, highlighting profile of variants that could be considered for future integration in cellular immunotherapy approaches.

5.2.1 Application of Synthetic Fas receptor to complement CAR-T cell therapy

Potentially, SyCyRs could be exploited to improve CAR T-cell treatment, also known as chimeric antigen receptor T-cell therapy, a groundbreaking immunotherapy approach that harnesses the power of a patient's own immune system to fight cancer (June, O'Connor et al. 2018).

CAR T-cell therapy has shown remarkable success in treating certain types of hematological cancers, particularly acute lymphoblastic leukemia (ALL) and certain forms of non-Hodgkin lymphoma. However, it also carries potential risks and side effects: the activation of CAR T-cells can lead to an excessive immune response known as cytokine release syndrome (CRS), which can cause flu-like symptoms, fever, and potentially severe complications. Neurological toxicities, such as confusion and seizures, have also been reported in some patients (Siegler and Kenderian 2020).

Therefore, in the recent years, efforts are being made to optimize the therapy and minimize these side effects through improved CAR designs and controlling strategies. For instance, my research aimed to provide a tenable novel strategy to overcome the negative effects, by stimulating proliferation or suppressing the activity of transgenic T-cells, respectively activating gp130 by HIL-6, a fusion protein composed by IL-6 and sIL-6R, and synthetic Fas by synthetic ligand, like mCherry or GFP. In order to achieve this goal, we tested whether combining gain-of-function (GOF) or LOF mutations would result in a stronger or weaker activation of synthetic wild-type Fas. This would allow us to induce a better (stronger or weaker) synthetic Fas activation in primary T-cells and subsequently suppress the lethal pro-inflammatory response.

To accomplish this goal, N223A and N329D, two GOF mutations, were combined; however, the combination led to a mild LOF phenotype. Although N223 of FADD is close to N136 and R135 of FADD, it doesn't appear to be in contact with FADD within the structure. FADD is located distant from N329. We were unable to explain the LOF phenotype of the N223A and N329D combination based on the structure. Since these two amino acids contribute to the overall protein stability with -9.7 KJ/mol (N223) and -32.1 KJ/mol (N329) in the closed conformation (PDB: 1DDF) and -86.3 KJ/mol (N329) in the open conformation (PDB: 3EZQ) (Galgonek, Vymětal et al. 2017), respectively, it is possible that the switch of both amino acids may result in a lower stability of Fas.

Unquestionably, after the preliminary screening, a future investigation that might be performed is to examine all the disease-related SNPs and mutations in primary immune cells that also express endogenous Fas for the purpose of identifying the most beneficial variant candidates in synthetic Fas for the effective activation and then inhibition of T-cells' activity.

In conclusion, I showed how synthetic Fas receptor is a proficient system to methodically validate possible loss-of-function mutations through experimental testing and demonstrated its potential role in turning off CAR T-cells after activation to minimize side effects.

REFERENCES

- Abou Ziki, M. D. and A. Mani (2016). "Metabolic syndrome: genetic insights into disease pathogenesis." *Curr Opin Lipidol* **27**(2): 162-171.
- Arkan, M. C., A. L. Hevener, F. R. Greten, S. Maeda, Z. W. Li, J. M. Long, A. Wynshaw-Boris, G. Poli, J. Olefsky and M. Karin (2005). "IKK-beta links inflammation to obesity-induced insulin resistance." *Nat Med* **11**(2): 191-198.
- Baek, M., F. DiMaio, I. Anishchenko, J. Dauparas, S. Ovchinnikov, G. R. Lee, J. Wang, Q. Cong, L. N. Kinch and R. D. Schaeffer (2021). "Accurate prediction of protein structures and interactions using a three-track neural network." *Science* **373**(6557): 871-876.
- Bazan, J. F. (1990). "Haemopoietic receptors and helical cytokines." *Immunology today* **11**: 350-354.
- Becker, C., M. C. Fantini, C. Schramm, H. A. Lehr, S. Wirtz, A. Nikolaev, J. Burg, S. Strand, R. Kiesslich, S. Huber, H. Ito, N. Nishimoto, K. Yoshizaki, T. Kishimoto, P. R. Galle, M. Blessing, S. Rose-John and M. F. Neurath (2004). "TGF-beta suppresses tumor progression in colon cancer by inhibition of IL-6 trans-signaling." *Immunity* **21**(4): 491-501.
- Bettinardi, A., D. Brugnani, E. Quiros-Roldan, A. Malagoli, S. La Grutta, A. Correr and L. D. Notarangelo (1997). "Missense mutations in the Fas gene resulting in autoimmune lymphoproliferative syndrome: a molecular and immunological analysis." *Blood, The Journal of the American Society of Hematology* **89**(3): 902-909.
- Bodmer, J. L., P. Schneider and J. Tschopp (2002). "The molecular architecture of the TNF superfamily." *Trends Biochem Sci* **27**(1): 19-26.
- Booth, F. W., C. K. Roberts and M. J. Laye (2012). "Lack of exercise is a major cause of chronic diseases." *Compr Physiol* **2**(2): 1143-1211.
- Boulangier, M. and D.-C. B. Chow "EE, and Garcia, KC (2003)." *Science* **300**: 2101-2104.
- Carswell, E. A., L. J. Old, R. L. Kassel, S. Green, N. Fiore and B. Williamson (1975). "An endotoxin-induced serum factor that causes necrosis of tumors." *Proc Natl Acad Sci U S A* **72**(9): 3666-3670.
- Chalaris, A., C. Garbers, B. Rabe, S. Rose-John and J. Scheller (2011). "The soluble Interleukin 6 receptor: generation and role in inflammation and cancer." *European journal of cell biology* **90**(6-7): 484-494.
- Chan, M. H., A. L. Carey, M. J. Watt and M. A. Febbraio (2004). "Cytokine gene expression in human skeletal muscle during concentric contraction: evidence that IL-8, like IL-6, is influenced by glycogen availability." *Am J Physiol Regul Integr Comp Physiol* **287**(2): R322-327.
- Chen, B., S. Zhang, B. Wang, H. Chen, Y. Li, Q. Cao, J. Zhong, M. Xie, Z. Ran and T. Tang (2021). "775b olamkicept, an IL-6 trans-signaling inhibitor, is effective for induction of response and remission in a randomized, placebo-controlled trial in moderate to severe ulcerative colitis." *Gastroenterology* **161**(2): e28-e29.
- Chowdhury, S., L. Schulz, B. Palmisano, P. Singh, J. M. Berger, V. K. Yadav, P. Mera, H. Ellingsgaard, J. Hidalgo, J. Brüning and G. Karsenty (2020). "Muscle-derived interleukin 6 increases exercise capacity by signaling in osteoblasts." *J Clin Invest* **130**(6): 2888-2902.
- Colombo, C., M. Haluzik, J. J. Cutson, K. R. Dietz, B. Marcus-Samuels, C. Vinson, O. Gavrilova and M. L. Reitman (2003). "Opposite effects of background genotype on muscle and liver insulin sensitivity of lipotrophic mice: role of triglyceride clearance." *Journal of Biological Chemistry* **278**(6): 3992-3999.
- Crabé, S., A. Guay-Giroux, A. J. Tormo, D. Duluc, R. Lissilaa, F. Guilhot, U. Mavoungou-Bigouagou, F. Lefouili, I. Cognet and W. Ferlin (2009). "The IL-27 p28 subunit binds cytokine-like factor 1 to form a cytokine regulating NK and T cell activities requiring IL-6R for signaling." *The Journal of Immunology* **183**(12): 7692-7702.
- de Carvalho-Neto, P. B., M. d. Santos, M. B. de Carvalho, A. M. d. C. Mercante, V. P. P. d. Santos, P. Severino, E. H. Tajara, I. D. Louro and A. M. Á. da Silva-Conforti (2013). "FAS/FASL expression profile as a prognostic marker in squamous cell carcinoma of the oral cavity." *PLoS One* **8**(7): e69024.
- Dendorfer, U. (1996). "Molecular biology of cytokines." *Artificial organs* **20**(6): 437-444.
- Deng, B., M. Wehling-Henricks, S. A. Villalta, Y. Wang and J. G. Tidball (2012). "IL-10 triggers changes in macrophage phenotype that promote muscle growth and regeneration." *J Immunol* **189**(7): 3669-3680.

Di Gregorio, G. B., L. Hensley, T. Lu, G. Ranganathan and P. A. Kern (2004). "Lipid and carbohydrate metabolism in mice with a targeted mutation in the IL-6 gene: absence of development of age-related obesity." *Am J Physiol Endocrinol Metab* **287**(1): E182-187.

Dinarello, C. A. (2007). "Historical insights into cytokines." *European journal of immunology* **37**(S1): S34-S45.

Dostert, C., M. Grusdat, E. Letellier and D. Brenner (2019). "The TNF Family of Ligands and Receptors: Communication Modules in the Immune System and Beyond." *Physiol Rev* **99**(1): 115-160.

Drenth, J. P., S. H. Van Uum, M. Van Deuren, G. J. Pesman, J. Van der Ven-Jongekrijg and J. W. Van der Meer (1995). "Endurance run increases circulating IL-6 and IL-1ra but downregulates ex vivo TNF-alpha and IL-1 beta production." *J Appl Physiol* (1985) **79**(5): 1497-1503.

Engelowski, E., A. Schneider, M. Franke, H. Xu, R. Clemen, A. Lang, P. Baran, C. Binsch, B. Knebel and H. Al-Hasani (2018). "Synthetic cytokine receptors transmit biological signals using artificial ligands." *Nature communications* **9**(1): 2034.

Esser, N., S. Legrand-Poels, J. Piette, A. J. Scheen and N. Paquot (2014). "Inflammation as a link between obesity, metabolic syndrome and type 2 diabetes." *Diabetes Res Clin Pract* **105**(2): 141-150.

Ettinger, M. P., T. W. Littlejohn, S. L. Schwartz, S. R. Weiss, H. H. McIlwain, S. B. Heymsfield, G. A. Bray, W. G. Roberts, E. R. Heyman and N. Stambler (2003). "Recombinant variant of ciliary neurotrophic factor for weight loss in obese adults: a randomized, dose-ranging study." *Jama* **289**(14): 1826-1832.

Fazel Modares, N., R. Polz, F. Haghighi, L. Lamertz, K. Behnke, Y. Zhuang, C. Kordes, D. Häussinger, U. R. Sorg, K. Pfeffer, D. M. Floss, J. M. Moll, R. P. Piekorz, M. R. Ahmadian, P. A. Lang and J. Scheller (2019). "IL-6 Trans-signaling Controls Liver Regeneration After Partial Hepatectomy." *Hepatology* **70**(6): 2075-2091.

Febbraio, M. A. and B. K. Pedersen (2002). "Muscle-derived interleukin-6: mechanisms for activation and possible biological roles." *Faseb j* **16**(11): 1335-1347.

Fernando, M. R., J. L. Reyes, J. Iannuzzi, G. Leung and D. M. McKay (2014). "The pro-inflammatory cytokine, interleukin-6, enhances the polarization of alternatively activated macrophages." *PLoS One* **9**(4): e94188.

Findeisen, M., T. L. Allen, D. C. Henstridge, H. Kammoun, A. E. Brandon, L. L. Baggio, K. I. Watt, M. Pal, L. Cron and E. Estevez (2019). "Treatment of type 2 diabetes with the designer cytokine IC7Fc." *Nature* **574**(7776): 63-68.

Fisher, G. H., F. J. Rosenberg, S. E. Straus, J. K. Dale, L. A. Middleton, A. Y. Lin, W. Strober, M. J. Lenardo and J. M. Puck (1995). "Dominant interfering Fas gene mutations impair apoptosis in a human autoimmune lymphoproliferative syndrome." *Cell* **81**(6): 935-946.

Fridy, P. C., Y. Li, S. Keegan, M. K. Thompson, I. Nudelman, J. F. Scheid, M. Oeffinger, M. C. Nussenzweig, D. Fenyö and B. T. Chait (2014). "A robust pipeline for rapid production of versatile nanobody repertoires." *Nature methods* **11**(12): 1253-1260.

Fu, Q., T.-M. Fu, A. C. Cruz, P. Sengupta, S. K. Thomas, S. Wang, R. M. Siegel, H. Wu and J. J. Chou (2016). "Structural basis and functional role of intramembrane trimerization of the Fas/CD95 death receptor." *Molecular cell* **61**(4): 602-613.

Galgonek, J., J. Vymětal, D. Jakubec and J. Vondrášek (2017). "Amino acid interaction (INTAA) web server." *Nucleic Acids Research* **45**(W1): W388-W392.

Garbers, C., H. M. Hermanns, F. Schaper, G. Müller-Newen, J. Grötzinger, S. Rose-John and J. Scheller (2012). "Plasticity and cross-talk of interleukin 6-type cytokines." *Cytokine & growth factor reviews* **23**(3): 85-97.

Garbers, C. and J. Scheller (2013). "Interleukin-6 and interleukin-11: same same but different." *Biological chemistry* **394**(9): 1145-1161.

George, M. J., N. H. Jasmin, V. T. Cummings, A. Richard-Loendt, F. Launchbury, K. Woollard, T. Turner-Stokes, A. I. Garcia Diaz, M. Lythgoe, D. J. Stuckey, A. D. Hingorani and D. W. Gilroy (2021). "Selective Interleukin-6 Trans-Signaling Blockade Is More Effective Than Panantagonism in Reperfused Myocardial Infarction." *JACC Basic Transl Sci* **6**(5): 431-443.

Grötzinger, J., T. Kernebeck, K.-J. Kallen and S. Rose-John (1999). "IL-6 type cytokine receptor complexes: hexamer, tetramer or both?"

Han, M. S., A. White, R. J. Perry, J. P. Camporez, J. Hidalgo, G. I. Shulman and R. J. Davis (2020). "Regulation of adipose tissue inflammation by interleukin 6." *Proc Natl Acad Sci U S A* **117**(6): 2751-2760.

Heink, S., N. Yogev, C. Garbers, M. Herwerth, L. Aly, C. Gasperi, V. Husterer, A. L. Croxford, K. Möller-Hackbarth and H. S. Bartsch (2017). "Trans-presentation of IL-6 by dendritic cells is required for the priming of pathogenic TH17 cells." Nature immunology **18**(1): 74-85.

Heinrich, P. (1998). "Behrmann I, Muller-Newen G, Schaper F, and Graeve L." Interleukin-6-type cytokine signalling through the gp130/Jak/STAT pathway. Biochem J **334**: 297-314.

Heinrich, P. C., I. Behrmann, S. Haan, H. M. Hermanns, G. Müller-Newen and F. Schaper (2003). "Principles of interleukin (IL)-6-type cytokine signalling and its regulation." Biochemical journal **374**(1): 1-20.

Hirano, T., K. Yasukawa, H. Harada, T. Taga, Y. Watanabe, T. Matsuda, S. Kashiwamura, K. Nakajima and K. Koyama (1986). "Iwano, A." Tsunasawa, S., Sakiyama, F., Matsui, H., Taniguchi, T., and Kishimoto, T., Complementary DNA for a novel interleukin (BSF-2) that induces B lymphocytes to produce immunoglobulin, Nature (London) **324**: 73.

Hotamisligil, G. S., N. S. Shargill and B. M. Spiegelman (1993). "Adipose expression of tumor necrosis factor- α : direct role in obesity-linked insulin resistance." Science **259**(5091): 87-91.

Jackson, C. E., R. E. Fischer, A. P. Hsu, S. M. Anderson, Y. Choi, J. Wang, J. K. Dale, T. A. Fleisher, L. A. Middleton and M. C. Sneller (1999). "Autoimmune lymphoproliferative syndrome with defective Fas: genotype influences penetrance." The American Journal of Human Genetics **64**(4): 1002-1014.

Jones, S. A. and B. J. Jenkins (2018). "Recent insights into targeting the IL-6 cytokine family in inflammatory diseases and cancer." Nature reviews immunology **18**(12): 773-789.

Jonsdottir, I. H., P. Schjerling, K. Ostrowski, S. Asp, E. A. Richter and B. K. Pedersen (2000). "Muscle contractions induce interleukin-6 mRNA production in rat skeletal muscles." J Physiol **528 Pt 1**(Pt 1): 157-163.

Jostock, T., J. Müllberg, S. Özbek, R. Atreya, G. Blinn, N. Voltz, M. Fischer, M. F. Neurath and S. Rose-John (2001). "Soluble gp130 is the natural inhibitor of soluble interleukin-6 receptor transsignaling responses." European journal of biochemistry **268**(1): 160-167.

Jumper, J., R. Evans, A. Pritzel, T. Green, M. Figurnov, O. Ronneberger, K. Tunyasuvunakool, R. Bates, A. Žídek and A. Potapenko (2021). "Highly accurate protein structure prediction with AlphaFold." Nature **596**(7873): 583-589.

June, C. H., R. S. O'Connor, O. U. Kawalekar, S. Ghassemi and M. C. Milone (2018). "CAR T cell immunotherapy for human cancer." Science **359**(6382): 1361-1365.

Kaiser, K., K. Prystaz, A. Vikman, M. Haffner-Luntzer, S. Bergdolt, G. Strauss, G. H. Waetzig, S. Rose-John and A. Ignatius (2018). "Pharmacological inhibition of IL-6 trans-signaling improves compromised fracture healing after severe trauma." Naunyn Schmiedeberg's Arch Pharmacol **391**(5): 523-536.

Kallen, K.-J., J. Grötzinger, E. Lelièvre, P. Vollmer, D. Aasland, C. Renné, J. r. Müllberg, K.-H. M. zum Büschenfelde, H. Gascan and S. Rose-John (1999). "Receptor recognition sites of cytokines are organized as exchangeable modules: transfer of the leukemia inhibitory factor receptor-binding site from ciliary neurotrophic factor to interleukin-6." Journal of Biological Chemistry **274**(17): 11859-11867.

Keller, C., A. Steensberg, A. K. Hansen, C. P. Fischer, P. Plomgaard and B. K. Pedersen (2005). "Effect of exercise, training, and glycogen availability on IL-6 receptor expression in human skeletal muscle." Journal of Applied Physiology **99**(6): 2075-2079.

Kistner, T. M., B. K. Pedersen and D. E. Lieberman (2022). "Interleukin 6 as an energy allocator in muscle tissue." Nature metabolism **4**(2): 170-179.

Kuehn, H. S., I. Caminha, J. E. Niemela, V. K. Rao, J. Davis, T. A. Fleisher and J. B. Oliveira (2011). "FAS haploinsufficiency is a common disease mechanism in the human autoimmune lymphoproliferative syndrome." The Journal of Immunology **186**(10): 6035-6043.

Kumar, P., S. Henikoff and P. C. Ng (2009). "Predicting the effects of coding non-synonymous variants on protein function using the SIFT algorithm." Nature protocols **4**(7): 1073-1081.

Larson, R. C. and M. V. Maus (2021). "Recent advances and discoveries in the mechanisms and functions of CAR T cells." Nature Reviews Cancer **21**(3): 145-161.

Leahy, D. J., W. A. Hendrickson, I. Aukhil and H. P. Erickson (1992). "Structure of a fibronectin type III domain from tenascin phased by MAD analysis of the selenomethionyl protein." Science **258**(5084): 987-991.

Lukaszuk, B., I. Bialuk, J. Górski, M. Zajączkiewicz, M. M. Winnicka and A. Chabowski (2012). "A single bout of exercise increases the expression of glucose but not fatty acid transporters in skeletal muscle of IL-6 KO mice." Lipids **47**(8): 763-772.

Lust, J. A., K. A. Donovan, M. P. Kline, P. R. Greipp, R. A. Kyle and N. J. Maihle (1992). "Isolation of an mRNA encoding a soluble form of the human interleukin-6 receptor." *Cytokine* **4**(2): 96-100.

Martin, D. A., L. Zheng, R. M. Siegel, B. Huang, G. H. Fisher, J. Wang, C. E. Jackson, J. M. Puck, J. Dale and S. E. Straus (1999). "Defective CD95/APO-1/Fas signal complex formation in the human autoimmune lymphoproliferative syndrome, type Ia." *Proceedings of the National Academy of Sciences* **96**(8): 4552-4557.

Matthews, V. B., T. L. Allen, S. Risis, M. H. Chan, D. C. Henstridge, N. Watson, L. A. Zaffino, J. R. Babb, J. Boon, P. J. Meikle, J. B. Jowett, M. J. Watt, J. O. Jansson, C. R. Bruce and M. A. Febbraio (2010). "Interleukin-6-deficient mice develop hepatic inflammation and systemic insulin resistance." *Diabetologia* **53**(11): 2431-2441.

McDonald, N., N. Panayotatos and W. Hendrickson (1995). "Crystal structure of dimeric human ciliary neurotrophic factor determined by MAD phasing." *The EMBO journal* **14**(12): 2689-2699.

Metcalfe, R. D., K. Aizel, C. O. Zlatić, P. M. Nguyen, C. J. Morton, D. S.-S. Lio, H.-C. Cheng, R. C. Dobson, M. W. Parker and P. R. Gooley (2020). "The structure of the extracellular domains of human interleukin 11 α receptor reveals mechanisms of cytokine engagement." *Journal of Biological Chemistry* **295**(24): 8285-8301.

Morel, J., A. Constantin, G. Baron, E. Dernis, R. M. Flipo, S. Rist, B. Combe, J. E. Gottenberg, T. Schaeffer and M. Soubrier (2017). "Risk factors of serious infections in patients with rheumatoid arthritis treated with tocilizumab in the French Registry REGATE." *Rheumatology* **56**(10): 1746-1754.

Mossner, S., D. M. Floss and J. Scheller (2021). "Pro- and anti-apoptotic fate decisions induced by di- and trimeric synthetic cytokine receptors." *Iscience* **24**(5): 102471.

Mossner, S., M. Kuchner, N. F. Modares, B. Knebel, H. Al-Hasani, D. M. Floss and J. Scheller (2020). "Synthetic interleukin 22 (IL-22) signaling reveals biological activity of homodimeric IL-10 receptor 2 and functional cross-talk with the IL-6 receptor gp130." *Journal of Biological Chemistry* **295**(35): 12378-12397.

Mossner, S., H. T. Phan, S. Triller, J. M. Moll, U. Conrad and J. Scheller (2020). "Multimerization strategies for efficient production and purification of highly active synthetic cytokine receptor ligands." *Plos one* **15**(4): e0230804.

Murakami, M., M. Hibi, N. Nakagawa, T. Nakagawa, K. Yasukawa, K. Yamanishi, T. Taga and T. Kishimoto (1993). "IL-6-induced homodimerization of gp130 and associated activation of a tyrosine kinase." *Science* **260**(5115): 1808-1810.

Murphy, R. M., M. J. Watt and M. A. Febbraio (2020). "Metabolic communication during exercise." *Nat Metab* **2**(9): 805-816.

Navarro, G., S. Taroumian, N. Barroso, L. Duan and D. Furst (2014). *Tocilizumab in rheumatoid arthritis: a meta-analysis of efficacy and selected clinical conundrums*. Seminars in arthritis and rheumatism, Elsevier.

Nehlsen-Cannarella, S. L., O. R. Fagoaga, D. C. Nieman, D. A. Henson, D. E. Butterworth, R. L. Schmitt, E. M. Bailey, B. J. Warren, A. Utter and J. M. Davis (1997). "Carbohydrate and the cytokine response to 2.5 h of running." *J Appl Physiol* (1985) **82**(5): 1662-1667.

Nowell, M. A., A. S. Williams, S. A. Carty, J. Scheller, A. J. Hayes, G. W. Jones, P. J. Richards, S. Slinn, M. Ernst, B. J. Jenkins, N. Topley, S. Rose-John and S. A. Jones (2009). "Therapeutic targeting of IL-6 trans signaling counteracts STAT3 control of experimental inflammatory arthritis." *J Immunol* **182**(1): 613-622.

Oberg, H.-H., D. Wesch, S. Grüssel, S. Rose-John and D. Kabelitz (2006). "Differential expression of CD126 and CD130 mediates different STAT-3 phosphorylation in CD4⁺ CD25⁻ and CD25^{high} regulatory T cells." *International immunology* **18**(4): 555-563.

Ostrowski, K., C. Hermann, A. Bangash, P. Schjerling, J. N. Nielsen and B. K. Pedersen (1998). "A trauma-like elevation of plasma cytokines in humans in response to treadmill running." *J Physiol* **513** (Pt 3)(Pt 3): 889-894.

Ostrowski, K., T. Rohde, M. Zacho, S. Asp and B. K. Pedersen (1998). "Evidence that interleukin-6 is produced in human skeletal muscle during prolonged running." *J Physiol* **508** (Pt 3)(Pt 3): 949-953.

Pal, M., M. A. Febbraio and M. Whitham (2014). "From cytokine to myokine: the emerging role of interleukin-6 in metabolic regulation." *Immunol Cell Biol* **92**(4): 331-339.

Päth, G. n., S. R. Bornstein, M. Gurniak, G. P. Chrousos, W. A. Scherbaum and H. Hauner (2001). "Human breast adipocytes express interleukin-6 (IL-6) and its receptor system: increased IL-6 production by β -adrenergic activation and effects of IL-6 on adipocyte function." *The Journal of Clinical Endocrinology & Metabolism* **86**(5): 2281-2288.

Pedersen, B. K. and M. A. Febbraio (2012). "Muscles, exercise and obesity: skeletal muscle as a secretory organ." Nat Rev Endocrinol **8**(8): 457-465.

Pedersen, B. K. and L. Hoffman-Goetz (2000). "Exercise and the immune system: regulation, integration, and adaptation." Physiol Rev **80**(3): 1055-1081.

Petersen, A. M. and B. K. Pedersen (2005). "The anti-inflammatory effect of exercise." J Appl Physiol (1985) **98**(4): 1154-1162.

Petersen, E. W., A. L. Carey, M. Sacchetti, G. R. Steinberg, S. L. Macaulay, M. A. Febbraio and B. K. Pedersen (2005). "Acute IL-6 treatment increases fatty acid turnover in elderly humans in vivo and in tissue culture in vitro." Am J Physiol Endocrinol Metab **288**(1): E155-162.

Pettersen, E. F., T. D. Goddard, C. C. Huang, E. C. Meng, G. S. Couch, T. I. Croll, J. H. Morris and T. E. Ferrin (2021). "UCSF ChimeraX: Structure visualization for researchers, educators, and developers." Protein Science **30**(1): 70-82.

Price, S., P. A. Shaw, A. Seitz, G. Joshi, J. Davis, J. E. Niemela, K. Perkins, R. L. Hornung, L. Folio, P. S. Rosenberg, J. M. Puck, A. P. Hsu, B. Lo, S. Pittaluga, E. S. Jaffe, T. A. Fleisher, V. K. Rao and M. J. Lenardo (2014). "Natural history of autoimmune lymphoproliferative syndrome associated with FAS gene mutations." Blood **123**(13): 1989-1999.

Quintana, A., M. Erta, B. Ferrer, G. Comes, M. Giralt and J. Hidalgo (2013). "Astrocyte-specific deficiency of interleukin-6 and its receptor reveal specific roles in survival, body weight and behavior." Brain Behav Immun **27**(1): 162-173.

Rakonczay, Z., Jr., P. Hegyi, T. Takács, J. McCarroll and A. K. Saluja (2008). "The role of NF-kappaB activation in the pathogenesis of acute pancreatitis." Gut **57**(2): 259-267.

Rauscher, R. and Z. Ignatova (2018). "Timing during translation matters: synonymous mutations in human pathologies influence protein folding and function." Biochemical Society Transactions **46**(4): 937-944.

Rieux-Laucat, F. (2017). "What's up in the ALPS." Current Opinion in Immunology **49**: 79-86.

Robert, F. and J. Pelletier (2018). "Exploring the impact of single-nucleotide polymorphisms on translation." Frontiers in genetics **9**: 507.

Rose-John, S., B. J. Jenkins, C. Garbers, J. M. Moll and J. Scheller (2023). "Targeting IL-6 trans-signalling: past, present and future prospects." Nature Reviews Immunology: 1-16.

Rothbauer, U., K. Zolghadr, S. Muyldermans, A. Schepers, M. C. Cardoso and H. Leonhardt (2008). "A versatile nanotrap for biochemical and functional studies with fluorescent fusion proteins." Molecular & cellular proteomics **7**(2): 282-289.

Russo, S., M. Kwiatkowski, N. Govorukhina, R. Bischoff and B. N. Melgert (2021). "Meta-Inflammation and Metabolic Reprogramming of Macrophages in Diabetes and Obesity: The Importance of Metabolites." Front Immunol **12**: 746151.

Saggio, I., I. Gloaguen, G. Poiana and R. Laufer (1995). "CNTF variants with increased biological potency and receptor selectivity define a functional site of receptor interaction." The EMBO Journal **14**(13): 3045-3054.

Scheller, J. and S. Rose-John (2006). "Interleukin-6 and its receptor: from bench to bedside." Medical microbiology and immunology **195**: 173-183.

Schindler, R., J. Mancilla, S. Endres, R. Ghorbani, S. C. Clark and C. A. Dinarello (1990). "Correlations and interactions in the production of interleukin-6 (IL-6), IL-1, and tumor necrosis factor (TNF) in human blood mononuclear cells: IL-6 suppresses IL-1 and TNF." Blood **75**(1): 40-47.

Schreiber, S., K. Aden, J. P. Bernardes, C. Conrad, F. Tran, H. Höper, V. Volk, N. Mishra, J. I. Blase, S. Nikolaus, J. Bethge, T. Kühbacher, C. Röcken, M. Chen, I. Cottingham, N. Petri, B. B. Rasmussen, J. Lokau, L. Lenk, C. Garbers, F. Feuerhake, S. Rose-John, G. H. Waetzig and P. Rosenstiel (2021). "Therapeutic Interleukin-6 Trans-signaling Inhibition by Olamkicept (sgp130Fc) in Patients With Active Inflammatory Bowel Disease." Gastroenterology **160**(7): 2354-2366.e2311.

Schuett, H., R. Oestreich, G. H. Waetzig, W. Annema, M. Luchtefeld, A. Hillmer, U. Bavendiek, J. von Felden, D. Divchev, T. Kempf, K. C. Wollert, D. Seegert, S. Rose-John, U. J. Tietge, B. Schieffer and K. Grote (2012). "Transsignaling of interleukin-6 crucially contributes to atherosclerosis in mice." Arterioscler Thromb Vasc Biol **32**(2): 281-290.

Schumacher, N., D. Meyer, A. Mauermann, J. von der Heyde, J. Wolf, J. Schwarz, K. Knittler, G. Murphy, M. Michalek and C. Garbers (2015). "Shedding of endogenous interleukin-6 receptor (IL-6R) is governed by a

disintegrin and metalloproteinase (ADAM) proteases while a full-length IL-6R isoform localizes to circulating microvesicles." *Journal of Biological Chemistry* **290**(43): 26059-26071.

Schuster, B. r., M. Kovaleva, Y. Sun, P. Regenhard, V. Matthews, J. Grötzinger, S. Rose-John and K.-J. Kallen (2003). "Signaling of human ciliary neurotrophic factor (CNTF) revisited: the interleukin-6 receptor can serve as an α -receptor for CNTF." *Journal of Biological Chemistry* **278**(11): 9528-9535.

Scott, F. L., B. Stec, C. Pop, M. K. Dobaczewska, J. J. Lee, E. Monosov, H. Robinson, G. S. Salvesen, R. Schwarzenbacher and S. J. Riedl (2009). "The Fas-FADD death domain complex structure unravels signalling by receptor clustering." *Nature* **457**(7232): 1019-1022.

Serrano, A. L., B. Baeza-Raja, E. Perdiguero, M. Jardí and P. Muñoz-Cánoves (2008). "Interleukin-6 is an essential regulator of satellite cell-mediated skeletal muscle hypertrophy." *Cell Metab* **7**(1): 33-44.

Service, R. F. (2021). AI reveals structures of protein complexes, American Association for the Advancement of Science.

Sharma, A., V. Madaan and F. D. Petty (2006). "Exercise for mental health." *Prim Care Companion J Clin Psychiatry* **8**(2): 106.

Siegler, E. L. and S. S. Kenderian (2020). "Neurotoxicity and cytokine release syndrome after chimeric antigen receptor T cell therapy: insights into mechanisms and novel therapies." *Frontiers in immunology* **11**: 1973.

Sindhu, S., R. Thomas, P. Shihab, D. Sriraman, K. Behbehani and R. Ahmad (2015). "Obesity is a positive modulator of IL-6R and IL-6 expression in the subcutaneous adipose tissue: significance for metabolic inflammation." *PloS one* **10**(7): e0133494.

Sprenger, H., C. Jacobs, M. Nain, A. M. Gressner, H. Prinz, W. Wesemann and D. Gerns (1992). "Enhanced release of cytokines, interleukin-2 receptors, and neopterin after long-distance running." *Clin Immunol Immunopathol* **63**(2): 188-195.

Starkie, R., S. R. Ostrowski, S. Jauffred, M. Febbraio and B. K. Pedersen (2003). "Exercise and IL-6 infusion inhibit endotoxin-induced TNF- α production in humans." *Faseb j* **17**(8): 884-886.

Steensberg, A., M. A. Febbraio, T. Osada, P. Schjerling, G. van Hall, B. Saltin and B. K. Pedersen (2001). "Interleukin-6 production in contracting human skeletal muscle is influenced by pre-exercise muscle glycogen content." *J Physiol* **537**(Pt 2): 633-639.

Steensberg, A., C. P. Fischer, C. Keller, K. Møller and B. K. Pedersen (2003). "IL-6 enhances plasma IL-1ra, IL-10, and cortisol in humans." *Am J Physiol Endocrinol Metab* **285**(2): E433-437.

Steensberg, A., G. van Hall, T. Osada, M. Sacchetti, B. Saltin and B. Klarlund Pedersen (2000). "Production of interleukin-6 in contracting human skeletal muscles can account for the exercise-induced increase in plasma interleukin-6." *J Physiol* **529 Pt 1**(Pt 1): 237-242.

Stranges, P. B., J. Watson, C. J. Cooper, C. M. Choisy-Rossi, A. C. Stonebraker, R. A. Beighton, H. Hartig, J. P. Sundberg, S. Servick, G. Kaufmann, P. J. Fink and A. V. Chervonsky (2007). "Elimination of antigen-presenting cells and autoreactive T cells by Fas contributes to prevention of autoimmunity." *Immunity* **26**(5): 629-641.

Taga, T. (1997). "Kishimoto T." *Gp130 and the interleukin-6 family of cytokines. Annu Rev Immunol* **15**: 797-819.

Temple, N. J. (2022). "The Origins of the Obesity Epidemic in the USA-Lessons for Today." *Nutrients* **14**(20).

Urnbach, P., R. Ley, M. Mahowald, V. Magrini, E. Mardis and J. Gordon (2006). "An obesity-associated gut microbiome with increased capacity for energy harvest [J]." *Nature* **444**(7122): 1027-1031.

Vaishnav, A. K., J. R. Orlicky, J.-L. Chu, P. H. Krammer, M. V. Chao and K. B. Elkon (1999). "The molecular basis for apoptotic defects in patients with CD95 (Fas/Apo-1) mutations." *The Journal of clinical investigation* **103**(3): 355-363.

Wagner, E.-M., M. Aurich, S. Aparicio-Siegmund, D. M. Floss, C. Garbers, K. Breusing, B. Rabe, R. Schwanbeck, J. Grötzinger and S. Rose-John (2014). "The amino acid exchange R28E in ciliary neurotrophic factor (CNTF) abrogates interleukin-6 receptor-dependent but retains CNTF receptor-dependent signaling via glycoprotein 130 (gp130)/leukemia inhibitory factor receptor (LIFR)." *Journal of Biological Chemistry* **289**(26): 18442-18450.

Wallenius, V., K. Wallenius, B. Ahrén, M. Rudling, H. Carlsten, S. L. Dickson, C. Ohlsson and J. O. Jansson (2002). "Interleukin-6-deficient mice develop mature-onset obesity." *Nat Med* **8**(1): 75-79.

Wan, Z., C. G. Perry, T. Macdonald, C. B. Chan, G. P. Holloway and D. C. Wright (2012). "IL-6 is not necessary for the regulation of adipose tissue mitochondrial content." *PLoS One* **7**(12): e51233.

Ward, L. D., G. J. Howlett, G. Discolo, K. Yasukawa, A. Hammacher, R. L. Moritz and R. J. Simpson (1994). "High affinity interleukin-6 receptor is a hexameric complex consisting of two molecules each of interleukin-6, interleukin-6 receptor, and gp-130." Journal of Biological Chemistry **269**(37): 23286-23289.

Wesolowski, J., V. Alzogaray, J. Reyelt, M. Unger, K. Juarez, M. Urrutia, A. Cauerhff, W. Danquah, B. Rissiek and F. Scheuplein (2009). "Single domain antibodies: promising experimental and therapeutic tools in infection and immunity." Medical microbiology and immunology **198**: 157-174.

Whitham, M., M. Pal, T. Petzold, M. Hjorth, C. L. Egan, J. S. Brunner, E. Estevez, P. Iliades, B. Zivanovic, S. Reibe, W. E. Hughes, M. Findeisen, J. Hidalgo and M. A. Febbraio (2019). "Adipocyte-specific deletion of IL-6 does not attenuate obesity-induced weight gain or glucose intolerance in mice." Am J Physiol Endocrinol Metab **317**(4): E597-e604.

Wilkinson, A. N., K. H. Gartlan, G. Kelly, L. D. Samson, S. D. Olver, J. Avery, N. Zomerdijs, S. K. Tey, J. S. Lee, S. Vuckovic and G. R. Hill (2018). "Granulocytes Are Unresponsive to IL-6 Due to an Absence of gp130." J Immunol **200**(10): 3547-3555.

Wueest, S. and D. Konrad (2020). "The controversial role of IL-6 in adipose tissue on obesity-induced dysregulation of glucose metabolism." Am J Physiol Endocrinol Metab **319**(3): E607-e613.

Wunderlich, F. T., P. Ströhle, A. C. Könnner, S. Gruber, S. Tovar, H. S. Brönneke, L. Juntti-Berggren, L. S. Li, N. van Rooijen, C. Libert, P. O. Berggren and J. C. Brüning (2010). "Interleukin-6 signaling in liver-parenchymal cells suppresses hepatic inflammation and improves systemic insulin action." Cell Metab **12**(3): 237-249.

Yamasaki, K., T. Taga, Y. Hirata, H. Yawata, Y. Kawanishi, B. Seed, T. Taniguchi, T. Hirano and T. Kishimoto (1988). "Cloning and expression of the human interleukin-6 (BSF-2/IFN β 2) receptor." Science **241**(4867): 825-828.

Yuan, M., N. Konstantopoulos, J. Lee, L. Hansen, Z. W. Li, M. Karin and S. E. Shoelson (2001). "Reversal of obesity- and diet-induced insulin resistance with salicylates or targeted disruption of Ikk β ." Science **293**(5535): 1673-1677.

Zhang, H., P. Neuhöfer, L. Song, B. Rabe, M. Lesina, M. U. Kurkowski, M. Treiber, T. Wartmann, S. Regnér, H. Thorlacius, D. Saur, G. Weirich, A. Yoshimura, W. Halangk, J. P. Mizgerd, R. M. Schmid, S. Rose-John and H. Algül (2013). "IL-6 trans-signaling promotes pancreatitis-associated lung injury and lethality." J Clin Invest **123**(3): 1019-1031.

Zheng, X., Y. Wu, J. Bi, Y. Huang, Y. Cheng, Y. Li, Y. Wu, G. Cao and Z. Tian (2022). "The use of supercytokines, immunocytokines, engager cytokines, and other synthetic cytokines in immunotherapy." Cell Mol Immunol **19**(2): 192-209.

ACKNOWLEDGEMENTS

I would like to express my deepest gratitude to my supervisor Prof. Dr. Jürgen Scheller, for his guidance, constant support, and profound knowledge throughout my doctoral journey. His expertise and enthusiasm have been truly inspiring, and I am grateful for the opportunities he provided me to grow as a researcher.

I also thank my second supervisor, Prof. Dr. Hadi Al-Hasani, for his feedback, criticism, and encouragement.

I extend my heartfelt appreciation to Dr. Doreen M. Floss, Dr. Christina Vogel, and Dr. Jens Moll, for their constant help, and for shaping my research ideas and refining my methodologies, to Petra Oprea Keremic for her ever-present support and encouragement, and to all my colleagues I crossed in AG Scheller during my entire doctoral studies. I am grateful for all the scientific discussions, for their support, and specially for friendship.

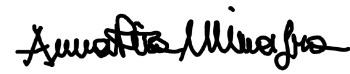
To my beloved family, I dedicate my doctoral thesis. I cannot thank you enough for your unwavering love, encouragement, and unlimited belief in me. Even if physically distant, your presence in my life has been my greatest strength.

Last but certainly not least, I am deeply grateful to my partner, Farhad Bazgir, for his endless belief in me and to be a constant source of inspiration and motivation, at work and in life.

EIDESSTATTLICHE ERKLÄRUNG

Ich versichere an Eides Statt, dass die Dissertation von mir selbständig und ohne unzulässige fremde Hilfe unter Beachtung der „Grundsätze zur Sicherung guter wissenschaftlicher Praxis an der Heinrich-Heine-Universität Düsseldorf“ erstellt worden ist. Diese Dissertation wurde in der vorgelegten oder einer ähnlichen Form noch bei keiner anderen Institution eingereicht und es wurden bisher keine erfolglosen Promotionsversuche von mir unternommen.

Düsseldorf, den Juli 2023

A handwritten signature in black ink, which appears to read 'Anna Rita Minafra', is written over a horizontal line.

Anna Rita Minafra